TARGETING OF EPIGENETIC MODIFIER EZH2 IN OROPHARYNGEAL SQUAMOUS CELL CARCINOMAS

by

CAMERON DAVID LINDSAY

A thesis submitted in partial fulfillment of the requirements for the degree of

Master of Science

in

Experimental Surgery

Department of Surgery

University of Alberta

ABSTRACT

Head and neck squamous cell carcinoma (HNSCC) is the 6th most prevalent cancer worldwide with rates of human papillomavirus (HPV)-positive oropharyngeal squamous cell carcinoma (OPSCC) dramatically increasing. The overexpression of enhancer of zeste homolog 2 (EZH2), a histone methyltransferase responsible for the trimethylation at lysine 27 of histone 3 (H3K27me3), is associated with a poor clinical prognosis and aggressive HPV-positive phenotypes. Three EZH2 pathway inhibitors; GSK-343, DZNeP, and EPZ-5687, were tested for efficacy in two HPV-positive (SCC-47 and SCC-104) and two HPV-negative (SCC-1 and SCC-9) HNSCC cell lines. Treatment with GSK-343 decreased H3K27me3 in all cell lines, whereas DZNeP decreased H3K27me3 in HPV-negative cell lines as determined by Western blot. Cells treated with EPZ-5687 displayed no appreciable change in H3K27me3. Epigenetic effect on gene expression was measured via ddPCR utilizing 11 target probes. Cells treated with DZNeP showed the most dramatic expressional changes, with decreased EGFR in HPV-positive cell lines and an overall increase in proliferation markers in HPV-negative cell lines. GSK-343-treated cells displayed moderate expressional changes, with CCND1 increased in HPV-positive cell lines and decreased TP53 in HPV-negative SCC-1. EPZ-5687 treated cell lines displayed few expressional changes overall. Only DZNeP-treated cells displayed anti-proliferative characteristics via wound-healing assay. Our findings suggest that EZH2 inhibitors remain a viable therapeutic option for the role of epigenetic effect, potentially limiting cell differentiation.

PREFACE

This thesis is an original work by Cameron Lindsay. Portions of the research conducted for this thesis forms part of a collaboration within the University of Alberta, led by Vincent Biron, MD, PhD, FRCSC, with Morris Kostiuk, PhD being the lead collaborator, and Hadi Seikaly, MD, MAL, FRCSC, Jeff Harris, MD, MHA, FRCSC, and Daniel O'Connell, MD, MSc, FRCSC contributing to this research. The technical aspects referred to in chapter 3 were performed by myself, with the assistance of Dr. Morris Kostiuk and Dr. Vincent Biron. The introduction and literature review in chapters 1 and 2 are my original work, as well as the data analysis in chapter 4 and concluding remarks in chapter 5.

Sections of Chapter 2 of this thesis have been published as C. Lindsay, H. Seikaly, and V. L. Biron. "Epigenetics of oropharyngeal squamous cell carcinoma: opportunities for novel chemotherapeutic targets." Journal of Otolaryngology-Head & Neck Surgery 46, no. 9 (2017). DOI 10.1186/s40463-017-0185-3. I was responsible for the data collection and analysis as well as the manuscript composition. Dr. Morris Kostiuk and Dr. Vincent Biron contributed to manuscript edits. Dr. Vincent Biron was the senior author, involved with concept design and manuscript composition.

Sections of Chapter 3-5 of this thesis have been published as C. Lindsay, M. Kostiuk, J. Harris, D. A. O'Connell, H. Seikaly, V. Biron. "Efficacy of EZH2 Inhibitory Drugs in Human Papillomavirus Positive and Negative Oropharyngeal Squamous Cell Carcinomas." Clinical Epigenetics 9, no. 95 (2017). DOI 10.1186/s13148-017-0390-y. I was responsible for the data collection and analysis as well as the manuscript composition. Dr. Morris Kostiuk and Dr. Vincent Biron contributed to manuscript edits. Dr. Vincent Biron was the senior author, involved with experimental design, data analysis and manuscript preparation.

DEDICATIONS

In loving memory of my Father, Murray Lindsay, and to my Mother, Dianne Lindsay, who raised me to be the man I am today. My accomplishments have not been without your love and support every step of the way. I hope to continue making you proud.

ACKNOWLEDGEMENTS

First and foremost, I would like to thank Dr. Vincent Biron and Dr. Morris Kostiuk for welcoming me into the OHRLA laboratory. You both have provided me with not only the knowledge and resources necessary to excel in my studies, but a fun and heavily sarcastic work environment that helped me look forward to every day. My examination committee; Dr. Michael Hendzel, Dr. Hadi Seikaly, and Dr. Thomas Churchill, I would like to thank for your time, knowledge, and resources. I would also like to thank Dr. Fred Berry's, Dr. Adetola Adesida's, and Dr. Nadr Jomha's laboratories for their advice and resources that aided in the completion of this project, as well as the Alberta Centre for Head and Neck Centre for Oncology and Reconstruction Fund and the University of Alberta Hospital Foundation for funding this project.

Melanie, Kezhou, Alex, Yan, and Brayden; without you all I doubt I would have been able to complete this project. Thank you for the laughs and your support. They are friendships that will endure for years to come. Dr. Kevin Friesen, you provided me with the skills necessary to bring me here, as well as the motivation to apply to this program in the first place. Thank you for your mentorship throughout my undergraduate degree as well as the uninvited coffee breaks in your office that followed.

TABLE OF CONTENTS

LIST OF TABLES

CHAPTER 2: LITERATURE REVIEW

LIST OF FIGURES

CHAPTER 1: GENERAL INTRODUCTION

CHAPTER 2: LITERATURE REVIEW

CHAPTER 4: RESULTS

LIST OF ABBREVIATIONS

5-FU	5-fluorouracil
AJCC	American Joint Committee on Cancer
BMI-1	B-cell specific Moloney murine complex 1
bp	base pair
CpG	cytosine preceding guanine
CT	Calcitonin
CT-imaging	computerized tomographic-based imaging
CPI	“Complete Protease inhibitor” cocktail
ddPCR	droplet digital polymerase chain reaction
DNMT	DNA methyltransferase
DNA	Deoxyribonucleic acid
DTT	Dithiothretiol
ECE	extracapsular extension
EED	embryonic ectoderm development
EGFR	epidermal growth factor receptor
EMT	epithelial to mesenchymal transition
EZH1	enhancer of zeste homolog 1
EZH2	enhancer of zeste homolog 2
FBS	fetal bovine serum
FOXM1	Forkhead box protein M1
H2AK119ub1	monoquitinylated histone H2A at lysine 119
H3K27me3	trimethylated histone 3 at lysine 27

H4K20me1	monomethylated histone 4 at lysine 20
H4K20me3	trimethylated histone 4 at lysine 20
HA	hyaluronic acid
HAT	histone acetyltransferase
HDAC	histone deacetylase
HDM	histone demethylase
HELLS	Helicase, Lymphoid Specific gene
HMT	histone methyltransferase
HNSCC	head and neck squamous cell carcinoma
HPV	human papillomavirus
HSPG	heparin sulphate proteoglycans
lncRNA	long non-coding RNA
MDM2	Mouse double minute homolog 2
miR	microRNA
MRI	magnetic resonance imaging
mTOR	mammalian target of rapamycin complex
ncRNA	non-coding RNA
OCSCC	oral cavity squamous cell carcinoma
OPSCC	oropharyngeal squamous cell carcinoma
PBS	phosphate buffered saline
PBST	phosphate buffered saline with 0.1% Tween20
PcG	Polycomb group
PDK1	phosphoinositide-dependent protein kinase 1
PI3K	phosphatidylinositol-3-kinase

PIP2	phosphatidylinositol 1,4-bisphosphate
PIP3	phosphatidylinositol 1,4,5-triphosphate
PMSF	phenylmethylsulfonyl fluoride
PRC1	polycomb repressive complex 1
PRC2	polycomb repressive complex 2
PTEN	phosphatase and tensin homolog
PVDF	polyvinylidene fluoride
Rb	Retinoblastoma
RNA	Ribonucleic acid
RT-PCR	reverse transcriptase polymerase chain reaction
SAM	S-adenosylmethionine
SAH	S-adenosylhomocysteine
siRNA	small interfering RNA
SUZ12	suppressor of zeste 12
piRNA	PIWI-interacting RNA
TEB	Triton extraction buffer
trxG	Trithorax
VEGF	vascular endothelial growth factor

CHAPTER 1

GENERAL INTRODUCTION

1.1 WHAT IS EPIGENETICS?

The term epigenetics was introduced by Conrad Waddington in the early 1940's as "the branch of biology which studies the causal interactions between genes and their products which brings phenotype into being" [1]. This definition encompasses all molecular pathways that modulate the expression of a genotype to produce a particular phenotype. The field of epigenetics has since evolved and narrowed in scope from its original definition. The field of epigenetics is now generally defined as "the study of changes in gene function that are mitotically and/or meiotically heritable and that do not entail a change in the DNA sequence" [2]. Epigenetic regulation has been implicated in multiple phenomena in both plants and animals. These include embryonic development, cell differentiation, imprinting, X chromosome inactivation, and various other gene expression patterns [3-5]. This definition is still quite limited, only accounting for normal, heritable physiological phenomena. When disease biology is included, this definition broadens and encompasses multiple facets. Aberrations within the epigenome have been implicated in a broad range of human diseases spanning immunologic disorders, metabolic and developmental abnormalities, psychiatric disorders, and cancer [6-10].

1.2 EPIGENETIC MECHANISMS IN CANCER

Cancer epigenetics is a steadily growing field that has demonstrated its importance in various aspects of carcinogenesis. Changes within the epigenome are known to influence tumor development, proliferation, metastasis, and resistance to chemotherapies and radiotherapies [6-10]. Literature focuses on three primary mechanisms of epigenetic carcinogenesis: DNA methylation, histone modification and their effects on chromatin structure and stability, as well as post-translational gene regulation through small and non-coding RNA (ncRNA) expression [3, 11-14].

1.2.1 DNA METHYLATION

Alterations in DNA methylation within the epigenome are recognized according to three general states; hypomethylated, hypermethylated, and loss of imprinting [15, 16]. Loss of imprinting will not be discussed, as its relevance to cancer biology is currently limited. While discovered much earlier (see section 1.3 History of Epigenetics), DNA methylation was recognized as the first encounter with epigenetic abnormalities in cancer in 1982 at a symposium at John Hopkins. It was shown a genome-wide loss of DNA methylation at the 5' position of a cytosine preceding guanine (CpG) dinucleotide in cancer cell lines relative to normal tissues [3, 17]. Current evidence remains coherent with the John Hopkins symposium, and it is a generally supported hypothesis that hypomethylation of promoter regions by DNA demethylases can be oncogenic via activation of various proto-oncogenes and chromatin restructuring [18]. The oncogenic activity associated with DNA hypermethylation tends to be site-specific, targeting promoter CpG islands catalyzed by a set of enzymes known as DNA methyltransferases (DNMTs). There are three DNMTs frequently observed in literature; DNMT1, responsible for the maintenance of the normal epigenome as well as DNMT3a and DNMT3b, which are responsible for *de novo* methylation patterns [19-22]. In cancers, DNA hypermethylation often results in the silencing of various genes, frequently tumor suppressors genes involved in the regulation of cell cycle control, DNA repair mechanisms, and apoptosis [6, 23-26].

1.2.2 HISTONE MODIFICATIONS

The structure of chromatin is a well-regulated system involving multiple complex pathways and interactions that regulate metabolic processes within a cell. The most basic unit of chromatin is the nucleosome, which is composed of 146 base pairs (bp) strand of DNA wrapped in a left-handed supercoil around an octamer core of histones approximately 1.7 turns [27, 28]. The octamer core consists of two of each four globular proteins; H2A, H2B, H3, and H4. At the level of the chromatosome, histone H1 provides linkage alongside an additional 20 bp of DNA [27-30]. Histone proteins have a net positive charge which form electrostatic interactions with the overall negatively charged DNA backbone [27]. At the amino-terminal ends of the histone

proteins, various post-translational modifications can be applied. Due to the net positive charge of these terminal ends, often lysine or arginine residues, the type and number of modifications can dramatically alter the electrostatic interactions between histone and DNA [31-33]. These modifications lead to changes in the chromatin structures and can alter gene expression via the allowance or blockage of access to various target genes to transcriptional machinery. These include acetylation, phosphorylation, methylation, ubiquitination, sumoylation, and ADP-ribosylation. These modifications, while all able to remodel chromatin structure, seem to be limited to aberrant acetylation and methylation profiles in carcinogenesis [4, 13, 34, 35]. The primary enzymes involved in histone methylation and acetylation processes include histone methyltransferases (HMTs), histone demethylases (HDMs), histone acetyltransferases (HATs), and histone deacetylases (HDACs) [6, 7].

Currently, there are two known types of HATs; A-type that are localized within the nucleus and are involved in the catalysis of transcription-related acetylation, and B-type localized within the cytosol that are involved in the catalysis of newly generated histones. While the exact mechanism behind HATs facilitation of transcriptional regulation is not fully understood, it is generally accepted that HAT's facilitate the opening of chromatin for recruitment of transcriptional machinery through the transfer of an acetyl group from an acetyl-CoA molecule to ε-amino groups of specific lysine residues [36-38]. Their overexpression has been associated with various cancers via encouragement of transcription factor binding, resulting in gene activation or overexpression. HAT overexpression can be seen in several cancers with histone 3 lysine 27 (H3K27) acetylation being one of the more well-documented modifications and can be seen in lung cancers and hematopoietic cancers [39, 40]. The overexpression of HDACs results in deacetylation and gene silencing events that can be oncogenic [40-42]. Histone methylation works in a slightly different process, where methylation, or multiple methylations, of lysine and arginine residues result in the structural rearrangement of chromatin to allow or block transcriptional machinery from accessing a particular gene of interest [43, 44]. Like histone acetylation, aberrant expression of HMTs and HDMs has been associated with carcinogenesis of various cancers via gene silencing or overexpression, respectively. Cancers frequently show altered methylation profiles on histone H3 at specific lysine sites including K4, K9, K27, K36, K79 [44]. Histone modifications remain a complex field of study in the context of disease

models, as modifications occurring at various sites act as part of a standard and temporary biochemical processes such as gene expression or DNA repair of distinct tissue types [45].

1.2.3 SMALL AND NON-CODING RNA

While a relatively new area of study, ncRNAs have shown numerous links to carcinogenesis and malignancy progression. Their first link to cancer was revealed by the altered expression profiles of miR-15 and miR-16 in chronic lymphocytic leukemia and they have since been discovered to have a role in multiple other cancer variants [46-50]. ncRNA are categorized based on size. Less than 200bp are known as small ncRNAs, while ncRNA molecules greater than 200bp are known as long non-coding RNAs (lncRNAs) [35]. Included within the small ncRNAs are the small interfering RNAs (siRNAs), micro RNAs (miRs), and PIWI-interacting RNAs (piRNAs). While all molecules contribute to gene silencing, much of cancer research focuses on miRs. miRs have been shown to silence genes via direct interaction with mRNA, either through mRNA translation inhibition or through targeting mRNA for degradation [47, 51]. Epigenetic silencing by specific miRs may have a direct causal link in carcinogenesis as evidence suggests their role may include that of tumor suppressor [52]. Unlike small ncRNAs, lncRNAs have no formal categorization. However, most are organized based on a particular transcripts function, including chromatin remodelling and transcription factor modulation. Knowledge of lncRNAs in carcinogenesis is limited, but evidence of lncRNAs chromatin remodeling function suggests a significant role in tumor formation and maintenance [35, 46, 53].

1.3 HISTORY OF EPIGENETICS

As our knowledge of biological mechanisms of gene expression has increased, so too has our definition of the term “epigenetics”. First coined by CH Waddington in 1942, epigenetics was a term broadly used to define all developmental regulatory processes occurring from a fertilized zygote to the mature organism [1, 54]. This paradigm had its origins in the study of cell biology and embryology, ultimately laying the groundwork for our current understanding of gene regulation and development. At that time, embryologists were divided into two different schools

of thought; “preformatism” where each cell contained preformed elements that expanded throughout development, and “epigenesis” where cells performed numerous chemical reactions that followed a complex plan of development. While both fields of thought had merits and pitfalls, the result of this rivalry brought forth a large influx of knowledge regarding the role of the cells’ nucleus and cytoplasm [45].

One of the most revolutionary theories introduced in the movement, also by CH Waddington, was the theory of “canalization” and the “epigenetic landscape”. This concept proposed that phenotype was not just the result of additive effects of multiple genes, but was driven by a unique developmental system. This theory was brought about by the resilience of phenotypic expression when eukaryotic developmental systems were subjected to multiple genetic and environmental variations. This ability to buffer or suppress phenotypic variations was known as canalization [54, 55]. It was proposed that developmental processes would lead to specific phenotypic endpoints or milestones from separate genetic starting points.

The concept of the epigenetic landscape was utilized to illustrate the theory of canalization via the “ball rolling down a hill” imagery seen in FIG. 1.1. Proposed were multiple paths that featured downward slopes with an undulating surface between each path. The ball represented a specific cell or tissue and the paths determining the ultimate fate of differentiation. If the ball rolled down the landscape, it would be forced to take a specific pathway to reach the “canalized” low point. To roll back up the hill or to take another path would be a difficult endeavour. How it suppressed the influence of the genetic and environmental factors is represented through small deviations in surface heights and widths. Ultimately, the changes to a surfaces height or width would do little to disrupt the ball, or cell’s, fate. Also proposed are the influences of gene expression, represented by pegs and strings underneath. The pegs and strings link to form the crevices and hills of the epigenetic surface. To summarize in biological terms, a cells fate is determined by gene interactions and once decided, its developmental endpoint is difficult to reverse. Waddington’s theory predicted genetic variations and mutations would accumulate until a decanalizing event would result in a gross change to the cell’s phenotype [37, 54, 55].

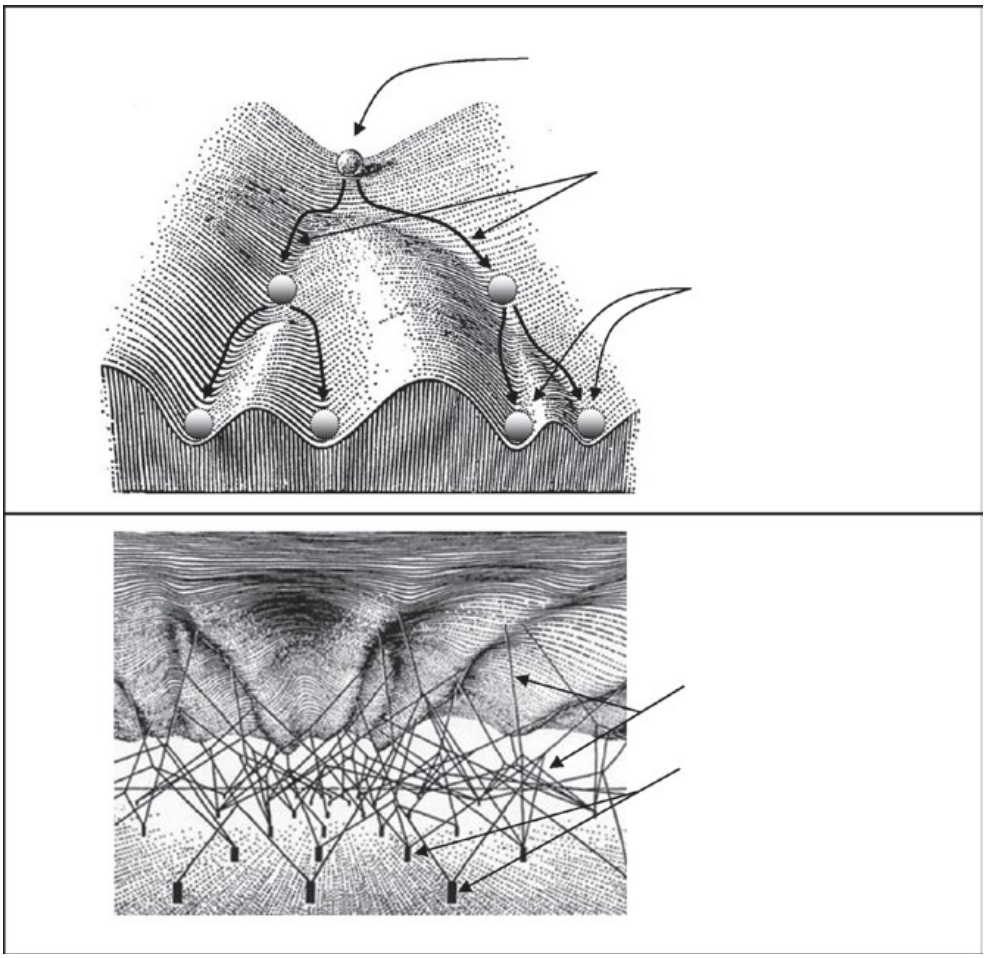

FIG. 1.1 Waddington's model of Epigenesis

Above: The landscape as imagined by Waddington. The surface begins at an elevated position, where elevations and depression on the surface form multiple lower end pathways. Each pathway is representative of a developmental endpoint. The cell, represented by the ball, will roll down to an ultimate developmental endpoint. Therefore, once a cell reaches a developmental pathway it cannot be reversed. The ball at its highest point is representative of a totipotent cell. Once canalized, its characteristics are relative to that of a committed cell. Below: Genetic interactions and pathways, represented by pegs and strings, respectively. They interact with one another to shape the genetic landscape depicted above, representing the collective genetic interactions required to ultimately shape a cells developmental fate.

(Figures reprinted from Waddington's The Strategy of Genes: A Discussion of Some Aspects of Theoretical Biology, 1957, Figure 4 on page 29 and Figure 5 on page 36, George Allen and Unwin, with permission from Taylor and Francis. Both figures have been modified)

The field of epigenetic regulation remained relatively dormant until approximately 65 years ago, when Watson and Crick brought forth the explanation of the molecular structure of DNA [56]. Following this time, multiple mechanisms of epigenetic regulation were discovered, such as the three primary mechanisms of epigenetic regulation (DNA methylation, histone modification, and ncRNA-mediated regulation). Some epigenetic phenomena were also documented during this time; including transvection, paramutation, and X chromosome inactivation. X chromosome inactivation in particular provided renewed interest regarding the epigenetic question. Its discovery clearly demonstrated random gene regulation with no evidence of change in the DNA sequence [5, 37, 57-59].

DNA methylation was technically discovered in 1925 by Johnson and Coghill when they identified 5-methylcytosine in *tubercle bacilli*. However, it was not formally accepted until 1948 when Hotchkiss viewed 5-methylcytosine on hydrolyzed nucleic acid [37, 60, 61]. This was further confirmed by GR Wyatt in 1950 [62]. Despite the discovery of methylated nucleic acids, the role of DNA methylation as a genetic regulator was not proposed until 25 years later by Holliday and Pugh (1975) and Riggs (1975) independently; suggesting this mechanism could account for processes such as X chromosome inactivation [59, 63].

Theories of a histones role in gene expression were proposed as early as the 1950s; long before the solidification of the chromatin structure by Kornberg in 1974 [29]. In 1964 Allfrey and colleagues performed a study on calf thymus nuclei with acetate and methionine precursors. Their study had demonstrated dynamic regulatory effects of histone acetylation on RNA polymerase reactions, suggesting a link between histone acetylation and transcriptional activation. Their conclusions on methylation were slightly different in relation, suggesting methylation only playing a role in posttranslational modification [64]. This linkage between histone acetylation and transcriptional activity was further supported by Riggs and colleagues in 1977, while the transcriptional regulatory role of histone methylation was not demonstrated until the late 1990s by Chen and colleagues and Strahl and colleagues [37, 65-67]. In 1991, work by Durrin and colleagues in *Saccharomyces cerevisiae* provided another monumental step forward regarding the involvement of histone modifications in gene regulation. They performed a series

of amino acid deletions and substitutions in the H4 N-termini, which resulted in a dramatic reduction in *GAL1* activation. They concluded that the histone H4 N-terminus is involved in transcription initiation and silencing [68]. Brownell and colleagues provided further detail on the mechanisms at work. Their study showed a histone acetyltransferase in *Tetrahymena* was homologous to a known yeast transcription regulator protein Gcn5. This parallel indicated a direct connection to histone acetylation and regulation of gene expression [45, 69]. From then till modern day, major breakthroughs in knowledge of the roles and mechanisms of various histone modification types have been quite frequent. We have seen the discovery of A- and B-type HATs, A-type HATs role as a transcriptional coactivator, the discovery and role of HMTs in transcriptional regulation, and the most recently discovered method of transcriptional regulation via sumoylation of histone H4 [45, 65, 66, 70-73].

Of the epigenetic regulators, ncRNAs are the most recently discovered. The first recognized of this category are miRs, and like the concept of epigenesis itself, began in the field of developmental biology. In 1993, Lee and colleagues identified the first miR by cloning the developmental gene *lin-4* in *Caenorhabididtus elegans.* They had noticed this process resulted in two separate transcripts being produced (*lin-4S and lin-4L)* without the translation of a protein. The transcripts produced also contained complementary sequences to the *lin-14* mRNA, suggesting the possibility of RNA-RNA interactions [45, 74]. This interaction, otherwise referred to as RNA interference, would not be identified until 1998 by Fire and collegues through their work with *C. elegans*. Their study showed the effects of specific gene suppression on the worms when injected with double stranded RNA [75]. lncRNAs remain far less studied in comparison, despite their discovery in the 1990s through cDNA library searches [76]. Currently their role and classification is still widely debated, but their implication in cancer biology has spurred great interest in the molecule [77].

1.3.1 THE HISTORY OF EPIGENETICS ROLE IN CANCER

The idea of epigenetic implications in tumorigenesis was first proposed by Markert in 1968, prior to the discovery of the epigenetic regulatory mechanisms. It was suggested that the

development of cancer was potentially instigated through the alteration of various genes via external epigenetic mechanisms [78]. This theory was refined further by Holliday in 1979, suggesting damage to DNA could result in the alteration or loss of specific DNA methylation which would result in a change in gene expression [79].

DNA methylation is recognized as the first encounter with epigenetic abnormalities in cancer cells, first described in 1982 at a symposium at John Hopkins. The study showed a genome-wide loss of DNA methylation at the 5' position of CpG dinucleotides in cancer cell lines relative to normal tissues, allowing nearby genes to become activated [3, 17]. While the exact mechanism behind global methylation interactions remain unknown, the SNF2 family of helicases remain an active area of investigation due to their regulatory role in DNA methylation. Evidence of genome-wide hypomethylation in multiple other cancers has been reported since the advent of high-throughput methylation techniques [3]. Cancers of multiple tissue origins including stomach, kidney, colon, cervix, and head and neck are associated with genome-wide hypomethylation in 5-methylcytosine [34, 80-83]. Hypomethylation's role in carcinogenesis remained relatively dormant until very recently with the discovery of drug, toxin, and viral effects on the epigenome [3]. Four years from the symposium at John Hopkins, Baylin and Nelkin (1986) observed the role of hypermethylation and its role in lung cancer. When using calcitonin (CT) as an expressional marker, *CT* expression was found to be silenced in lung cancer relative to normal adult tissues. This silencing was shown to be a direct result of hypermethylation at the 5′-region of the *CT* promotor [84]. Hypermethylation's direct role in carcinogenesis was revealed shortly afterwards in 1989, with the discovery of retinoblastoma tumor suppressor gene *RB* demonstrating site-specific hypermethylation in a retinoblastoma model [85]. Research within this area was slow to progress following this discovery until 1994, when a rapid increase in knowledge of cancer specific gene promoters were hypermethylated. The most notable publications included *CDKN2A, VHL,* and *MLH1*; coding a cyclin-dependent inhibitor, an E3 ubiquitin ligase, and DNA mismatch repair enzyme, respectively [86-88]. Multiple progressions in the field of cancer epigenetics have been made with much focus on the alteration of DNMTs via chemical inhibitors, RNA silencing, and or knockout studies for targeted gene reactivation. From these studies, mixed results have been obtained [1]. Queries obtained from these studies question whether initial hyper/hypomethylation is a direct result of

DNMT dysregulation or whether it is a secondary to other modifications like histone modifications. Bachman and colleagues provided an answer to this question, acknowledging the methylation of H2K9 occurs in conjunction with the re-silencing of *CDKN2A* following a DNMT knockout [89].

The concept of histone modifications as a form of transcriptional regulation was first proposed by Vincent Allfrey and colleagues in 1964 through their work with histone acetylation [64]. However, implications with regard to cancer did not come into the spotlight until much later through the discovery of interactions with DNMT's in the 1980's [90-93]. Histone methylation's role in gene regulation was formally recognized in 1999 by Strahl and colleagues [67]. They were able to show regulatory gene silencing being a result of cyclical histone methylation mediated by histone methyltransferase SUV39H1 [67]. Inspired by this research, Nguyen and colleagues demonstrated H3K9 methylation was correlated with *CDKN2A* silencing [94]. In this study, chromatin immunoprecipitation assays were utilized to view methylation status of H3K9 and H3K4 in bladder cancer cells following treatment with 5-aza-2′-deoxycytidine, a cytosine methylation inhibitor. Their results showed reduced levels of dimethylated H3K9, increased levels of dimethylated H3K4, and 5-aza-2′-deoxycytidine treated cells displayed increased H3K4 acetylation and methylation at the *p14ARF* promoter [3, 94].

The recently discovered ncRNAs have shown numerous and diverse links in both carcinogenesis and malignancy progression. The first link to cancer was shown by the different expression profiles of miR-15a and miR-16-1 in B-cell chronic lymphocytic leukemia [46-50]. 2005 proved to be a breakthrough year for miR knowledge, beginning with the first direct implication of miR function as oncogenes by He and colleagues [95]. Their study observed the overexpression of miR-17-92 cluster enhanced lymphoma *in vivo* within a mouse model via the *c-MYC* oncogene [95]. O'Donnell and colleagues further expanded on this evidence, showing *c-MYC*`s ability to regulate miR-17-92 expression [96]. Johnson and colleagues also demonstrated the mechanical role of miR's in cancer progression, exhibiting Let-7's targeting of oncogene *RAS* involving multiple cancer types [97].

The complexity of miR regulation was exemplified in 2006 by Saito and colleagues [98]. Their study demonstrated the role of both DNA methylation and histone modifications in regulating

the expression of miRs. Of focus was miR-127, a miRNA often silenced in cancer cells. When Saito and colleagues utilized chromatin demethylation and deacteylation agents, miR-127 was found to be overexpressed [98]. The role miRs play in cancer progression and malignancy was observed in 2007. In breast cancer cells, miR10b was shown to play a role in both tumor invasion of nearby tissues as well as metastasis [99]. Tavazoie and colleagues had demonstrated the opposite, with miR-126 suppressing tumor growth and proliferation while miR-335 and miR-206 were regulating migration and cell morphology [100]. Fortunately in 2010, Medina and colleagues introduced an interesting phenomenon in miR regulation and tumorigenesis - the concept of "oncomiR addiction", otherwise known as the dependence of one or a few genes for maintenance of a malignant phenotype [101]. Their study found through the manipulation of a single miR (miR-21) that its overexpression was enough to stimulate neoplastic development in a mouse model. Additionally, tumor size showed significant decrease and survival rates significantly increased following miR-21 inactivation [101]. Melo and colleagues later provided strong evidence that breast cancer miRs can enter normal cells and induce transcriptome alterations that lead to tumor formation [102]. This line of evidence has further spurred research into miR chemotherapeutics.

An exciting development in cancer epigenetics is the link between diet, lifestyle, and environmental factors leading to the development of neoplasia. The most well studied example is between dietary methionine and DNA methylation. In normal cells, methionine is an essential amino acid that acts as a methyl donor [103]. In a study by Chen and colleagues, patients with higher dietary methionine displayed lower incidences of cancer, suggesting increased methylation content [103]. Reduction of methylenetetrahydrofolate reductase, an enzyme involved in methionine metabolism, has been associated with alcohol consumption. Alcohol has well established cytotoxic properties [3, 103]. Certain dietary agents such as green tea polyphenols and phenethyl isothiocyanate have shown an ability to act as DNMT and HDAC inhibitors in cells [104]. These agents were more effective than current epigenetic chemotherapeutics. This would suggest cancer prevention could potentially be achieved through dietary and/or non-pharmaceutical intervention [104].

CHAPTER 2

LITERATURE REVIEW

2.1 OROPHARYNGEAL SQUAMOUS CELL CARCINOMA EPIDEMIOLOGY

Head and neck squamous cell carcinoma (HNSCC) is the sixth leading cancer worldwide, with over 600 000 new cases per year [105]. Males appear to be affected significantly more than females worldwide, with rates being two to four times higher [106]. In the United States, approximately 60 000 new cases are diagnosed annually with 12 000 patients dying from the disease [107, 108]. The primary risk factors associated with head and neck cancers include the consumption of alcohol, cigarettes, chewing tobacco, and betel quid due to their mutagenic and cytotoxic properties combined with consistent exposure to the epithelial layers of the upper aerodigestive tract [105, 107-109]. Exposure to various microbes has also been implemented in the acquisition of head and neck cancers. The Epstein-Barr Virus is associated with nasopharyngeal carcinoma, whereas human papillomavirus (HPV) is found in the majority of oropharyngeal squamous cell carcinomas (OPSCC) [97-99].

In many parts of the world, the incidence of HNSCC has decreased since the 1980s and is attributed to successful smoking cessation public health campaigns. However, the incidence of OPSCC has been rapidly increasing over the past decade due to HPV-associated infections. In the 1990s, studies suggested HPV-positive tumors composed approximately 40–60% of total OPSCCs, while recent studies have shown rates have risen to 70-80% in developed countries [108, 109]. HPV serotypes 16, 18, 31, 33, 35, 39, 51, 52, 56, 58, 59, and 66 have causal links with HPV-associated carcinogenesis; however, HPV-16 has shown a much higher level of incidence (approximately 88%) relative to other serotypes [110-112].

2.2 HUMAN PAPILLOMAVIRUS BIOLOGY

HPV is a nonenveloped, double-stranded DNA virus that is approximately 8000 bp [113]. There are over 150 known serotypes of HPV that have been obtained from human epidermal and mucosal epithelium. HPV is classified as a sexually transmitted virus, with the majority of infections being spread human-to-human via genital-to-genital or oral-to genital contact. Viruses are categorized as either “low-risk” or “high-risk” with regard to their oncogenic potential. Low-risk serotypes often manifest in the form of epithelial warts or oral papillomas. 12 HPV serotypes

(16, 18, 31, 33, 35, 39, 51, 52, 56, 58, 59, and 68) are included within this high-risk category, with HPV-16 and 18 alone being accountable for approximately 71% of cervical (90% when including other high-risk serotypes), over 85% of head and neck (90% when including other high-risk serotypes), and over 87% of anogenital cancers (anus, vulva, vagina and penis, 96% when including other high-risk serotypes) [114]. Their viral genome consists of 8 encoded proteins (E1, E2, E4, E5, E6, E7, L1, L2) involved in viral replication, maintenance, and capsid proteins [115, 116]. Viral proteins E6 and E7 have been shown to play an integral role in carcinogenesis and will be discussed in greater detail in later sections.

The mechanism of entry into cells by HPV starts when a virion binds to cell surface heparin sulphate proteoglycans (HSPG) and cyclophilin B. Through this binding, the virion is uncoated and internalized into the cell [117, 118]. This process is likely mediated by a secondary receptor, as HSPG binding is not sufficient for entry [119]. Epidermal growth factor receptors (EGFR) have been shown to play an integral role in HPV infection as well. HPV capsids pre-coated with HSPG-growth factor form a complex and activate EGFR, thus inhibiting cellular autophagy and allowing further uptake of the virus [120, 121]. Upon infection of the host cell, low pH exposure by host cell endosomes allow viral capsid proteins which are bound to viral DNA to be released into the host cell's cytoplasm. The viral protein-DNA complex travels along host cell microtubules into the nucleus [122]. Once in the nucleus, HPV integrates into the host genome and begins replication. In cancer cells, this integration into human chromosomes has been shown to increase and stabilize the expression of viral oncoproteins E6 and E7 [123]. HPV integration sites are distributed along the entire human genome, with various serotypes displaying degrees of favoritism on specific chromosomal regions. For instance, HPV-16 favors integration at chromosomes 1, 2, 3, 5, 8, and 9 [124]. An interesting discovery by Akagi and colleagues has shown an association between the number of HPV integrants and their effects on neighboring gene expression [125]. They found as the number of viral integrants increased, the chances of direct disruption of neighboring genes via alterations in genomic structures increased alongside [125]. While an interesting line of research, it is still very much in its infancy and further investigation into HPV integration-associated mutagenesis is required prior to making any definitive claims.

2.3 MOLECULAR MECHANISMS OF CARCINOGENESIS IN OPSCC

Research demonstrates distinct differences in HPV-positive OPSCCs host gene expression profiles relative to HPV-negative OPSCCs, with these changes being present within multiple genomic modification mechanisms. Each change observed provides further insight into the mechanisms of cancer tumorigenesis, proliferation, invasion, and metastasis in both HPV-positive and HPV-negative OPSCC. This biological distinction based on HPV status is directly reflected by both clinical presentation and response to current treatment modalities, as HPV-positive OPSCCs have significantly better prognostic outcomes [126, 127]. The use of biomarkers in determining clinical diagnosis and prognostic outcome is widely used within the medical field. One of the best-known examples for use in oncological fields today is marker of proliferation, Ki-67, chosen for its reliability of expression only in proliferating cells [128, 129]. The field of genetics, specifically epigenetics, has shown an increase in popularity of epigenetic markers as the advents of high throughput genetic technologies becomes increasingly more affordable, accessible and efficient. Clinical biomarkers are detected in the human body through various means including resected tumors, blood plasma DNA, and urine sediments. Cancer biomarkers are typically observed through biopsy or sample of resected tumor [4].

Specific DNA methylation patterns are showing increased promise as biomarkers, some claiming superiority to current markers, as they hold increased levels of stability and can be amplified in a cost-effective manner [4, 130, 131]. Histone modifications may also provide potential utilization as prognostic markers. Histone methyltransferase enhancer of zeste homolog 2 (EZH2) and subsequent H3K27 trimethylation is found to be overexpressed in numerous cancer types and is frequently indicative of a poor prognosis [7, 132, 133]. EZH2 is of primary focus within this study. Unfortunately, the study of histone modifications faces the limitation of unknown gene activity changes following gross chromatin remodeling typically associated with histone modifiers. This would suggest further study is required before diagnostic use [7].

Despite being the most recently discovered of the epigenetic modifiers, miR's have shown some of the greatest potential as prognostic markers. As mentioned in 1.3.1, their role in cancers

appears to be quite significant to all stages of cancer, including tumorigenesis, invasion, metastasis, and response to therapy [7, 134]. A summary of the potential epigenetic biomarkers involved in OPSCC can be found in Table 1.

2.3.1 THE p53/Rb PATHWAY

Frequently encountered in both mutational and epigenetic modification-mediated OPSCC are alterations directly involved, or alterations that indirectly affect the p53/Rb pathway [135, 136]. This pathway can generally be split into two separate directions according to splicing variants of the *CDKN2A* gene.

A key factor involved in the response of cell cancer stress signal such as DNA damage or oncogene activation, is the tumor suppressor protein p53. Once activated, p53 can elicit the expression of multiple cellular responses resulting in growth arrest, senescence, and apoptosis [137]. Because of this dramatic response from activation, physiological levels of p53 are typically quite low. Low levels of p53 can be attributed to regulation by mouse double minute 2 homolog (MDM2), an E3 ubiquitin protein ligase that targets p53 for rapid degradation via ubiquitination. MDM2 is in turn regulated by protein alternative transcript reading frame variant p14ARF encoded by the *CDKN2A* gene. Frameshift transcription of *CDKN2A* is triggered by the aforementioned stress signal, leading to the expression of p14ARF which then inhibits MDM2 [138].

Tumor suppressor protein, retinoblastoma (Rb), is responsible for the repression of gene activity during the transition from G1 to the S phase of the cell cycle [139]. This process is mediated via the formation of a complex containing Rb bound to E2F. Release of Rb from E2F occurs by phosphorylation of Rb via cyclin-dependent kinase complexes CCND1/CDK4/CDK6. Both p21 and another alternative splicing variant of the *CDKN2A* gene, p16INK4A, are cyclin-dependent kinase inhibitors responsible for the binding and inhibition of these kinases. Their function prevents progression of the cell into the S phase [139]. Induced growth arrest mediated by p53 occurs through the transactivation of multiple genes, including the tumor suppressor protein p21 [138].

The large majority of HPV-negative HNSCC cases are a direct result of mutation within the p53/Rb pathway. Suggested rates of 50-80% of HNSCC cases containing a mutation in the *TP53* gene directly, as well as a large number of cases reporting reduced *CDKN2A* or amplified *CCND1*[140-143]. HPV's oncogenic activities are also largely attributed to interference within this pathway by oncoproteins E6 and E7. HPV E6 binds and targets p53 for degradation via ubiquitination, thereby contributing to unstable G1/S phase that would normally follow an apoptotic death following cellular stress [144, 145]. HPV oncoprotein E7 binds and targets Rb for degradation, freeing transcription factor E2F to activate S phase [146, 147]. Free E2F also transcribes *CDKN2A* resulting in the overexpression of p16INK4A, for this reason p16INK4A is used a surrogate marker for HPV status in both cervical and HNSCC [148].

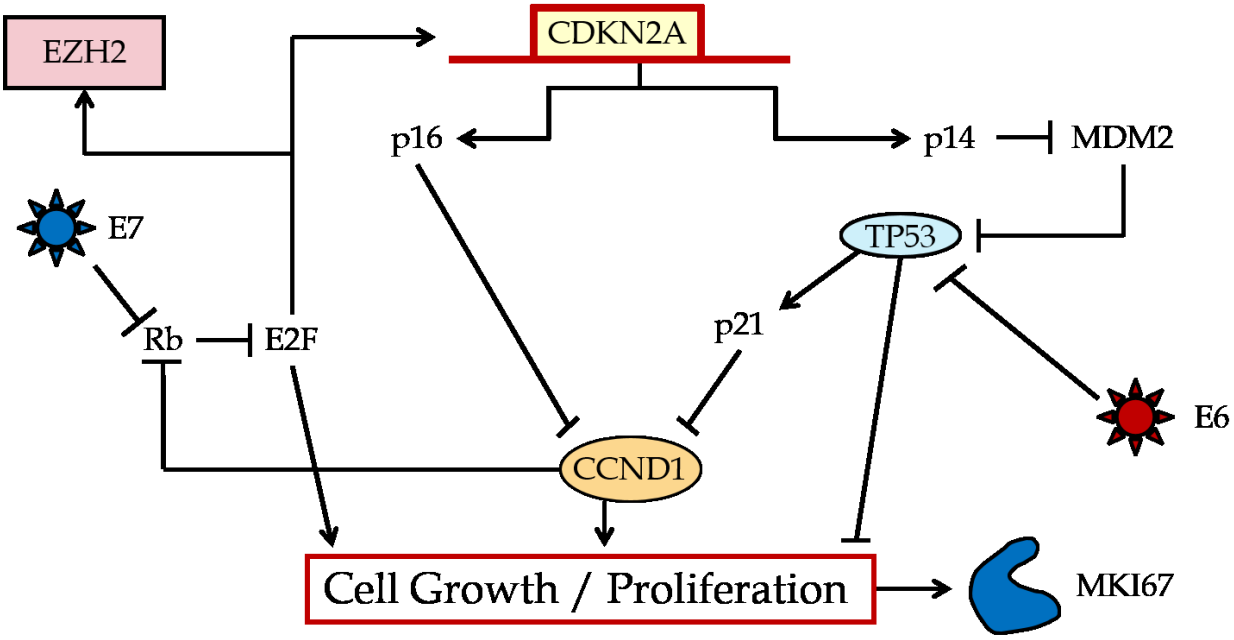

FIG. 2.1 Summary of CDKN2A and TP53 pathways in HNSCC.
Inhibition of Rb by HPV viral oncoprotein E7 results in the release of transcription factor E2F. E2F transcribes tumor suppressor p16. Other downstream targets of E2F become transcribed ultimately leading to increased cell proliferation as well as EZH2 expression. Cell stress signals trigger the transcription of tumor suppressor protein p14 that prevent the degradation of p53 and

lead to apoptosis/cell cycle arrest. Viral oncoprotein E6 inhibits p53 activation, thereby inhibiting apoptotic checkpoints from being activated.

2.3.2 THE PI3K/Akt PATHWAY

Phosphatidylinositol-3-kinases (PI3Ks) are an enzyme family responsible for the regulation of various cell functions. PI3Ks are divided into three different classes: Class I, Class II, and Class III [149]. Of most interest in cancer biology are the Class I, specifically IA, PI3Ks. Class IA subtypes are activated by receptor tyrosine kinases, which are often found to be dysregulated in cancers [150]. Functions of the PI3K family include regulation of cell growth, differentiation, proliferation and survival via the phosphorylation of the 3'OH position of phosphatidylinositols. PI3K phosphorylates phosphatidylinositol 1,4-bisphosphate (PIP2) to form phosphatidylinositol 1,4,5-triphosphate (PIP3) [136]. The tumor suppressor phosphatase and tensin homolog (PTEN) functions antagonistically to the PI3K, converting PIP3 to PIP2 [151]. PIP3 is formed through a catalytic reaction that recruits phosphoinositide-dependent protein-kinase 1 (PDK1) and Akt [152]. Following phosphorylation of Akt by PDK1, Akt then targets serine/threonine protein kinase mammalian target of rapamycin complex (mTOR). mTOR has two structurally distinct complexes: mTORC1 and mTORC2, both of which play an important role in the regulation of cell growth, transcription, motility, and proliferation. The activity of mTORC1 is stimulated by insulin, various growth factors and oxidative stress that stimulates cell growth through the phosphorylation of S6K and 4E-BP1 [153]. mTORC2 phosphorylates and activates Akt [154]. mTOR activation results in an increased level of proteins such as CCND1 and vascular endothelial growth factor (VEGF), thereby stimulating proliferative processes leading to tumorigenicity and malignancy [155].

Genetic aberrations in the PI3K pathway are relatively common in OPSCC, and more commonly found in HPV-positive cancers. The *PI3KCA* gene has been shown to be mutated/amplified in anywhere from 6-20% of HPV-negative patients and over 50% of HPV-positive patients. Physical mutations of *PTEN* have been reported in approximately 7% of HNSCC with

unspecified HPV status, promoting proliferation and cell survival through the utilization of mTOR interactions [156-158].

2.3.3 THE EGFR PATHWAY

EGFR is a member of the ErbB/HER family transmembrane receptor tyrosine kinases. Included within this family are three other members: ErbB2/HER2, ErbB3/HER3, and ErbB4/HER4. These receptor types are involved in gross physiological changes related to cell proliferation, differentiation, migration, and survival [159]. Often ErbB family members are implicated in cancer, be it through their over expression, gene amplification, or mutation resulting in overactivity [160]. EGFR is activated by multiple ligands, yet EGF is often found to be of focus in carcinogenic processes [161]. Upon binding, a large signal transduction cascade is triggered, often including Ras/Raf/MAPK pathways, PI3K/Akt pathways, and JAK/STAT3 pathways [161, 162]. This cascade can lead to gross metabolic changes within a cell. The EGF/EGFR complex formed following binding is also able to translocate to the nucleus and function as a transcription factor. Often targeted is the *CCND1* gene involved in S-phase cell cycle progression [131].

In HNSCC, 10-30% of cancers display EGFR gene amplification, with 42% displaying the mutant phenotype, EGFRvIII [163, 164]. These altered profiles often result in a significant overexpression of EGFR, which has been routinely linked to a poor prognosis in multiple cancer types including HNSCC and lung cancer. Because of this, EGFR is frequently utilized as a prognostic biomarker [160, 164].

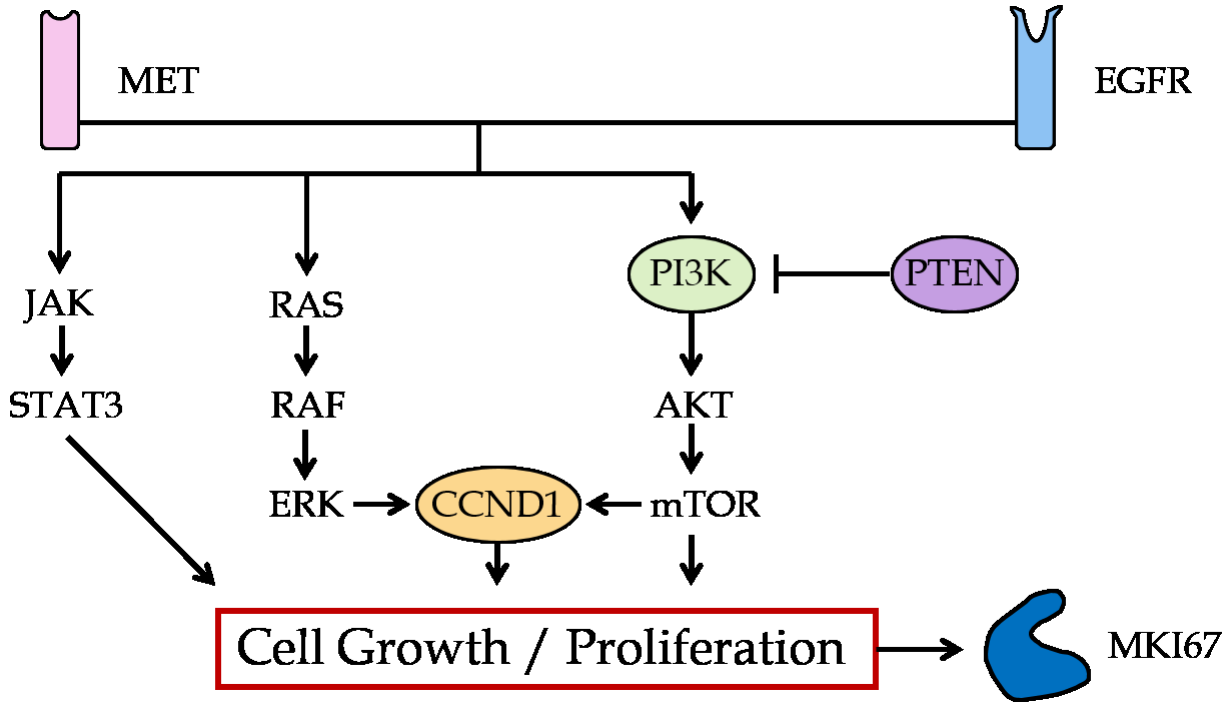

FIG. 2.2 Summary of EGFR and PIK3CA pathways in HNSCC.
Activation of EGFR or MET results in a signal cascade through interconnected pathways including PI3K and mTOR, RAS, and JAK. Pathway activation ultimately leads CCND1 activation and progression through the G1 checkpoint. PI3K is inhibited by PTEN resulting in cell cycle arrest. MKI67 indicates a marker for cell proliferation.

2.3.4 HNSCC STEM CELLS

While still a contested theory, evidence is quickly accumulating regarding the formation of cancer stem cells as an explanation regarding chemoradiotherapy resistance, self-initiation, and propagation of various cancers. The theory describes the heterogeneous nature of tumors with rapidly replicating cells surrounding a small subpopulation of cells capable of initiating and propagating tumorigenesis [165]. These cancer stem cells are often located in hypoxic regions of tumors and are often slowly dividing or senescent, implicating them in therapeutic resistance and recurrence [166]. Resistance mechanisms are described in further detail in Section 2.4. As research into cancer stem cells continues, biomarkers of proposed stem cells are being identified. Two prominently featured biomarkers in HNSCC literature are CD44 and ALDH1A1.

CD44 and its isoforms are transmembrane glycoprotein receptors for hyaluronic acid (HA), extracellular matrix components, and act as cofactors for multiple growth factors and cytokines [167]. This diverse set of interactions has resulted in CD44's involvement in multiple cellular processes; of which include cell adhesion and migration [168]. CD44's role in cancer is that of a cancer stem cell receptor, mediating cell-cell and cell-matrix interactions necessary for malignancy. CD44 expression in HNSCC is one of the first and most reliable stem cell biomarkers for determination of cancer aggressiveness, with higher expression in primary tumor samples to be positively correlated with cancer recurrence [169, 170]. Evidence of CD44's role in malignancy was demonstrated following the blockage of HA binding in a melanoma model of liver metastasis. HA blockage significantly reduced epithelial to mesenchymal transition (EMT) as well as metastasis formation [171]. Animal models utilizing HNSCC xenografts have also shown CD44+ cells to be sufficient to initiate tumorigenesis as well as display self-renewal properties following serial passaging [170]. These self-renewal properties may be a result of interactions with several pathway molecules associated with cell cycle progression including the differential expression of *BMI-1* (discussed in further detail in 2.3.5) as well as complex formation and enhancement of EGFR, leading to signal cascades associated with tumor mitigation downstream of EGFR such as Ras, RhoA, and PI3K [170, 172, 173]. However, CD44 expression as a biomarker alone is not sufficient to identify cancer stem cells. Frequently CD44 expression is seen in both benign and normal epithelia of the head and neck in addition to malignant tissue thereby requiring an additional marker to be paired [174].

Frequently implicated as a HNSCC stem cell marker is ALDH, specifically isoform ALDH1A1, an enzyme involved in the conversion of retinol to retinoic acid [165, 175]. Its expression in HNSCC has been associated with stem cell-like properties, including tumorigenicity, chemoradiotherapy resistance, as well as mediating a role in the EMT of cells [176]. When co-expressed with CD44 in immunodeficient mice, cells additionally displayed self-renewal properties and increased *BMI-1* expression [177]. While the overall mechanism behind ALDH1A1's role in cancer is unclear, signaling pathways involving retinoic acid and retinoid derivatives are theorized to be the primary means of developing tumorigenic and self-renewing properties characterized by cancer stem cells [178]. Retinoid signaling pathways are responsible for many cellular processes including the regulation of gene expression for multiple genes

associated with morphogenesis and development, including *c-MYC, RARβ,* and *CCND1* [178-181]. A genetic positive feedback loop is also created as a result retinoid pathway products, stimulating the expression of *ALDH1* and allowing further catalysis of retinoic acid. This positive feedback loop is the primary theory behind chemoradiotherapy resistance, as ALDH's primary function is the breakdown of potentially harmful aldehydes, like cyclophosphamide-based chemotherapeutics, within the cytosol [182, 183].

Promising biomarkers for HNSCC cancer stem cells are being identified quite frequently, often with aberrant expression in various other cancer types outside of HNSCC. Studies utilizing oral HNSCC observed CD133 expression to develop chemotherapeutic resistance to cisplatin and CD10 to develop resistance to both cisplatin and radiotherapy. Suppression of either CD10 or CD133 saw a reduction in these resistance mechanisms [184, 185]. Cancer stem cells also utilized regular stem cell pathways to preserve stemness and avoid apoptosis, allowing for tumorigenesis. Therefore, proteins such as Oct-4, Nanog, and Notch are frequently associated with cancer stem cells as they all play roles in regulation of cell pleuripotency, differentiation, and self-renewal [186-189]. Aberrant expression of these proteins has also been correlated with resistance mechanisms in HNSCC as well as mediation of EMT in hepatocellular carcinoma [190, 191]. Dysregulated expression of Notch is present in HPV-positive cervical tumors despite the better prognosis associated with HPV status [116, 192]. As theorized by Swanson and colleagues in their review, the primary mechanism behind aberrant Notch expression is due to p53 suppression by HPV oncoprotein E6. Typically p53 inhibits the Notch pathway, but becomes activated upon infection with HPV and increases the likelihood of cancer stem cell propagation and malignancy [186, 193].

2.3.5 DNA METHYLATION

The most well documented epigenetic event occurs directly at the level of DNA, with 5' methylation of CpG residues, primarily at gene promoter regions. In OPSCC, distinct host methylation profiles can be witnessed in HPV-positive cancers when compared to HPV-negative cancers [126, 194]. This distinction has been described as nearing 3 times as much differentiation

in methylation profiles between HPV-positive and HPV-negative disease when compared to adjacent somatic cells [195]. HPV-positive cancers have shown higher levels of methylation in specific regions of the genome (promoters, genic, and LINE-1), while HPV-negative cancers show a much higher degree of genome-wide hypomethylation. This evidence suggests HPV-negative cancers to be far less genomically stable relative to their HPV-positive counterparts. This genomic instability, in turn, leads to widespread deregulation of cellular processes characteristic of aggressive tumors [23, 126, 196].

One potential mechanism to account for the altered DNA methylation profiles is through DNMT dysregulation. HPV-positive HNSCCs have shown increased expression in DNMT1 and DNMT3a, a pattern also shared by cervical cancers. This suggests a common mechanism of carcinogenesis by HPV [126, 197, 198]. This process is known to occur through HPV viral oncoproteins E6 and E7. As mentioned previously, HPV E6 causes the inhibition of p53. Anayannis and colleagues suggested this inhibition allows for the overexpression of DNMT1 by activation of transcription factor Sp1 [34, 199-201]. The more notable interaction is seen by HPV E7 as it has been shown to directly interact with the tumor suppressor Rb, allowing the release of E2F from its protein complex to promote the transcription of DNMT1 [202]. E7 has also been shown to directly interact with DNMT1 *in vitro*; however, functional implications require further investigation [203].

Low expression of *CDKN2A* is seen in HPV-negative cancers, while high expression is found in HPV-associated disease [204]. Schlecht and colleagues has identified 4 *CDKN2A* loci downstream of the p16INK4A and p14ARF transcription start sites that are frequently hypermethylated in HPV-positive OPSCC, suggesting an additional mechanism of p16 overexpression in HPV-positive OPSCC. Their study also identified multiple Sp1 binding sites within the *CDKN2A* locus, further supporting the role of Sp1 in carcinogenesis [197].

The oncogene *FOXM1* has been found to have aberrant expression in multiple cancers including esophageal SCC [12, 24]. Teh and colleagues (2009) first identified *FOXM1* role in the regulation of HELLS, a SNF2/helicase involved in DNA methylation, and later performed a knockdown experiment. Their research showed upregulation of *FOXM1* to emulate a comparable methylation pattern as head and neck SCC, suppressing the tumor suppressor gene *CDKN2A* via

hypermethylation [24, 205]. They later performed a knockdown of HELLS that restored *CDKN2A* mRNA expression and downregulated DNMT1 and DNMT3b expression [22]. This evidence makes *FOXM1* a good candidate as a potential biomarker in early cancer screening, prognostic, or potentially future chemotherapeutic target.

2.3.6 HISTONE MODIFICATION

Polycomb group (PcG) and trithorax (trxG) genes are believed to serve in the preservation and maintenance of gene expression programs that control cellular differentiation in tissues of complex organisms, with roles as gene repressors and activators, respectively [206]. Mutations of PcG these genes in vertebrates results in altered body plan development, suggesting a role in homoeotic gene regulation; however, PcG genes have shown roles in multiple cellular processes outside of differentiation including, chromosome X-inactivation, cell fate, and cell senescence [207-210]. PcG proteins have been found to form two chromatin-associating complexes: the Polycomb Repressive Complex 1 (PRC1) and the Polycomb Repressive Complex 2 (PRC2) [211].

B-cell–specific Moloney murine leukemia virus integration site 1 (BMI1) is a central component of the PRC1 and its overexpression has been highly associated with carcinogenesis. BMI1 functions by stabilizing H3K27me3 through the monoquitinylation of histone H2A at lysine 119 (H2AK119ub1) and in doing so prevents the initiation of transcription via prohibition of Pol II occupancy at the tagged site [212-214]. Huber and colleagues have shown BMI1 expression to play a potential role as a significant prognostic biomarker of OPSCC, as its aberrant expression in conjunction with p16INK4A silencing is negatively correlated with recurrence-free survival in OPSCC [212].

A novel study by Biron and colleagues had shown the differences in histone methylation profiles in OPSCC based on HPV status. Observed were overall increased levels of monomethylated histone H4 at lysine 20 (H4K20me1) and reduced levels of H4 trimethylated lysine 20 (H4K20me3) in HPV-positive cancers, while HPV-negative tumors had reduced levels of H4K20me1 and H3K27me3 with increased levels of H4K20me3 [215]. Histone H4 methylation

is catalyzed by multiple HMT's including SETD8, SUV4-20H1, and SUV4-20H2. [216-219]. The role of H4 methylation in multicellular organisms appears to be that of development and cell viability, with knockout studies in *Setd8* producing embryos that do not exceed the 8-cell stage of their development [220]. While no formal information regarding SETD8, SUV4-20H1, and SUV4-20H2's role in OPSCC is published at time of writing, the evidence brought forth by Biron and colleagues study would suggest their potential role as an OPSCC biomarker.

2.3.6.1 EZH2

A recurring histone modifier in cancer literature as well as the primary focus of this study is histone methyltransferase EZH2, a catalytic subunit within the PRC2. EZH2 catalyzes the trimethylation of lysine 27 on histone 3 (H3K27me3) and, with the aid of PRC1, appears to regulate transcriptional processes involved with cell proliferation and cell-cycle progression [221]. EZH2's catalytic activity requires the presence of at least two other subunits of the PRC2: embryonic ectoderm development (EED) and suppressor of zeste 12 (SUZ12) [222-224]. Two additional subunits, the histone-binding protein RbAP46/48 and the Zinc finger protein AEBP2 together further activate EZH2's catalytic activity [225]. The catalytic subunit of the PRC2 is not limited to EZH2 alone. EZH1, a paralog of EZH2, has been shown to control several overlapping target genes of EZH2 but does so without the cofactor S-adenosyl methionine (SAM), albeit weakly [226]. Expression differences between catalytic proteins may provide explanations as to their roles in maintaining the epigenome. EZH1 expression is often found in dividing or differentiating cells and tissues, whereas EZH2 is primarily expressed in proliferating tissues [226, 227]. Purposed by Völkel and collegues (2015), the mechanistic and expressional differences between PRC2 complexes suggest EZH1 may be partly responsible for the restoration of H3K27me3 profile following demethylation or histone exchange activity, while EZH2 is responsible for the establishment of H3K27me3 repressive marks [228].

Dysregulated EZH2 expression is often correlated with a malignant phenotype [228]. The overexpression of EZH2 is typically found in solid tumors; yet, activating or inactivating mutations are commonly found in hematologic malignancies and pediatric gliomas [229-231].

Solid tumors displaying overexpression of EZH2 are frequently found to display an increased malignancy potential and poor clinical prognosis, with its implication in aggressive HPV-positive OPSCC variants as well [132, 133, 228]. HPV status and EZH2 overexpression are closely related, as *EZH2* is a downstream target of E7 via the release of transcription factor E2F from Rb [232]. As expected, HPV-positive OPSCC have increased levels of H3K27me3 [42]. As proposed by Holland et. al. (2008), p53 suppression via E6 may also provide a mechanism for EZH2 overexpression, with *EZH2* promotor repression being a direct result of p53 activation [232, 233].

Although the Rb-E2F pathway is frequently implicated in many tumors outside of HNSCC including breast, bladder, and lung cancers, the overexpression of EZH2 may be the result of several different transcriptional signals [227, 234, 235]. ELK1 and its related pathway, which has commonly been associated with many cancers, has been found to be responsible for EZH2 overexpression in HER2-overexpressing and the triple-negative (estrogen receptor-negative, progesterone receptor-negative, and HER2-negative) breast cancers [236]. Transcription factors MYC and ETS have also been shown to directly induce transcription of EZH2 in prostate cancers, while NF-YA, STAT3, ANCCA/ATAD2, EWS/FLI1, and mutant BRAF (V600E) have all been shown to regulate EZH2 expression in various other cancers including ovarian, colorectal, breast, sarcoma, and melanoma (respectively); however, their mechanism of regulation has yet to be determined [228, 237-242]. Another interesting regulator of EZH2 is through a hypoxic tumor microenvironment (described in further detail within Section 2.4.2), specifically through transcription factor HIF1α, which binds and activates a specific sequence found within the EZH2 promoter to enhance tumor proliferation [243].

Commonly documented EZH2 mutations associated with cancer can be located within the catalytic C-terminal SET domain (residues 520-746), responsible for the H3K27 methyltransferase function [228, 244]. Frequently seen in lymphomas is the Y641F mutant, a tyrosine replacement within the SET domain that results in EZH2 overactivation [229]. When utilized in a mouse model, lymphocytes containing the Y641F mutants when combined with Eμ-Myc expression displayed increased H3K27me3 in spleen cells [245]. Comparable mutations within the SET domain, like EZH2-A677 and EZH2-A687, are also frequently seen in

lymphomas and share this hypermethylation at H3K27 [246-248]. Loss of function mutations can also present with malignancy in myeloid disorders, namely pediatric cancers, with EZH2 deletions enough to instigate myelodysplastic syndrome in a mouse model [249-251]. These results would suggest the potential role of EZH2 as a tumor suppressor, in addition to its known role as an oncogene.

Within normal cells, EZH2 has been shown to regulate transcriptional activity via promotor silencing of multiple genes, including those responsible for morphogenesis [252] and cell fate responses following DNA damage. [253]. Aberrant EZH2 activity resulting in silencing of genes within the latter category, as well as related tumor suppressor genes, is generally accepted to be the primary mechanism of oncogenesis by EZH2 [254, 255]. Known tumor suppressor target genes of note include *CDKN1A*, *CDKN2A*, *CDKN2B*, *TP53*, *RARβ, Rassf1a* and *PTEN* [256-261]. However, PRC2-mediated gene regulation appears to be widespread across the genome, with H3K27me3 associated with the majority of non-transcribed CpG islands [262]. This in theory could place PRC2 involvement in both an oncogenic or tumor suppressive role, depending on which genes are being silenced. Studies have confirmed this dual role theory of PRC2 in cancers, with PRC2 activation displaying anti-tumorigenic properties [263, 264].

EZH2 appears to have a specific role in gene regulation. The histone H1 protein, has been shown to be a key factor in the preferential binding of EZH2 to specific substrates [265]. An additional method of targeted gene regulation by EZH2 may be through its association with DNMTs. Within the PRC2 complex, EZH2 has shown to directly associate with DNMT1, DNMT3a, and DNMT3b *in vivo* [266]. It should also be noted that PRC1 is able to recruit and bind DMNT1 and DNMT3b as well [267]. Further support for this is seen through the use of chromatin immunoprecipitation and bisulfite sequencing analysis, where binding activity of DNMTs to EZH2-repressed gene promoters is dependent on the presence of EZH2 [266]. However, while EZH2 has been shown to recruit DNMT3a *in vivo*, the *de novo* functionality of DNMT3a is not directly activated by this process [268].

There are several modifications that can regulate EZH2 function within the PRC2 complex, which suggest EZH2 acts mainly through gene silencing mechanisms . AKT1, a serine/threonine kinase that plays a key role in several signalling pathways, has been shown to phosphorylate

EZH2 at serine 21 [269-271]. This modification results in EZH2's conversion from gene silencer to activator. This modification in castration-resistant prostate cancers as well as glioblastomas does not require the other PRC2 subunits to utilize EZH2 methyltransferase activities [269, 270]. S21 phosphorylation studies suggests EZH2 interacts with androgen receptors in castration-resistant prostate cancers to interact with multiple target genes and enhancement of transcription factor STAT3 via lysine 180 trimethylation in glioblastoma [269, 270]. Several EZH2 threonine residues have also demonstrated phosphorylation; however, depending on which location the modification is located, its effect on EZH2 activity can vary dramatically. CDK1 and CDK2 have been found to phosphorylate these EZH2 threonine residues at T350 and T492, with T350 phosphorylation promoting EZH2 recruitment at chromatin through interaction with lncRNAs, namely HOTAIR (HOTAIR discussed in further detail in Section 2.3.7) [272-274]. Gene regulation by EZH2 may also be through coordination with lncRNAs, as recent findings found that PcG proteins work with non-coding RNAs to silence target genes [258, 275, 276]. T492 phosphorylation, in turn, disrupts EZH2 interaction with other PRC2 subunits and resulting in the disruption of methyltransferase activity [274]. Interestingly, an additional study by Wu and Zhang (2011) demonstrated phosphorylated EZH2 at residues T350 and T492 demonstrated a much shorter half-life relative to unmodified EZH2 [277]. This would suggest a potential method of cell cycle regulation via CDK1-mediated EZH2 phosphorylation.

EZH2 is thought to have enzymatic activity independent of the other PRC2 subunits. In breast cancers, EZH2 acts as a transcriptional activator of several different target proteins that vary depending on cell type [228]. In estrogen receptor positive MCF-7 cells, EZH2 binds to the estrogen receptor α and β-catenin to functionally enhance Wnt signalling pathways [278]. The downstream targets of this complex include the transcription of *CCND1* as well as *MYC*, phenotypically promoting cell cycle progression [278]. In colon cancers, EZH2 couples with β-catenin to form the PAF-EZH2-β-catenin complex to activate Wnt target genes [279]. Estrogen receptor-negative MDA-MB-231 breast cancer cells display EZH2 interactions with RELA and RELB to activate NF-κB target genes, including *TNF* and *IL6* [280]. This dynamic nature of EZH2 suggests its highly complex nature, with both the potential to transcriptionally regulate genes independently of the PRC2 as well within the PRC2 via its methyltransferase activity.

2.3.7 SMALL AND NON-CODING RNA

Our current knowledge of the ncRNAs role in carcinogenesis is relatively limited, largely due to the novelty of the molecules discovery. For the purposes of this section, the field of study will be expanded slightly to include ncRNAs implicated in other head and neck cancers, in addition to those found in OPSCC.

HPV status in HNSCC is associated with distinct epigenetic profiles and clinical outcomes. A comparison of epigenetic distinctions in HPV-positive and HPV-negative cancers is well outlined in a review by Lajer and colleagues, who compared epigenetic profiles of HPV-positive cervical and head and neck cancers. Their study identified a significant overlap in several miR clusters. These included miR-15a, miR-16, miR-195, miR-497 family, miR-143, miR-145 and the miR-106-363 cluster [281].

Sethi and colleagues (2014) outlined a comprehensive list of multiple miRs with aberrant expression patterns in head and neck cancers in addition to those mentioned by Lajer and colleagues. When comparing HPV-positive to HPV-negative OPSCC miR-150, miR-146 family, Let-7 family, miR-625, miR-155, miR-15 family, miR-29a, miR-125 family, miR-26b, miR-342-3p, miR-768-3p, miR-34a, miR-596, miR-598, miR-33, miR-9 were found to be upregulated. miR-223, miR-31, miR-193b, miR-1180, miR-99 family, miR-877, miR-744, miR-423-5p, miR-324-5p, miR-1275, miR-200c, miR-517, miR-101, miR-409 family, miR-126, miR-1201, miR-199b-5p, miR-381, miR-433, miR-432, miR-379, miR-127-3p were downregulated in addition to those described above [282]. This draws the conclusion of distinct miR expression as a result of HPV-associated disease. This concept is further enforced by the direct interaction of some miRs, such as miR-15 and miR-16, with viral E6 and E7 [283].

In addition to those described above, several aberrant patterns were described when OPSCCs were compared to normal tissues. These included several from the miR-106b-25 cluster, miR-193a, Let7i, several from the miR-17-92 cluster, miR-27a, miR-142-3, miR-210, miR-29 family, miR-130b, miR-205, miR-422b, miR-23b, miR-142-3p, miR-146c, miR-181 family, miR-491, miR-455, miR-130b, miR-221, miR-7083, miR-7, miR-34b, miR-182, miR-185, miR-93, Let-7

family, miR-107, miR-103, miR-221 were upregulated. miR-7029, miR-23b, miR-140-3p, miR-375, miR-494, miR-205, miR-133a, miR-1, Let-7 family, miR-26a, miR-127, miR-365, miR-30c, miR-100, miR-140, miR-10a, miR-375 appeared to be downregulated [282]. A systematic meta-analysis performed by Jamali and colleagues showed frequent overlap of results to those found by Sethi and colleagues [282, 284]. Of these miRs, four were directly implicated in OPSCC: miR-363, miR-210, Let-7d, and miR375 [284].

Several miRs indicated above have been associated in multiple cancer variants. Some have greater potential as prognostic biomarkers due to their targeting tumor suppressor genes or key tumor suppressor proteins. Those that have the greatest potential include the miR-17-92 and miR-106b-25 clusters, shown to target *c-MYC* and p21, respectively [285, 286]. Individual miRs include upregulated levels of miR-21, miR-205, and miR-181; with miR-21 and miR-205 targeting *PTEN* and miR-181 targeting *TCL-1* [287-289]. Downregulated levels of Let-7 have also been shown to target *RAS* [97].

One miR not acknowledged in literature, but which provides great interest, is miR-101. The aberrant downregulation of miR-101 has been involved in multiple cancers and has shown to mediate the overexpression of EZH2 [290, 291]. The restoration of miR-101 via DNMT3a inhibition has also been shown to suppress lung tumorigenesis [291]. As seen with both DNMT3a and EZH2 overexpression in HPV-positive OPSCC, miR-101 may have a direct role in carcinogenesis [34].

Of the ncRNAs present within head and neck cancer literature, lncRNAs mirror the scarcity of miR counterparts. However, one lncRNA in particular, HOTAIR, has shown great promise as a biomarker. HOTAIR is a non-coding RNA transcript of 2.2 kb transcribed from the HOXC locus to transcriptionally silence HOXD [292, 293]. Interactions of HOTAIR have shown the 5`domain to bind to the PRC2 complex as well the 3`domain binding the histone demethylase KDM6A. These interactions potentially suggest methods of carcinogenesis, as its overexpression has been demonstrated in multiple cancer types including esophageal, nasopharyngeal, breast, pancreatic, and colorectal cancers [46, 292-300]. In addition, overexpression of HOTAIR has been associated with an overall poor clinical prognosis, demonstrating increased lymph node metastasis and resistance to apoptosis [158]. At the time of writing, HOTAIRs direct linkage to

OPSCC has not been performed and requires further study. Other lncRNAs of interest are FTH1P3, PDIA3F and GTF2IRD2P1, as they have been associated with the progression and metastasis of oral SCC via the targeting of multiple tumor regulator genes [301]. SOX2OT alternative splicing patterns and nc886 (pre-miR-886) have also shown potential roles in esophageal cancers [302, 303].

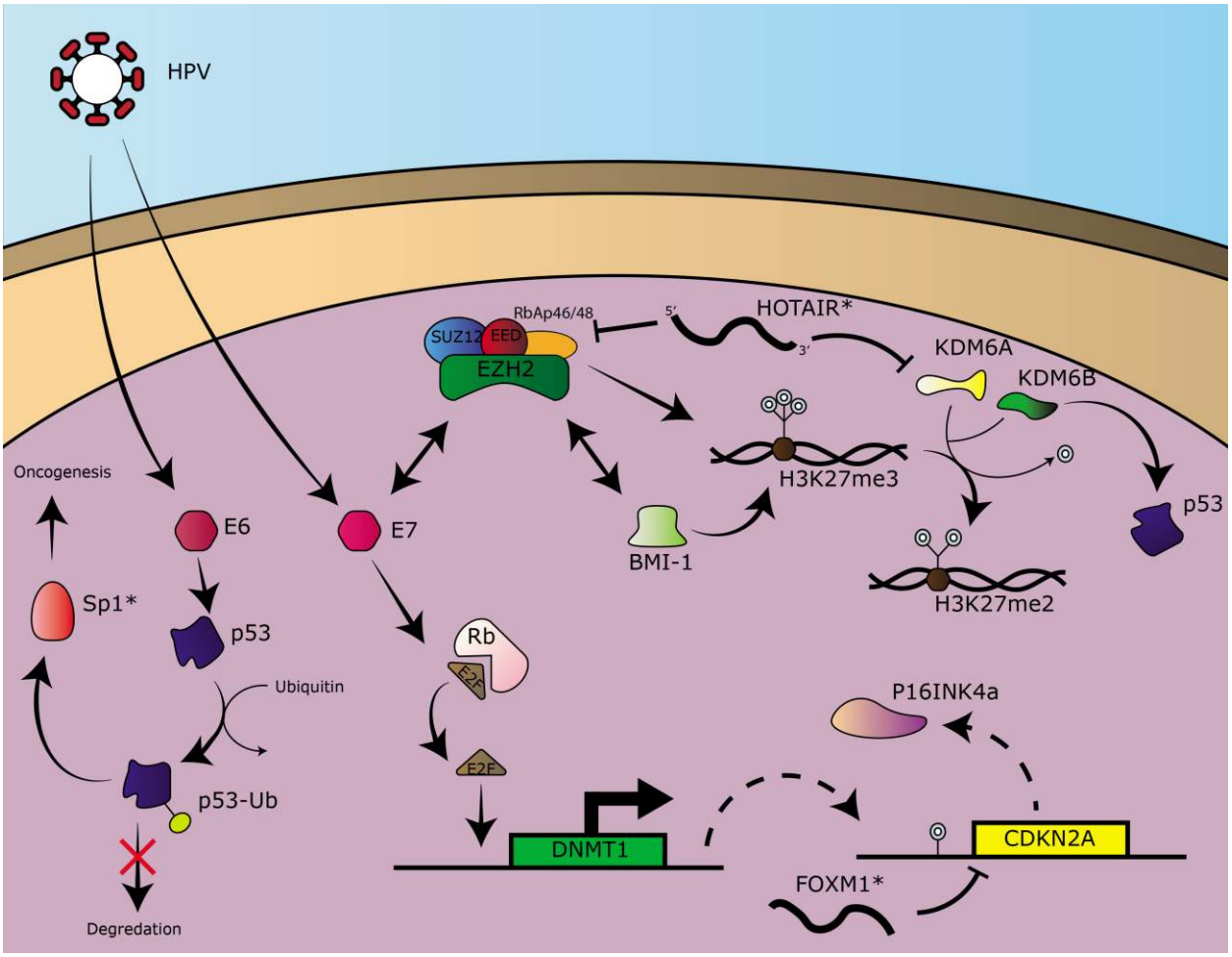

FIG. 2.3 Summary of epigenetic pathways involved in OPSCC.

Oncogenic human papillomavirus integrated into the human genome, resulting in the expression of HPV-associated proteins E6 and E7. This results in alterations of p53, Rb and Polycomb Repressive Complex 2 (shown here including EZH2, SUZ12, EED and RbAp46/48) related pathways with downstream epigenetic deregulation in OPSCC. Overexpression of P16INK4a

occurs as a result of loss of Rb and is used as clinical surrogate marker for HPV-positive OPSCC. *FOXM1 and HOTAIR are presumed to have a role in OPSCC based on studies in OCSCC. *Image from [304]*

2.4 CURRENT THERAPEUTIC MODALITES

The molecular characteristics of OPSCC are heterogeneous in nature and as a result there is a great impact on clinical prognosis and interventional strategy. Two genes are frequently implemented in tumor differentiation and clinical prognosis; *TP53,* encoding for p53 and *CDKN2A,* encoding for p16INK4A. Overall implications of these pathways in head and neck cancers display approximately 80% p53 pathway aberrations, and nearly 94% *CCND1* or *CDKN2A* aberrations [305, 306]. Four molecular subtypes of HNSCC have been identified through the advent of high throughput genetic technologies: the basal subtype, associated with *TP63* overexpression; classical subtype, with *KEAP1* and *NFE2L2* mutations; mesenchymal, with *FGR1* and *FGR2* mutations; and atypical, described with frequent mutations in the *PIK3CA* gene and HPV status [110, 305].

HPV status is an established prognostic factor in OPSCC, repeatedly showing higher survival rates for HPV-positive patients relative to HPV-negative patients. Regardless of treatment protocols utilized, HPV-positive tumors have shown a minimum of a 50% reduction in disease progression and death due to cancer than HPV-negative patients [116, 307]. The improved rates seen in HPV-positive patients have been attributed to multiple factors, including increased loco-regional control, reduced rates of recurrence, and reduced rates of prognostic factors associated with poor outcomes [116]. Improved survival outcomes following surgical resection have also been shown in HPV-positive tumors [308]. Current practices in establishing HPV positivity is through indirect measure of p16INK4A content in tumor histology. While still providing a high degree of correlation, p16 INK4A only plays a surrogate role for HPV status and its overexpression may not always be present in a sample [148]. Fortunately, efforts are being made to more accurately determine infection status. Of which includes the direct measure of HPV16

E6 and E7 transcripts within an oral swab using droplet digital polymerase chain reaction (ddPCR) [309].

Current therapeutic practices for treatment of HNSCC will vary on a case-to-case basis, with TNM staging classification playing a significant role in treatment protocol. Treatments will often utilize combination therapies including surgical intervention, radiotherapy, and chemotherapy [310].

2.4.1 RADIATION THERAPY

Radiotherapy (RT) utilized in the treatment of HNSCC is most commonly in the form of 2-3 photon beam arrangements directed from a linear accelerator [310]. These arrangements are aided through the use of volumetric imaging like 3D computed tomographic (CT)-based imaging to avoid as much radiation exposure to surrounding normal tissues [310]. Fluctuations in radiation intensity of treatment beams is also implemented to ensure lower doses to surrounding tissue. Often CT-imaging techniques will be supplemented with magnetic resonance imaging (MRI) for greater site detail. Standard radiation dose fractionation involves once daily treatment ranging from 1.8 to 2 Gy 5 days a week for 6 weeks [310]. However multiple clinical trials have deviated from this practice by utilizing altered fractionation schedules, including delivery twice a day with a six-hour separation between doses, as well as treatments extending to 7 days per week and combinations of the two [311-314]. These altered schedule changes have shown minor benefit (3.4% survival benefit over 5 years), but significantly higher levels of acute toxicity [315]. Acute effects of radiotherapy in HNSCC include increased inflammation and pain in the target site, with significant weight loss being a secondary side effect of pain while eating or swallowing. Mucosal imbalances in pH and increased mucosal viscosity can also occur, resulting in an increased chance of infection and dysphagia [316]. Fortunately, the majority of these effects are resolved within 12 weeks post treatment, with some chronic effects lingering post-treatment. Chronic effects most commonly being xerostomia, or dryness of the mouth as a result of reduced mucous production by salivary glands [317]. Future surgical practices have demonstrated a method of resolving xerostomia post-radiotherapy. In a breakthrough technique

developed by Seikaly and colleagues, surgical relocation of the submandibular gland outside of the radiotherapy target site prior to radiotherapy has shown dramatic reduction in xerostomia [318, 319].

2.4.2 CHEMOTHERAPEUTICS FOR USE IN SOLID TUMORS

Synchronous treatment of combined radiotherapy and chemotherapy is generally favored over an alternating modality as it is theoretically more favorable at combating accelerated repopulation of tumor cells. This of course increases the risk of acute toxicity, but its implementation in multiple clinical trials has demonstrated significant improvement in overall patient survival [320, 321].

5-fluorouracil (5-FU) has been utilized in conjunction with radiotherapy more frequently than any other chemotherapeutic agent since its initial use in oral squamous cell carcinoma in 1976 [321, 322]. 5-FU has antitumoral effects through both DNA-directed and RNA-directed mechanisms. Mechanistically 5-FU inhibits thymidalate synthase, a key enzyme in the early stages of DNA biosynthesis, which ultimately leads to cell death through additive DNA damage effects induced by radiotherapy once cells enter into S phase of their life cycle. Targeting cells in S phase is also believed to be one of the primary mechanism of radiosensitization by 5-FU, as cells in S phase frequently display radioresistant characteristics [323]. 5-FU is also shown to incorporate into DNA and RNA in human tissues. This leads to DNA strand breaks mediated by excision by uracil-DNA-glycosylase [324]. However, there is no apparent relationship between antitumoral efficacy and incorporation [325].

Cisplatin and is an additional chemotherapeutic often used in combination with radiotherapy as it has known radiosensitization properties [326]. Cisplatin's antitumoral properties have shown to occur through multiple mechanisms that are often enhanced through treatment with radiotherapy. These include the formation of toxic platinum intermediates that enhance oxidative stress [327], increased platinum uptake by cells [328], as well as inhibition of DNA repair mechanisms [329]. Its best-known interaction is through the formation of covalent bonds with purine DNA bases and its platinum compound, resulting in disruptions during the synthesis phases of a cells life

cycle [330, 331]. This covalent interaction is believed the primary mechanism behind its cytotoxic side effects [332], including nephrotoxcicity [333], hepatotoxicity [334, 335], and cardiotoxicity [336]. Both tumor resistance and these severe side effects have spurred the synthesis of multiple platinum-based analogs. Of the thousands developed, approximately 13 are currently at the stage of clinical trials [337]. One analog in particular, carboplatin, is gaining ground as a superior alternative chemotherapeutic for use in ovarian cancer, lung, and HNSCC's [337]. The clearest benefit to carboplatin is its reduced side effects, in particular its non-nephrotoxic side effects, as well as its increased retention half-life. Unfortunately, this comes at a cost of decreased potency relative to cisplatin, and myelo-suppressive effects [338].

One of the largest hurdles in the development and implementation of chemotherapeutics for solid tumors is the ability of the agent to be specifically target and penetrate tumor cells. If anticancer drugs are unable to access regenerative cells within the tumor core (such as cancer stem cells), a drugs efficacy is severely limited [339]. For a chemotherapeutic to be curative, it must be able to access and destroy every cancer cell, as the survival of one regenerative cell is sufficient for tumor recurrence [340]. This need for penetrative effect is also exemplified by the physiology of solid tumors. Often there will be poor vasculature organization surrounding tumors, which would naturally limit drug delivery to tumor cores. Poor vasculature also results in hypoxic tumor cores, often seen by increased metabolic product accumulation such as lactic and carbonic acid [341, 342]. These hypoxic regions have shown evidence of resistance to radiotherapy and are capable of repopulating following radiotherapy [339]. Anticancer drugs are potentially affected by these hypoxic regions, as conventional chemotherapies target rapidly dividing cells and hypoxic cells are generally less metabolically active, displaying low to no proliferation [343, 344]. Resistance mechanisms are not limited to hypoxia as genetic mutation and epigenetic variation are associated with resistant phenotypes [3, 339]. For these reasons, targeted therapies designed to sensitize resistant tumor cells to chemoradiotherapies are readily sought after.

There are several targeted therapies currently in the clinical trial stages for use in HNSCC. The majority of these inhibitors target pathways discussed earlier in section 2.3. These include, but are not limited to: VEGF, EGFR, PI3K, mTOR, AKT, c-Met, ATR, and PARP inhibitors [321]. The most widely studied of these targeted therapies are inhibitors of EGFR which are currently

in phase II and III clinical trails (gefitinib and cetuximab, respectively) for combined use with surgery and radiotherapy in HNSCC, but are now commonly used in clinical practice [345, 346]. EGFR inhibitors are separated into two classes: monoclonal antibodies (eg. cetuximab) and small molecule inhibitors (eg. gefitinib) with both displaying radiosensitization potential comparable to that of current antitumoral agents. EGFR inhibitors are thought to reduce systemic toxicities typically associated with agents like 5-FU or cisplatin [310, 345, 346]. However, one phase II trial utilizing cetuximab contradicts this claim, displaying higher acute toxicity rates relative to cisplatin in their cetuximab treatment arm [347]. Current trials are looking at the curative potential of combined EGFR inhibitors with other antitumoral agents [310].

2.4.3 STAGING AND INTERVENTION

The American Joint Committee on Cancer (AJCC) TNM staging classification is currently the accepted standard in defining tumor extent and progression. This system is anatomically based and is important for assessing prognosis, planning treatment, and evaluating treatment outcomes Categories are utilized to create anatomic stage groups (I to IV) that stratify for survival outcome [348].

The TNM prognostic staging system implemented by the AJCC remains controversial with its utilization on head and neck cancer patients. An analysis conducted by Ang and colleagues (2010) demonstrated tumor HPV status and smoking history were more reliable with regard to determining patient prognosis than AJCC TNM staging practices utilized [349]. This was further confirmed by retrospective analyses performed by Dahlstrom and colleagues (2013) and Huang and colleagues (2015) demonstrating TNM staging to be inaccurate in determining head and neck cancer patient survival and outcomes [350, 351].

Extracapsular extension (ECE) is a well-known marker for overall poor prognosis in surgical resection patients; including loco-regional recurrence, distant metastases, and reduced survival in head and neck cancers [116]. Current treatment protocols largely dictate the use of adjuvant-based cisplatin chemotherapeutics in conjunction with surgical resection. Adjuvant-based cisplatin therapies have proved to be more effective than radiotherapy in patients with high-risk

features such as ECE [352]. However, current practices do not account for gross tumor heterogeneity associated with head and neck cancer, namely HPV status [353].

Revised AJCC TNM staging classifications for HNSCC were developed and global implementation began January 2017. While not limited to head and neck cancers, the most dramatic changes were seen in the clinical staging of OPSCC. The use of p16 immunohistochemistry, the surrogate marker of HPV status, from a tumor sample is utilized to allow for not only more accurate staging, but determination of less invasive therapeutic interventions [354].

2.4.4 CURRENT AND FUTURE EPIGENETIC CHEMOTHERAPEUTICS

Aberrant events within the epigenome are suggested to occur more readily than structural gene modification through mutation. Given the reversible nature of epigenetic modifications, they have become an attractive target for cancer prevention and therapeutic intervention [4, 26, 355]. Epigenetic chemotherapeutics currently in use are classified into two primary classes; HDAC inhibitors and DNMT inhibitors [4, 355]. These classes are likely to expand as our knowledge of epigenetics advances and further chemotherapeutics are developed and tested. There are currently five USFDA-approved epigenetic chemotherapeutics on the market. Two are DNMT inhibitors; 5-acactidine (Vidaza) and 5-aza-2'-deoxycitidine (Decitabine). Three are HDAC inhibitors; suberoylanilide hydroxamic acid (Vorinostat), F-228 (Romidepsin), and LAQ-824 (Farydak) [4, 355-358]. Current epigenetic chemotherapeutics in clinical trials or approved by the USFDA are summarized in Table 2**.**

Both DMNT inhibitors, Vidaza and Decitabine, are the only epidrugs that have been approved for the treatment of patients with acute myeloid leukemia and myelodyplastic syndrome [359]. Vidaza and Decitabine are nucleoside analogs of cytosine modified in position 5 of their pyrimidine ring [360]. Upon exposure, Vizdaza is incorporated into RNA and Decitabine is incorporated into DNA where they disrupt interactions between DNMTs and DNA. During this process, a covalent bond is formed with DNMT, triggering a DNA damage signal and targeting the DNMT for degradation [361, 362]. When utilized in clinical practice, their applicability

encountered major limitations. These are characterized by poor bioavailability, poor activity with solid tumors, severe toxic effects, instability in physiological media, and gross non-specific changes to the epigenome of both normal and cancer cells [363, 364]. Fortunately, several new specific inhibitors are under development. Of these are MG98, small molecule RG108, nucleoside analog Zebularine, and arsenic trioxide. These inhibitors have shown increased specificity, chemical stability, increased bioavailability, and lower cytotoxic effects relative to their older counterparts [363, 365-369].

HDAC inhibitors are regularly divided into four separate groups based on their chemical structure. These are hydroximates, aliphatic acids, cyclic peptides, and benzamides. Within the hydroximate class are two USFDA approved agents, Vorinostat and the newly approved Farydak, as well as JNJ-26481585 (Quisinostat) currently in clinical trials [30, 355-358]. Aliphatic acids contain three agents currently in clinical trials; valproic acid, phenylbutyrate, and Belinostat [355]. Cyclic peptides contain the USFDA approved Romidepsin and benzamides contain three agents in the clinical trial stages; MS-275 (entinostat), MGCD-0103 (Mocetinostat), CI-994 [4, 355, 357]. The mechanisms of HDAC inhibitors are not fully understood but are thought to alter gene expression via regulation at both epigenetic and post-translational modification levels [370, 371]. Evidence also suggests HDAC inhibition may alter tumor progression through the inhibition of tumor-mediated angiogenesis [371]. HDAC inhibitors are well tolerated relative to other epigenetic chemotherapeutics. However, they still display poor activity against solid tumors when utilized on their own. Suggested application to combat these shortfalls is specific timing of administration in conjunction with current chemotherapeutics [372-374].

The use of miRs as potential targets for chemotherapeutics is still in its infancy. Multiple studies have shown the significant effects of upregulation and downregulation of specific miRs on cancer. Of note is the study described in 1.3.1, describing miR-21s direct role in tumorigenesis following upregulation and reduced tumor survival and progression following its downregulation [101]. Formal usage as a chemotherapeutic epidrug is not present at time of writing.

Histone methyltransferases undergoing current testing are not limited in number, but their designed targets currently are. One histone methyltransferase inhibitor currently in the clinical trial stage is EPZ-5676 (Pinometostat), an inhibitor of histone 3 lysine 79 methyltransferase DOT1L [375]. While still requiring further study for conclusive data, initial studies suggest its efficacy and tolerance in leukemias [375]. The majority of histone methyltransferase inhibitors currently available target EZH2, most likely due to the enzymes continued role as a molecular target and biomarker in multiple cancers. Of these include UNC1999, ZLD1039 and PF-06726304 acetate, small molecule inhibitors of EZH2 [376-379]. Our study focuses on three histone methyltransferase inhibitors of EZH2 all of which are currently in the preclinical stage of development: GSK-343, DZNeP, and EPZ-5687.

2.4.4.1 GSK-343

GSK-343 is a highly potent and selective small molecule inhibitor of EZH2 that functions through the competitive binding of EZH2 with cofactor SAM. The selectivity over other SAM-utilizing molecules is over 1000-fold, with exception of enhancer of zeste homolog 1 (EZH1) at 60-fold selectivity due to EZH1's high degree of homology to EZH2 [380]. The mechanism behind the differences in EZH1 and EZH2 selectivity are currently unknown at time of writing [380]. While the studies investigating this inhibitor are few, GSK-343 has shown promising results in its ability to variably alter epigenetic profiles as well as phenotypic expression in multiple cancer types. Sato and colleagues have demonstrated significant gene expressional changes following treatment while maintaining a high degree of gene expressional selectivity relative to other investigated inhibitors in breast, colon, and leukemia cell lines [381]. When utilized in hepatocellular carcinomas GSK-343 had also induced autophagy [382]. The most convincing evidence of GSK-343's potential as a chemotherapeutic agent was in a study performed by Ding and colleagues [383]. Their study had observed the phenotypic reprogramming of cervical cancer cell lines following treatment with GSK-343 both *in vitro* and *in vivo*. Cells had displayed reduced cell proliferation and motility theorized to be a result of E-cadherin induced tumor suppression, as cell lines displayed a mesenchymal phenotype to epithelial in the form of increased E-cadherin levels and decreased N-cadherin and vimentin post

treatment [383]. In essence, treatment with GSK-343 had reversed EMT, a key development process during cancer cell invasion and metastasis [383, 384].

2.4.4.2 DZNeP

With its reported discovery in 1986, DZNeP is one of the first known inhibitors of EZH2 and was originally theorized for potential use as both an antitumoral and antiviral agent. DZNeP is a highly potent small-molecule inhibitor of S-adenosylhomocysteine-hydrolase (SAH-hydrolase), a key enzyme in the methionine cycle, and was found to have a greater than 250-fold binding efficacy to its leading competitor, 3-deazaaristeromycin [385]. While historically documented as an EZH2-specific inhibitor, a study performed by Miranda and colleagues had solidified DZNeP's mechanism of inhibition to have global effects on multiple histone methyltransferases rather than EZH2 specifically [386]. Further evidence provided by Tan and colleagues showed only 140 out of 751 DZNep-activated genes appeared to be regulated by EZH2 [387]. The global effects of DZNeP may account for its overall success since its discovery, as treatment with the inhibitor has shown significant epigenetic, antiproliferative, and antiangiogenic effects in multiple cancer types.

When treated alone, epigenetic changes were observed in glioblastoma stem cell lines in the form of decreased c-myc expression, a molecule believed to be essential for glioblastoma stem cell development [388]. When used as a single agent inhibitor, as well as combined with HER2 and HDAC inhibitors, DZNeP has shown antiproliferative and apoptotic activity in breast cancer, with evidence of synergistic effects [389]. As a single agent in hepatocellular carcinoma, DZNeP-treated cells showed impaired growth as well as a clear decrease in the number of tumor initiating epithelial cell adhesion molecule-positive cells. This decrease in tumor initiating cells was also significantly higher in DZNeP-treated cells relative to 5-FU, suggesting hepatocellular carcinoma tumorgenicity to be dependent on pathways targeted by DZNeP [390]. Treatment in malignant pleural mesothelioma cells displayed inhibited proliferation, migration, clonogenicity, and tumorigenicity believed to be a result of the observed differential gene expression profiles [391]. Comparable results were seen in both leukemia and prostate models, with induction of

apoptosis in acute myeloid leukemia cells and a reduction in cancer stem cell markers in prostate cancer cell lines [392, 393].

In vivo cancer models utilizing DZNeP are relatively limited in literature; however, in a glioblastoma xenograft model treatment with DZNeP had also reduced tumor-mitigated angiogenesis without significant toxic effects [394]. A prostate cancer model had also shown reduced invasion and tumor size post treatment [393]. DZNeP's toxicity profiles overall seem to continue this trend, with DZNeP treatments being generally well tolerated at lower concentrations [393, 395]. Unfortunately, DZNeP's global histone methylation properties combined with its relatively short half-life *in vivo* limit applicable dosages [386, 396].

2.4.4.3 EPZ-5687

EPZ-5687 is a SAM-competitive inhibitor of EZH2 with a >500-fold selectivity to EZH2 and a >50-fold selectivity to EZH1 over other human protein methylases [397]. Like GSK-343, very little has been published at time of writing. However, published results of EPZ-5687's utilization in cancers have shown promise. When utilized in synovial sarcoma, treatment with EPZ-5687 was able to suppress cell migration and proliferation [398]. A non-Hodgkin's lymphoma model showed comparable results, with specified induction of apoptosis in Tyr641 or Ala677 mutants over wild-type cells [397].

Table 2.1: Epigenetic regulators specific to OPSCC

Name	Description	Role in OPSCC	Reference
Histone Modifying Protiens			
EZH2	PRC2 protein subunit	Hypermethylation of H3K27me3	[132]
BMI1	PRC1 protein subunit	Stabilization of H3K27me3	[212]
DNA Methylation			
DNMT1	DNA methyltrasferase	Overexpression	[126]
DNMT3A	DNA methyltrasferase	Overexpression, de novo	[126]

		methylation	
*ncRNAs**			
miR-21	microRNA	Overexpression	[282]
miR-205	microRNA	Overexpression	[282]
miR-181	microRNA	Overexpression	[282]
miR-17-92 cluster	microRNA	Overexpression	[282]
miR-106b-25 cluster	microRNA	Overexpression	[282]
miR-106-363 cluster	microRNA	Overexpression	[281, 282]
Let-7d	microRNA	Downregulation	[282]

**compared to normal tissues, only miRs frequently associated with cancer diagnosis; EZH2* Enhancer of zeste 2 polycomb repressive complex 2 subunit, *DNMT* DNA methyltransferase, *BMI1* B-cell–specific Moloney murine leukemia virus integration site 1

Table 2.2: Current and potential epigenetic chemotherapies

Chemotherapeutic Agent	Status	Target	Reference
DNMT inhibitors			
Arsenic trioxide	Clinical Trials	DNMT1, DNMT3a, and DNMT3b	[365, 366, 399]
5- azacytidine (Vidaza, Celgene)	USFDA Approved	DNMT1	[4, 364]
5-aza-2′-deoxycytidine (Decitabine, Dacogen, SuperGen)	USFDA Approved	DNMT1	[4, 364]
MG98	Clinical trials	DNMT1	[367, 368]
HDAC inhibitor			
LAQ-824 / LBH 589 (Farydak, Dacinostat, panobinostat)	USFDA Approved	HDAC	[355, 356]
PXD-101(Belinostat, Beleodaq)	Clinical trials	HDAC	[355]

Valproic acid (Mg valproate)	Clinical trials	Class I HDAC	[355, 400]
suberoylanilide hydroxamic acid (vorinostat, SAHA)	USFDA Approved	Class I & II HDAC	[4]
FK-228 (FR901228, romidepsin)	USFDA Approved	HDAC1 and HDAC2	[4]
Phenylbutyrate (4-sodium phenylbutyrate)	Clinical trials	Class I & II HDAC	[355, 401]
MS-275 (entinostat)	Clinical trials	HDAC1 and HDAC 3	[355, 357]
CI-994	Clinical trials	Class I HDAC	[355]
MGCD-0103 (Mocetinostat)	Clinical trials	Class I & IV HDAC	[355]
JNJ-26481585 (Quisinostat)	Clinical trials	Class I HDAC	[357, 358]
HMT inhibitor			
EPZ-6438 (EPZ006438, Tazemetostat)	Clinical trials	EZH2	[402]
DZNeP	Preclinical	HMT	[386]
EPZ-5676 (Pinometostat)	Clinical trials	DOT1L	[375]
EPZ-5687 (EPZ005687)	Preclinical	EZH2	[403]
GSK-126	Clinical Trials	EZH2	[404]
GSK-343	Preclinical	EZH2	[403]
PF 06726304 acetate	Preclinical	EZH2	[378, 379]
UNC1999	Preclinical	EZH2 & EZH1	[376]
ZLD1039	Preclinical	EZH2	[377]
UNC0638	Preclinical	EMHT2	[381]
CPI‑1205	Clinical Trials	EZH2	[405]
E11	Preclinical	EZH2	[257]

USFDA United States Food and Drug Association

2.4.5 PREVENTATIVE MEASURES

The rise of HPV-associated head and neck cancers remains a prevalent and very treatable problem in modern society. Given HPV's typical method of transmissibility mentioned in 2.2, safe sex practices are an obvious recommendation. Outside of behavioral modifications, preventative vaccinations like Gardasil are available to men and women ages 9-26. Advertisement strategies for the vaccine have been largely targeted towards a female demographic, with statistics reflecting this decision [406]. Previous Gardasil vaccines were quadrivalent, protecting against HPV-6, 11, 16, and 18 [407]. The latest vaccine, Gardasil 9, expands the protected serotypes to include HPV-31, 33, 45, 52, and 58 [408]. It is given intramuscularly in a three-dose series of injections [407, 409]. Efficacy of the vaccine have been reported as high as 98.2% against high-grade cervical lesions with related HPV serotypes and reports of only non-serious adverse reactions (pain, swelling, and erythema) [407, 409]

Despite the staggering evidence suggesting efficacy and safety of the vaccine, the vaccination rates in the United States are much lower than the advocated 80% coverage rates [410]. In a study by Stokley and colleagues (2014), they found only 57.3% of girls ages 13-17 had one or more doses in the vaccine series, 47.7% received two or more, and 37.6% received all three doses [411]. These rates are lower in women ages 19-26, with 34.5% reporting received one or more doses [412]. Reported barriers to the lack of receptiveness towards the vaccine are largely due to both patient and parent refusal. The most prevalent objection described by parents was a lack of knowledge regarding the vaccines safety and long-term effects. Parents had also felt a risk of HPV contraction for their child is low and a vaccination is not warranted. In addition, parents reported a lack of recommendation by their physician. Mature patients reported either a lack of efficacy of the vaccine, not required due to a lack of sexual activity, or being in a monogamous relationship [406].

While their role has lessened dramatically over the last decade, tobacco products play a significant part in carcinogenesis. Tobacco smoke contains at least 60 known carcinogenic, mutagenic, cytotoxic or antigenic compounds. Hydrocarbon compounds produced from tobacco combustion have been shown to act as DNA adducts, interfering with DNA replication mechanisms [413]. Smoke derivatives have also shown to upregulate antiapoptotic mechanisms

and various transcription factors associated with carcinogenesis [414]. Damage to the epithelium as well as decreased immune function have also shown tobacco smoke to promote infection by various pathogens, including HPV [408]. Alcohol, more specifically the acetaldehyde metabolite, has also shown cytotoxic, mutagenic, and carcinogenic properties as well. Acetaldehyde has been shown to interfere with multiple enzymes involved in DNA synthesis and repair mechanisms, DNA directly, as well as cellular metabolic proteins to cause both gross chromosomal aberrations and morphological changes [415].

2.5 THESIS OBJECTIVES

HNSCC is the 6th most prevalent cancer worldwide with rates of HPV-positive OPSCC dramatically increasing within developed world [107, 108]. The heterogenous nature of OPSCC presents multiple hurdles to clinical treatment including drug penetration, hypoxia, angiogenesis, and the likelihood of disease recurrence [416]. HPV positivity, while clinically given a better prognosis, still requires patients undergo highly invasive surgical intervention often combined with aggressive chemoradiotherapeutics [320, 321]. For these reasons, interventions with increased accuracy, efficacy, and safety are a necessity to improve prognostic outcome and potentially prevent unnecessary invasive interventions. EZH2 is the catalytic subunit of the PRC2 complex responsible for H3K27me3. This H3K27me3 results in transcription repression of a target gene through the aid of the PRC1 complex and effectively blocks transcriptional machinery from binding [212-214]. EZH2 overexpression has been reported in multiple cancer types, including HPV-positive variants, and is associated with a poor clinical prognosis [132, 133, 228]. EZH2 has known oncogenic and malignant properties, with its primary mechanism of action to target and silence tumor suppressor expression. While EZH2's physiological role may be ambiguous, the frequency of its overexpression in aggressive cancers still makes EZH2 an attractive chemotherapeutic target [228, 262-264].

With the historical knowledge of EZH2's role in oncogenesis, we hypothesized that EZH2 inhibition will result in gene expressional and phenotypic changes sufficient to act as a viable chemotherapeutic modality. The objective of this research project was to determine the efficacy

EZH2 inhibition in an OPSCC model *in vitro* utilizing three EZH2 pathway inhibitors currently in the preclinical stage of their development. We aimed to compare and contrast any effects HPV status would have on drug efficacy and gene expression, given the differences HPV-positive status has on the cancer epigenome [126, 127]. We designed the experiment to observe the expressional changes of nine frequently altered oncogenes or tumor suppressors in OPSCC including: *EGFR, MET, CDKN2A, CCND1, MKI67, PIK3CA, PTEN, EZH2,* as well as two OPSCC stem cell markers *ALDH1A1,* and *CD44 [136, 173, 178, 417]*.

The three EZH2 pathway inhibitors utilized in this study are GSK-343, EPZ-5687, and DZNeP, all of which have previously shown their ability to inhibit EZH2 in various cancer types. GSK-343 and EPZ-5687 are two novel SAM-competitive inhibitors of EZH2; early literature suggests these agents to provide much more specified inhibition of EZH2, but is relative limited given their infancy [380, 385, 398]. DZNeP, an older SAH hydrolase inhibitor, was also utilized in this study and provides well established evidence of its efficacy in multiple cancer variants, despite its global inhibitory effects on histone methyltransferases [386]. This study provides the first documented evidence of these epigenetic inhibitors usage in HPV-positive and HPV-negative OPSCC models and aims to further the knowledge of EZH2's viability as a chemotherapeutic target.

CHAPTER 3

MATERIALS AND METHODS

3.1 CELL CULTURES AND DRUG TREATMENT PROTOCOL

3.1.1 CELL CULTURE

Cell culture work and other protocols requiring sterile environments for reduction of bacterial contamination were performed in a Class II biological safety cabinet (cat: NU-425-400, Nuaire). Preparation of the biological safety cabinet (hood) involved liberal coating the walls and any exposed regions of instrumentation entering the hood with a spray bottle containing 70% isopropanol. Any pipet tips used in the hood were kept in sealed in original packaging with the outside sprayed with 70% isopropanol. Packaging was opened inside the hood. Autoclaved glass pipette tips were used for aspiration of liquids. If autoclave was unavailable, glass pipette tips were sprayed with 70% isopropanol and allowed to dry in the hood for 5 minutes before use. Waste media was collected in a 4L Erlenmeyer flask and treated with approximately 200mL 7.4% bleach (Clorox) for a minimum of 1 hour before being discarded. Isotemp general purpose water bath (cat: FSGPD05, ThermoFisher) was utilized for the purposes of warming media or rapid thawing or reagents. The water bath contained 5L of H2O purified via Milli-Q A10 Advantage system (EMD Millipore) utilizing a 0.22µm filter supplemented with 10mL Aquaguard-2 (cat: 01-916-1E, BI Biological Industries) with a maintained temperature of 37°C. All cell lines were cultured in sterile incubators (cat: 3403, ThermoFisher or cat: MCO-5AC-PA, Panasonic) with environmental conditions of 37°C and 5% CO2. Routine cleaning of incubators and water bath was targeted at a frequency of once per month. Cleaning entailed the removal of any trays, racks, dishes, and recommended small parts (per manual instructions) which were transferred to the hood. 70% isopropanol was liberally sprayed on all removed parts as well as the interior of incubators and wiped down with paper towel. All sprayed components were wiped again with new dry paper towel to ensure all isopropanol was removed prior to re-assembly.

3.1.2 THAWING CELL LINES FROM FROZEN

SCC-9 is a HPV-negative tongue squamous cell carcinomas established from a 25 year old male in 1981 by Rheinwald and Beckett [418]. UM-SCC cell lines (SCC-1, SCC-47, SCC-104) were

developed by Dr. Carey and colleagues at the University of Michigan from Head and Neck cancer patients. SCC-1 is a HPV-negative floor of mouth tumor established from a male. SCC-47 and SCC-104 are HPV 16-positive cancers established from the lateral tongue tumor established from a male and a recurrent oral cavity tumor of a 56-year old male, respectively [419]. Cell lines stored in 1.8mL Nunc Cryotube Vials (cat: 375418, ThermoScientific) were extracted from liquid nitrogen wearing insulated gloves and rapidly thawed in a 37°C water bath until no ice formation was visible. Cells were transferred to a labeled 15mL centrifuge tube (cat: 430055, Corning) and 10mL of appropriate culture media (see section 3.1.3) was added dropwise. Tubes were spun at 1500rpm (approximately 500xg) for 7 minutes. Media was aspirated and cells were resuspended in 10mL of appropriate cell culture media. Resuspended cells were transferred to labeled 10cm BioLite culture dishes (cat: 130182, ThermoScientific).

3.1.3 CELL CULTURING AND SUBCULTURING

SCC-9 cell lines were cultured in DMEM + F12 HAMS medium (cat: D6421, Sigma-Aldrich) supplemented with 10% fetal bovine serum (FBS) (cat: F1051, Sigma-Aldrich), 0.5% sodium pyruvate (cat: 11360-070, Gibco), 1% Antibiotic-Antimycotic (cat: 15240-062, Gibco), and 2mg Hydrocortisone (dissolved in DMEM + F12 HAMS using 0.22µM MCE filter; cat:H0396, Sigma-Aldrich). SCC-1, UM-SCC-47, SCC-104 cell lines were cultured in DMEM high glucose medium (cat: 11965-092, Gibco) supplemented with 10% FBS (cat: F1051, Sigma-Aldrich), 1% non-essential amino acids (cat: 11140-050, Gibco), and 1% Penicillin-Streptomycin Solution (cat: SV30010, ThermoScientific). Media was stored at 4°C and heated in a 37°C water bath for 1 hour prior to use with cell cultures. Changing of the media involved aspiration of old media with a glass pipette tip and the addition of 10mL of appropriate media per 10cm dish. Media changes were performed every 2-3 days. Cells were routinely subcultured once every 7 days with cell quantities seeded into three “maintenance dishes” containing approximately 25% of original cell quantity. Routine subculturing was performed by first aspirating old media and washing cells twice with 10mL of phosphate buffered saline (PBS) pH 7.4 (cat: 10010-023, Gibco). Aspiration of PBS was performed after each wash. To suspend adherent nature of cells, 1mL of 0.25 % Trypsin/EDTA (cat: 25200-056, Gibco) was added to the 10cm dish. The dish was swirled in a

circular motion to ensure adequate coverage of all cells. Cells were incubated in sterile incubators with 0.25% Trypsin/EDTA at variable times depending on cell line. SCC-1 and SCC-9 cell lines required incubation times of 5-7 minutes and SCC-47 and SCC-104 cell lines required incubation times of 12-15 minutes. Confirmation of non-adherence was performed prior to completion of subculturing protocol via brief shaking of the 10cm dish containing cells. Cells were considered non-adherent if white "film" of cells was visibly mobile during shaking. Non-adherent cells were lifted from the 10cm dish using 7mL of fresh media. Pipetting up and down was repeated until no visible patches were apparent on the dish and no cell clumping was visible. 2mL of lifted cells were added per labeled 10cm dish containing 8mL of fresh media. Swirling of media and newly added cells was performed in a clockwise and counterclockwise motion for a total of 30 seconds. Labeled dishes included cell line name, passage number (n+1), and date of subculture. Cells were stored in sterile incubators. Trypsinization of cells into 6-well (3.5cm) culture plates (cat: C153477P, eppendorf) procedure was functionally equivalent until the end step of transferring trypsinized cells into new culture plates. A cell seeding density of a complete 6-well culture plate was considered to be functionally equivalent to that of a single 10cm culture dish. Seeding density values were established according to ThermoFisher recommendations [420]. A seeding density of 25% of original cell quantity is maintained. Functionally, cells were lifted using 7mL of fresh media and 2mL of cells were added to 10mL of fresh media. Dilution steps varied based on number of plates required. 2mL of diluted cells were added to each well of a 6-well culture plate. Dilution was either performed in a 15mL or 50mL conical tube (cat: 430290, Corning) containing desired amount of appropriate media.

3.1.4 FREEZING CELLS FROM CULTURE

Cells were harvested at logarithmic growth (approximately 48 hours following subculture) and subjected to the trypsinization protocol described in 3.1.3. Lifted cells were transferred to a labeled 50mL conical tube containing 10mL of fresh media. Cells were centrifuged at 1500rpm (approximately 500xg) for 7 minutes. Media was aspirated leaving only the pellet and resuspended in freezing media. Quantity of freezing media for resuspension dependent on number of lifted cells and cryotubes desired. 1mL of cells were designated per cryotube.

Freezing media used dependent on cell line: SCC-9 freezing media composed of prepared (as described in 3.1.3) DMEM + F12 HAMS supplemented with 5% DMSO. SCC-1, SCC-47, and SCC-104 freezing media composed of prepared (as described in 3.1.3) high glucose DMEM supplemented with 10% DMSO. Cryotubes containing cells in freezing media were subjected to a slow freeze in a Styrofoam enclosure at -80°C for 24 hours. Following slow freeze, cryotubes were placed in liquid nitrogen for long term storage.

3.1.5 DRUG PREPARATION AND TREATMENT PROTOCOL

GSK-343 (cat: SML0766-5MG, Sigma-Aldrich), DZNeP (cat: S7120, Selleckchem), and EPZ-5687 (cat: S7004, Selleckchem) were received in powder form and dissolved in DMSO (cat: D2650, Sigma-Aldrich) within the inhibitors original containers. Masses of inhibitors, as labeled by manufacturer, were assumed to be accurate and were not formally weighed. Inhibitors were filtered using a 0.2µM nylon membrane filter (cat: PN4433, PALL) and syringe following the addition of DMSO. 100µL of individual inhibitors were then aliquoted into sterile 1.7mL centrifuge tubes. 5mg of EPZ-5687 was dissolved in 4.6325mL of DMSO resulting in a working solution concentration of 2mM. 1mg of DZNeP was dissolved in 3.3475mL of DMSO for a working solution concentration of 1mM. 1mg of GSK-343 was dissolved in 1.2560mL of DMSO for a solution concentration of 1mM. Aliquoted GSK-343 solutions were further diluted with DMSO into a working concentration of 200µM (1:4 dilution) into separate sterile 1.7mL centrifuge tubes per required need. Prepared inhibitors were stored at -80°C. Cells were seeded at 25% confluency in either 10 cm dishes or 6-well plates and allowed to settle and recover for 3 days. On the third day, old media was aspirated and replaced with 10mL or 2mL (respectively) of appropriate media. Inhibitors and DMSO were added directly to plates to desired concentrations via pipet using sterile tips with barrier (ART series, ThermoScientific). With the exception of untreated groups, inhibitor treatments not totaling 50µL (10cm dishes) or 10µL (individual well of a 6-well plate) were brought to desired total using DMSO, thereby maintaining a concentration of approximately 5.0µM DMSO throughout. Inhibitors were mixed by pipetting up and down prior to addition to plates. Cells treated with inhibitor for greater than 4

days received fresh media and inhibitors on day 4 of treatment. Fresh media was added every third day in maintenance cultures.

3.2 WESTERN BLOTTING

Day 7 Western blots utilizing inhibitor gradient (FIG. 4.1) as well as baseline EZH2 and H3K27me3 (FIG. 4.2) were performed three times (n=3). Western blots measuring time of inhibition (FIG. 4.3) were performed once (n=1).

3.2.1 WHOLE CELL LYSATE EXTRACTION AND QUANTIFICATION

Whole cell lysates were utilized in the analysis of EZH2 protein content and were obtained from harvesting cells in 200 µL 50mM TRIS + 1% SDS pH 7.6, supplemented with 1mM phenylmethylsulfonyl fluoride (PMSF) and 1x complete protease inhibitor (CPI) (Cat#: 11697498001 Roche). Cells were incubated on ice for 20 minutes, sheared through a 25-gauge syringe, and centrifuged for 15 minutes at 16000xg at 4°C. 100µL of supernatant was transferred to new centrifuge tubes and was either stored at -20°C or subjected to SDS-PAGE and Western Blot. Quantification of cell lysates were performed using an ND-1000 Spectrophotometer and accompanying ND-1000 v.3.3.0 software (Nanodrop Technologies, Inc). Measurements were based from absorbance at 280nm with blanks being measured using the buffer above. An average of 3 separate reads was used for deciding sample concentration with reader being wiped off and washed between samples. Measurement were re-blanked following change of cell line.

3.2.2 HISTONE ENRICHMENT

Histones were enriched from cell lysates following a modified abcam histone extraction protocol [421]. Cells were cultured and treated according to 3.1.3 and 3.1.5 in 10cm dishes or 6-well plates depending on experiment. All steps were carried out at 4°C, on ice or with ice-cold buffers. Media was aspirated from the dishes and the cells were washed twice with 10 ml PBS.

1ml Triton Extraction Buffer (TEB) (1xPBS supplemented with 0.5 % Triton X-100, 2mM PMSF and 1x CPI [Cat#: 11697498001 Roche]) was added to the dish and swirled to ensure adequate coverage of all cells. Cells were scraped using a 3cm bladed (10cm dish) or 1.8cm bladed (6-well plate) cell scraper (cat: 353089 and 353085, respectively, BD Falcon) and transferred via 1mL pipette to a labeled pre-chilled 1.7mL microfuge tube. Cell scrapers were changed between cell lines and wiped clean with a Kim Wipe (cat: 34120, Kimberley-Clark) between treatment groups. Cell membranes were lysed by end over end rotation for 10 minutes. End over end rotation was followed by centrifugation at 650xg for 10 minutes. The supernatant was aspirated and pellets were resuspended in 500ul TEB. TEB originally prepared in initial steps was supplemented with an additional 2mM PMSF prior to resuspension. Resuspended pellets were submitted to centrifugation again at 650xg for 10 minutes. The supernatant was once again aspirated and the pellets were resuspended in either 400µL (10cm dish) or 100µL (6-well plate) of 0.2N HCl and incubated at 4°C overnight.

3.2.3 TCA PRECIPITATION

Following incubation in 0.2N HCl, the tubes were briefly vortexed then centrifuged for 10 minutes at 6500xg and 4°C. The histone-containing supernatant was transferred via pipette to new labeled pre-chilled 1.7mL tubes containing either 100µL (10cm dish) or 25µL (6-well plate) of trichloroacetic acid. The tubes were vortexed briefly and incubated on ice for approximately 1.5 hours. Following incubation, tubes were submitted to centrifugation for 15 minutes at 16000xg and 4°C. The supernatant was aspirated and the pelleted protein was washed twice with 300µL acetone stored at -20°C. Washes involved tubes containing pelleted histones and acetone being vortexed for 5 seconds and submitted to centrifugation for 5 minutes at 16000xg. Acetone was then aspirated. Pelleted proteins were allowed to dry with acetone removed and the lid open at room temperature for 1.5 hours. Drying times were increased as necessary until no acetone was recognizably present via appearance and smell. Pelleted histones were either stored at -20°C or immediately resuspended in 0.1N NaOH and subjected to SDS-PAGE and Western blot.

3.2.4 RESUSPENSION OF HISTONES AND QUANTIFICATION

Pelleted histones were resuspended in 100µL (10cm dish) or 60-80µL (6-well plate) of 0.1N NaOH. Given the pelleted histone slow time for resuspension, histones incubated in 0.1N NaOH for 1.5 hours at room temperature and were spun down for 15 minutes at 16000xg. The supernatant was transferred to a new labeled 1.7mL centrifuge tube, thereby ensuring no remaining pellet would dissolve during the quantification process. Quantification of histones utilized the Qubit Fluorometric Quantitation system (ThermoFisher Scientific). Quantification reactions were prepared in a 0.5mL PCR tube (cat:321-05-051, AXYGEN) utilizing 5µL sample and 195µL reaction mixture (working reaction mixture contained 1µL protein detection reagent and 199µL protein buffer per sample). Samples were incubated in reaction mixture for 15 minutes at room temperature prior to reading.

3.2.5 SDS-PAGE AND TRANSFER

SDS-PAGE and transfer were performed utilizing the Mini-Protean Vertical Electrophoresis Cell with Mini Trans Blot Module and PowerPac HC power supply (cat: 1658036, BIO-RAD). Samples were prepared for SDS-PAGE according to common Laemmli methodology. A target of 3-5µg (histones) or 15µg (whole cell lysate) of protein per well was obtained and diluted to appropriate well volume using MilliQ. Samples were supplemented with appropriate volume of 4x Laemmli's buffer (cat: 161-0747, BIO-RAD) + Dithiothreitol (DTT) (working solution composed of 185µL 4x Laemmeli's buffer in 15µL 4M DTT) and boiled for 5 minutes prior to loading. Samples were subjected to SDS-PAGE on 12-well Mini-PROTEAN TGX 4-15% gradient gels (cat: 456-1085, BIO-RAD) or 15-well Mini-PROTEAN TGX 4-20% gradient gels (cat: 456-1096, BIO-RAD) in approximately 1L of running buffer (10x Tris/Glycine/SDS buffer (cat: 161-0732, BIO-RAD) in 1L MilliQ). Molecular weight marker (cat: 161-0374, BIO-RAD) and 4x Laemmli's buffer mixture (5:4 Molecular weight marker to 4x Laemmli's buffer ratio; 7.5µL per well) were run alongside treatment groups in separate wells. Gels were run at a constant target of 0.05A for 45 minutes. Following electrophoresis, gels were transferred to the transfer apparatus with an 8.5cm by 6cm polyvinylidene fluoride (PVDF) membrane (cat: 162-

0177, BIO-RAD). Protein transfer was performed with constant amperage of 0.2A for 1 hour in approximately 1L or transfer buffer (25mM Tris, 190mM glycine, and 20% methanol in MilliQ, pH 8.3). Membranes were blocked overnight at 4°C in PBS with 0.1% Tween20 (PBST) + 5% milk solution (rocking) following transfer.

3.2.6.1 WESTERN BLOTTING AND DETECTION: EZH2

Membranes were transferred from blocking solution to a 1:1000 dilution of anti-EZH2 primary antibody (cat: 5246 Cell Signalling Technology) in PBST + 5% milk solution and incubated for 1 hour at ambient temperature (rocking). Primary antibody was either discarded or stored at -20°C in a 15mL conical tube. The reuse of primary antibodies did not exceed 5 uses. Membranes were then washed 4x in PBST and incubated in 1:5000 HRP-conjugated anti-rabbit secondary antibody (polyclonal goat, cat: 170-6515, BIO-RAD) for 1 hour at room temperature in PBST + 5 % milk (rocking). Washes were performed by the addition of approximately 15mL of PBST, swirling for 30 seconds by hand, and discarding PBST. Following incubation, membranes were washed 8x with PBST via alternating previous washing methodology and mechanical rocking for 5 minutes. Membranes were then transferred protein side down to a clean, flat surface containing 350µL Amersham ECL Western Blotting Detection Reagents kit (cat: RPN2106, GE Healthcare) or Amersham ECL Prime Western Blotting Detection Reagent kit (cat: RPN2236, GE Healthcare) to reveal chemiluminescence. Membranes were manipulated to ensure coverage on the entire surface and incubated 2 minutes. Membranes were wrapped in saran-wrap and affixed via tape to a film cassette. Film (Fugifilm Medical XRAY Film Super RX) was applied to the membrane for variable time durations and developed. Once films were developed, membranes were washed 3x with hot water, stained with Coomassie blue (0.1% Coomassie Brilliante Blue R-250, 45% methanol, and 10% acetic acid in MilliQ) for 20 seconds, and washed an additional 3x with hot water. Membranes were dabbed gently with Kim Wipes to remove excess water and further dried in paper towel overnight at ambient room temperature.

3.2.6.2 WESTERN BLOTTING AND DETECTION: H3K27ME3

Membranes were transferred from blocking solution to a 1:1000 dilution of anti-H3K27me3 primary antibody (monoclonal mouse, cat: ab6002, abcam) in PBST + 3% milk solution and incubated for 1 hour at ambient temperature (rocking). Primary antibody was either discarded or stored at -20°C in a 15mL conical tube. The reuse of primary antibodies did not exceed 5 uses. Membranes were then washed 4x in PBST and incubated in 1:5000 HRP-conjugated anti-mouse secondary antibody (polyclonal donkey, cat: 170-5047, BIO-RAD) for 1 hour at room temperature in PBST + 5 % milk (rocking). Washes, detection, exposure, and membrane staining were performed as previous (see section 3.2.6.1).

3.2.7 QUANTIFICATION AND ANALYSIS

Quantification of Western Blots was performed using ImageJ (v. 1.51j8 bundled with Java v. 1.8.0_112 National Institutes of Health) on scans of exposed films and Coomassie-stained PVDF membranes. Scans were performed at 600DPI using an EPSON XP-610 All-In-One Printer (C11CD31201 Epson). Scans with lowest exposure while maintaining visible band differentiation were chosen for quantification. Values were calculated according to mean grey value of band and standardized via subtraction of nearby background. Grey value of standardized blots were normalized through division by a common, standardized Coomassie-stained band. Quantification area was maintained between band and subtracted background. Ratios were obtained by dividing treatment group values by either the highest expression values or DMSO-only values.

3.3 DROPLET DIGITAL POLYMERASE CHAIN REACTION

ddPCR gene expression analysis (FIG. 4) was performed twice (n=2).

3.3.1 RNA EXTRACTION AND PURIFICATION

Cells were cultured and treated according to 3.1.3 and 3.1.5 in 6-well cell culture plates for 7 days. On day of harvest, media was aspirated cells were washed 3 times with 2mL PBS. Cells were scraped using a 1.8cm bladed cell scraper in 300µL RNA Later and transferred via 1mL pipette to a labeled 1.7mL microfuge tube. Cell scrapers were changed between cell lines and cleaned with a hydrogen peroxide-based surface cleaner (cat: ACCDISR1-TB, Viroxaccel), distilled H2O, and dried with a Kim Wipe between treatment groups. Cells were vortexed briefly and 20µL of sample was transferred to a new to a labeled 1.7mL microfuge tube. RNA purification was performed using the RNeasy Plus Mini Kit (cat: 74134, Qiagen). The 20µL of sample was lysed in 350µL Bufffer RLT + 40mM dTT and transferred to the QIAshredder (cat: 79656, Qiagen) spin column. Samples in QIA shredder spin column were centrifuged for 30 seconds at 8000xg. The supernatant was loaded onto a gDNA Eliminator mini Spin Column and centrifuged for 30 seconds at 8000xg. An equal volume (375µL) of 70 % ethanol was added to the flow through, mixed by pipetting, and 700µL of the mixture was transferred to an RNeasy Mini spin column. The RNeasy Mini spin column was centrifuged for 15 seconds at 8000xg and the supernatant was aspirated**.** Given the limited capacity of the RNeasy Mini spin column, this step was repeated with the remaining supernatant/70% EtOH mixture. Following RNA binding, 700µL of Buffer RW1 was added to the RNeasy Mini spin column and samples were centrifuged for 15 seconds at 8000xg. The supernatant was aspirated and the RNeasy Mini spin column was washed twice with 500µL Buffer RPE supplemented with EtOH (44mL anhydrous ethanol added to 11mL stock solution as per manufacturer's instructions) with supernatant aspirated between washes. The membrane containing bound RNA was transferred to a new 2mL collection tube and dried via centrifugation at 16000xg for 1 minute. The membrane was transferred to a new 1.7mL microfuge tube and the RNA was eluted with 60µL RNase free H2O. Eluted RNA was transferred to new labeled 0.5mL PCR tubes and stored at -20°C.

3.3.2 QUANTIFICATION OF RNA

Quantification of RNA utilized the Qubit Fluorometric Quantitation system. Quantification reactions were prepared in a 0.5mL PCR tube utilizing 2µL sample and 198µL reaction mixture (working reaction mixture contained 1µL RNA detection reagent and 199µL RNA buffer per

sample). Samples were incubated in reaction mixture for 4 minutes at room temperature prior to reading.

3.3.3 CDNA SYNTHESIS

Reactions were prepared in 0.2mL PCR tubes (cat: 321-02-051, AXYGEN) with a target of 40-80ng of RNA utilized per 20µL reaction. Per the manufacturer's protocol, 4µL (20%) iScriptTM Reverse Transcription Supermix for RT-qPCR (BIO-RAD) was used per reaction. Nuclease-free H2O was used to bring samples to 20µL. cDNA reactions were performed in a C1000 Touch Thermal Cycler (cat: 185-1197, BIO-RAD) using the following parameters: Step 1) 25°C for 5 minutes, Step 2) 42°C for 30 seconds, Step 3) 85°C for 5 minutes and Step 4) 4°C infinite hold. All steps had a ramp rate of 3°C/second. Following the thermocycling reaction, transferred to 0.5mL PCR tubes where the cDNA was diluted with 0.125mM EDTA to a working concentration of 1 ng/µl. Diluted cDNA was either stored at -20°C or used directly for ddPCR.

3.3.4 REACTION FORMATION AND DROPLET SYNTHESIS

ddPCR reactions were set up and thermocycled in a twin.tec 96-well PCR plate (cat: 951020362, eppendorf). Reactions were set up following the manufacturer's protocols using 12µl/reaction of 2x ddPCR Supermix for Probes (No dUTP) (BIO-RAD), 1.2uL/reaction of 20x target primers/probe (FAM or HEX, BIO-RAD), 1.2µL/reaction 20x reference primers/probe (FAM or HEX, BIO-RAD), 2.4µL cDNA (at 1 ng/µL) and 7.2µL H2O. Primers/probes utilized are as follows: EGFR (unique assay ID: dHsaCPE5038080/dHsaCPE5038081 BIO-RAD), TP53 (unique assay ID: dHsaCPE5037520/dHsaCPE5037521 BIO-RAD), MKI67 (unique assay ID: dHsaCPE5050322/dHsaCPE5050323 BIO-RAD), CDKN2A (unique assay ID: dHsaCPE5045104/dHsaCPE5045105 BIO-RAD), CCND1 (unique assay ID: dHsaCPE5051730/dHsaCPE5051731 BIO-RAD), MET (unique assay ID: dHsaCPE5034172/dHsaCPE5034173 BIO-RAD), PTEN (unique assay ID: dHsaCPE5030136/dHsaCPE5030137 BIO-RAD), PIK3CA (unique assay ID: dHsaCPE5058352/dHsaCPE5058353 BIO-RAD), EZH2 (unique assay ID:

dHsaCPE5034224/dHsaCPE5034225 BIO-RAD), EEF2 (unique assay ID: dHsaCPE5050048/dHsaCPE5050049 BIO-RAD), ALDH1A1 (unique assay ID: dHsaCPE5056918/dHsaCPE5056919 BIO-RAD), and CD44 (unique assay ID: dHsaCPE5051600/dHsaCPE5051601 BIO-RAD). Where an internal reference for gene expression was required, human EEF2 primers/probe were used. GAPDH primers/probe (unique assay ID: dHsaCPE5031596/dHsaCPE5031597 BIO-RAD) were utilized as a secondary internal reference and compared to EEF2 values against a probe with known trends, EGFR. When set up, reactions were mixed 3 times in a Mixmate Vortex Shaker (eppendorf) and 20µL of the reaction mixture was transferred to DG8TM Cartridge for QX200/QX100 Droplet Generator (cat:186-4008, BIO-RAD) followed by 70µL of Droplet Generation Oil for Probes (cat: 186-3005, BIO-RAD) into the oil wells, according to the QX200 Droplet Generator Instruction Manual (cat: 10031907 BIO-RAD). Droplet generation was carried out using the QX200TM Droplet Generator (cat: 186-4002, BIO-RAD) and 40µL of the reaction was transferred to wells of a new 96-well PCR plate. When complete plates were sealed using a pierceable foil heat seal cover (cat: 1814040, BIO-RAD) and the PX1TM PCR Plate Sealer (cat: 181-4000, BIO-RAD) as per manufacturer's instructions. When sealed, plates were transferred to the thermal cycler and the reactions were carried out using the following parameters: Step 1) 95°C for 10 minutes, Step 2) 94°C for 30 seconds and 60°C for 1 minute (Step 2 repeat 39 times for a total of 40), Step 3) 98°C for 10 minutes and Step 4) 4°C infinite hold. All steps had a ramp rate of 3°C/second. Following thermocycling, the reactions were read in the QX200 Droplet Reader QX200 Droplet Reader (cat: 186-4003, BIO-RAD) and the RNA targets were quantified using the QuantaSoftTM Software (BIO-RAD).

3.3.5 ANALYSIS

Reactions were read in the QX200 Droplet Reader and the RNA targets were quantified using the QuantaSoft Software (BIO-RAD). If QuantaSoft software was unable to accurately quantify sample, adjustments to amplitude discrimination were made manually. If event number was fewer than 3000, experiment was repeated. ".CSV" files were exported from QuantaSoft

software and graphed in Microsoft Office Excel 2010 (Microsoft). Graphs were observed for trends relative to DMSO-treatment controls.

3.4 WOUND HEALING ASSAY

Wound healing assays (FIG. 5) were performed three times (n=3).

3.4.1 PLATE PREPARATION AND TREATMENT

With the aid of a 30cm ruler, alternating 2xred and 2xblue reference points 2mm apart spanning 2cm were made using a ultra-fine tip sharpie on the underside of individual wells of a 6-well culture plate prior to addition of cells. Cells were cultured and seeded according to 3.1.3. Following the recovery period, cells were either treated with various inhibitors or left untreated depending on treatment group (see 3.1.5). 5 days following recovery, both treatment groups were subjected to wound application.

3.4.2 WOUND APPLICATION

Wound was made 5 days following recovery period, whereby media was aspirated and cells were washed once with PBS. PBS was aspirated and a 2 cm “wound” was made across the reference points using a 1 mm diameter ART10 pipette tip (cat: 2139, ThermoScientific). A ruler was used to ensure wound made followed reference points. Cells were then washed an additional two times (as above) with PBS to remove excess cellular debris, followed by the addition of 2mL of appropriate media and treatment. Pre-treated media was utilized to allow for efficient re-application of treatment every 24 hours prior to photographs. Changes every 24 hours were necessary to remove cellular debris and ensure wound clarity. Pre-treated media was made according to 3.1.5 stored in 50mL conical tubes at 4°C. Pre-treated media was heated in a 37°C water bath for 1 hour prior to use with cell cultures.

3.4.3 PHOTOS AND PHOTO MANIPULATION

Digital photographs of the wound were taken at 50X magnification using the ZEISS Stemi 2000-C Stereo Microscope mounted with AxioCam ERc5s (ZEISS) and developed using ZEN 2011 Imaging software (ZEISS). Photos were taken at twelve-hour intervals for 72 hours. Levels and sharpness of images were corrected manually for purposes of clarity utilizing Photoshop CC 2015 (Adobe Systems).

3.5 CASPASE 3 ASSAY

Caspase 3 assays (FIG. 5) were performed at n=8.

3.5.1 CELL SEEDING, TREATMENT, AND LYSIS

Cells were cultured and treated according to 3.1.3 and 3.1.5 in a Corning flat-bottom 96-well cell culture plates (cat: 07-200-588, ThermoFisher Scientific) at a seeding density of 7500 cells per well. Treatment with inhibitor occurred over 48 hours. Staurosporine treatment group remained untreated until time of harvest, where 1.0μM staurosporine (cat:S4400, Sigma-Aldrich) was added, incubated at 37°C for 4 hours, and subjected to the same protocol as other treatment groups. Protocol and reagents utilized were from the Caspase 3 Assay Kit (cat: ab39383, abcam). All steps were performed at 4°C or on ice unless stated otherwise. Following treatment, 96-well plate was centrifuged for 2 minutes at 2000xg where media was aspirated and 50μL of lysis buffer was added. Cells in lysis buffer were incubated on ice for 10 minutes and transferred to -80°C for storage.

3.5.2 CELL STAINING AND READING

Protocol and reagents utilized were from the Caspase 3 Assay Kit (cat: ab39383, abcam). All steps were performed on ice unless stated otherwise. Cells stored in -80°C were thawed on ice for 10 minutes before proceeding with the remainder of assay. 50 μL of a prepared 2x Reaction

Buffer containing 1.0µM dTT was added to individual wells followed by 5µL of 1mM DEVD-AFC substrate. Following addition of the Reaction Buffer and DEVD-AFC substrate, the 96-well plate was shaken at 3000rpm for 30 seconds and centrifuged for 30 seconds at 1500xg. Lysed cells were then incubated at 37°C for 2 hours and read at 400nm+/-20nm emission and 505nm +/-20nm excitation wavelengths using the Cytation 5 Hybrid Multi-Mode Reader and Gen5^{TM} Software (BioTek).

3.5.3 STATISTICAL ANALYSIS

Due to the investigation of multiple scenarios and an expectation of a non-normal distribution of outcome variables, only nonparametric analyses were applied. Tests were applied to individual cell lines. Within-subjects design dictated a Friedman's Test to be utilized to look for equal medians between groups. All test values yielded a significant difference ($p<0.05$) whereby a Sign Test was applied with a Bonferroni correction conservatively for post hoc analysis. Sign Test comparisons were made versus non-treatment groups or versus DMSO treatment groups. All p-values derived from the Sign Test were multiplied by 5. All p-values were two-sided and statistical significance was determined with $p<0.05$. Statistical analysis was performed using Stata 13 MP (Stata 2013).

CHAPTER 4

RESULTS

4.1 DRUG EFFECTS ON H3K27ME3 LEVELS VARY BETWEEN CELL LINE'S HPV STATUS

To determine the individual drug efficacy of EZH2 inhibition, western blot analysis was utilized to detect changes in the levels of the EZH2 catalysis product, H3K27me3. This was performed on individual cell lines with an anti-H3K27me3 monoclonal antibody (FIG. 1).

Treatment with GSK-343 displayed a clear reduction of H3K27me3 that was consistent in all cell lines (FIG. 1). In contrast, inspection of western blots shows clear differences in H3K27me3 reduction based on HPV status in the SAH-hydrolase inhibitor DZNeP treated cells. Analysis of the western blots show DZNeP-treated cell lines have a reduction of H3K27me3 only present in HPV-negative cell line SCC-1 , while HPV-negative SCC-9 and HPV-positive cell lines (SCC-47 and SCC-104) appear have H3K27me3 levels comparable to untreated or DMSO only-treated cells. This reduction in H3K27me3 is also not as dramatic when compared to GSK-343-treated cell lines (FIG. 1C-D). Treatment with the other SAM-competitive inhibitor, EPZ-5687, resulted in no apparent demethylation in any cell lines, with H3K27me3 levels comparable to DMSO or untreated cells.

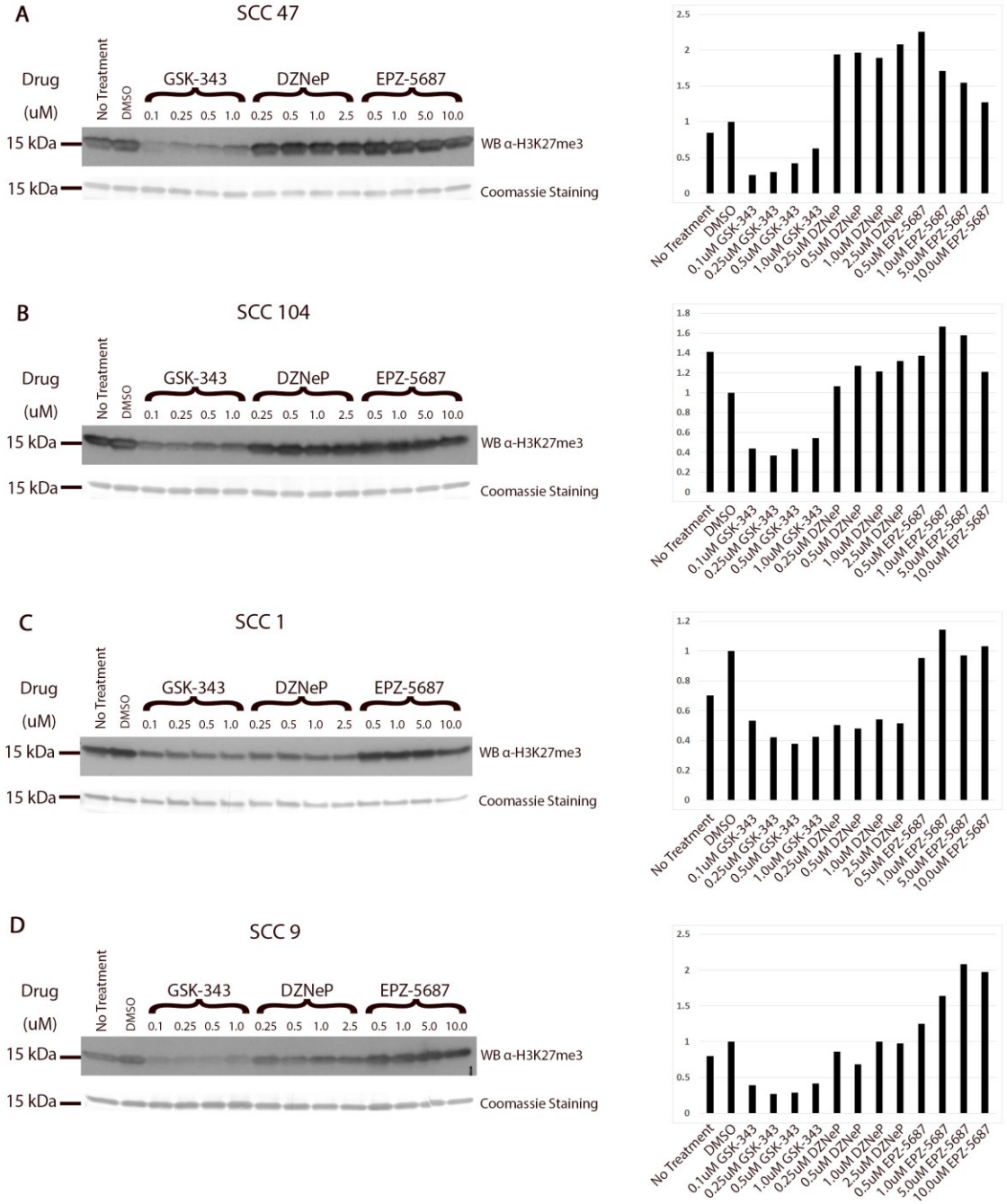

FIG. 4.1 Drug effects on H3K27me3 levels vary between cell line's HPV status.

Left: Western Blot analysis of H3K27me3 following 7-day treatments with GSK-343, DZNeP, or EPZ-5687. Coomassie blue staining (shown below western blot) utilized as loading control. Right: Quantification of Western blot to left of graph based on fold differences to DMSO-treated cells.

4.2 H3K27ME3 BASELINE VARIES BETWEEN CELL LINES, WITH INHIBITOR EFFECTS ON METHYLATION STATUS OCCURRING AS EARLY AS 48 HOURS POST TREATMENT

To compare the baseline protein levels of EZH2 and H3K27me3 in individual cell lines, western blot analysis was performed utilizing either an anti-EZH2 or anti-H3K27me3 antibody (FIG. 4.2). Both baseline EZH2 and H3K27me3 status showed clear variability between individual cell lines. However, this variability appears to contradict what one would expect, that being higher EZH2 levels would result in higher levels of H3K27me3 [422]. HPV-negative SCC-9 is the caveat to this, as it displays the lowest amount of EZH2 and H3K27me3 expression relative to other cell lines. HPV-positive SCC-104 displayed moderately elevated levels of H3K27me3, while its EZH2 expression displays the highest amount of EZH2 relative to the other cell lines utilized. SCC-1 and SCC-47 show the highest levels of H3K27me3 relative to the other cell lines; however, HPV-positive SCC-47 displays low EZH2 expression and HPV-negative SCC-1 displays high EZH2 expression.

The timeline of drug effect was determined via western blotting analysis utilizing an anti-H3K27me3 monoclonal antibody as above. Cell lines were treated with midline concentrations of GSK-343, DZNeP, or EPZ-5687 (FIG. 3). Endpoint (168 hours) western blotting results remained consistent with the results presented in FIG. 1. All GSK-343-treated cell lines displayed decreased H3K27me3. DZNeP-treated cell lines displayed decreased H3K27me3 in HPV-negative SCC-1 cell line. EPZ-5687-treated cell lines displayed no change in H3K27me3. GSK-343-treated cell lines displayed the most immediate drug effects in all cell lines, with demethylation occurring between 24 and 48 hours post treatment and maximum H3K27me3 reduction occurring at 96 hours post treatment. DZNeP-treated SCC-1 displayed demethylating

effects later than GSK-343-treated cell lines, with demethylation first appearing between 48 and 72 hours post treatment and maximum H3K27me3 reduction at 144 hours post treatment. Again, EPZ-5687 had no appreciable reduction in H3K27me3, with levels remaining comparable to DMSO or untreated cells. There are apparent reductions in H3K27me3 levels at 120 hours and 144 hours in DZNeP and EPZ-5687-treated SCC47 cells. However, when observing drug effect timeline patterns observed in other cell lines, combined with 7 day post-treatment H3K27me3 levels returning to repeatable levels, these reductions are most likely the result of random artefact and not drug effect.

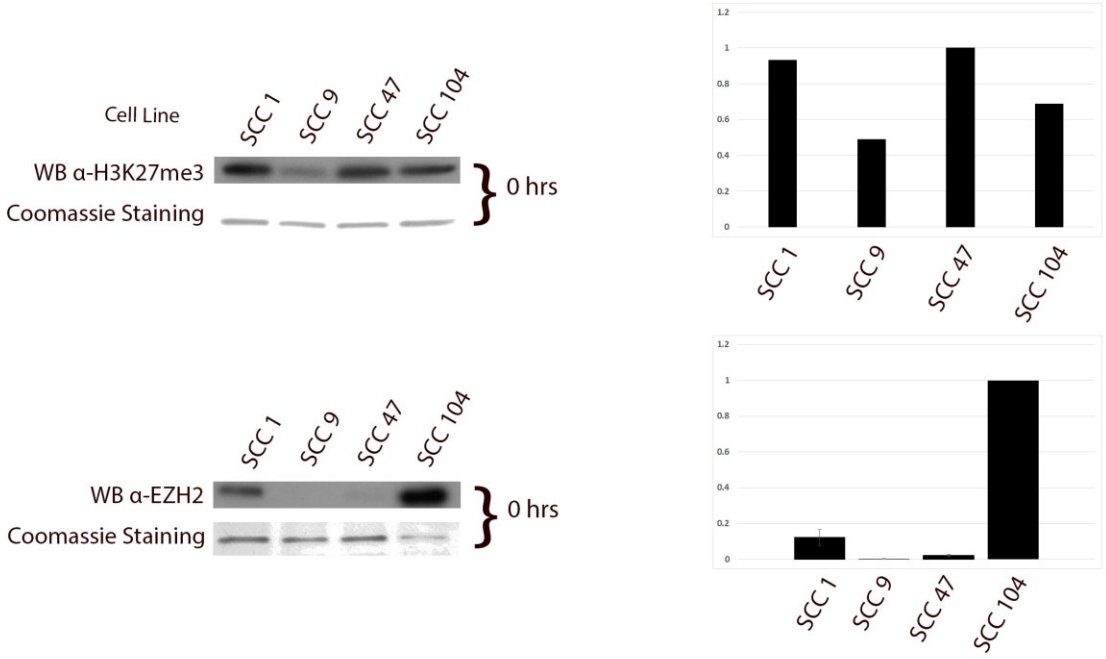

FIG. 4.2 EZH2 and H3K27me3 baseline varies between cell lines.

Left: Western Blot analysis of baseline EZH2 and H3K27me3 within individual cell lines. Coomassie blue staining (shown below western blot) utilized as loading control. Right: Quantification of Western blot to left of graph based on fold differences to highest expressing cell line (EZH2 values versus SCC-104 expression, H3K27me3 values versus SCC-104 expression.

SCC 47

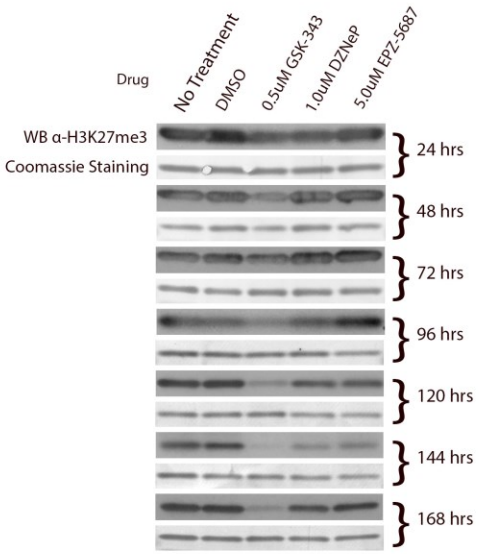

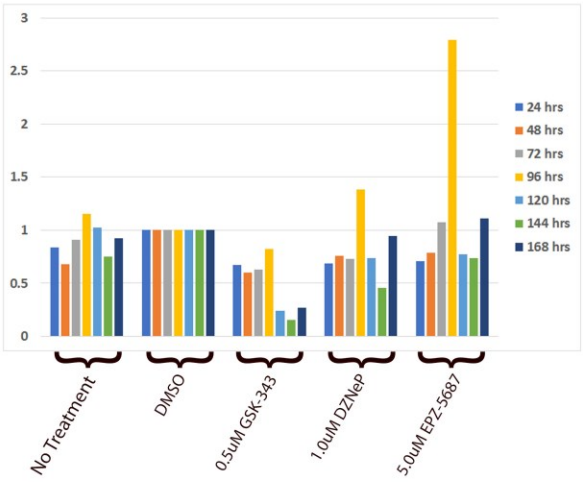

SCC 104

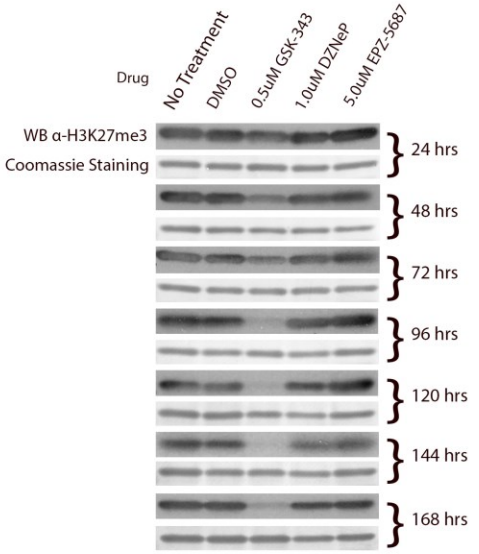

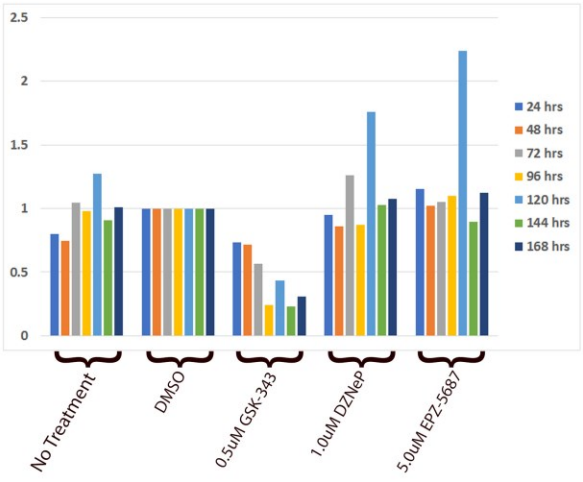

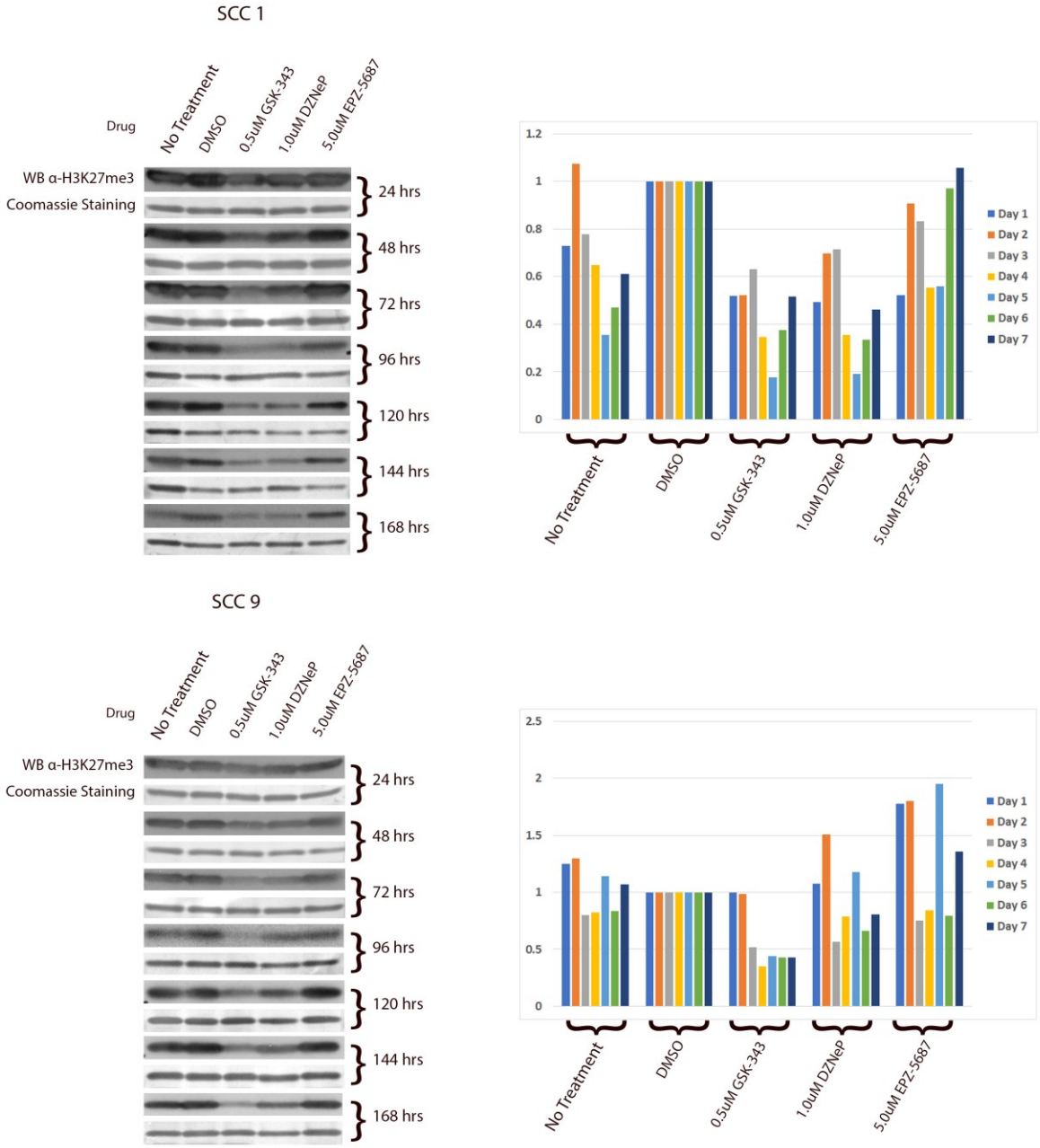

FIG. 4.3 H3K27me3 baseline varies between cell lines, with inhibitor effects on methylation status occurring as early as 48 hours post treatment.

Left: Western Blot analysis of H3K27me3. Coomassie blue staining (shown below western blot) utilized as loading control. Cells were harvested and subjected to Western Blot analysis of H3K27me3 in 24 hour intervals from 24 hours to 168 hours (1-7 days) following the addition of

an inhibitor (0.5μM GSK-343, 1.0μM DZNeP, or 5.0μM EPZ-5687) at hour 0. Right: Quantification of Western blot to left of graph based on fold differences to DMSO-treated cells.

4.3 TREATMENT WITH INHIBITORS VARIABLY ALTERS GENE EXPRESSION IN ALL CELL LINES

Numerous gene products have been shown to have direct oncogenic properties, or have shown a high degree of correlation in OPSCC. Using ddPCR in conjunction with reverse transcriptase PCR (RT PCR), a selection of 11 different genes (EGFR, TP53, MKI67, CDKN2A, CCND1, MET, PIK3CA, PTEN, EZH2, ALDH1A1, and CD44) frequently associated with HPV-positive and negative OPSCC were quantified for expressional changes against an internal normalization control EEF2 (FIG. 3). Reported results were noted according to differences and trends that deviated from DMSO-treated cells in both runs.

GSK-343-treated cell lines displayed only moderate changes in gene expression of targeted genes. A discriminatory trend based on HPV status was also identified. Of the observable changes, HPV-positive SCC-47s and SCC-104s showed an upward trend of CCND1 expression following treatment with increasing GSK-343 concentrations. Of the HPV-negative cell lines, only SCC-1 showed a slight decreasing trend in TP53 expression following treatment with increasing concentrations of GSK-343. SCC-9 showed no clear changes following treatment with GSK-343.

Treatment with DZNeP displayed the greatest variability and overall amount of expressional changes within the cell lines relative to GSK-343 and EPZ-5687. A slight discriminatory trend based on HPV status was also identified. HPV-positive SCC-47 and SCC-104 both displayed a downward trend in EGFR expression with increasing DZNeP concentrations. SCC-47 also showed slightly elevated TP53 that increased with increasing DZNeP concentrations and SCC-104 showed static decreases in CCND1, MET, CD44, EZH2, and PTEN:PIK3CA following treatment with DZNeP. The HPV-negative cell line SCC-1 displayed an upward trend of increasing EGFR and TP53, slight increases in MET and CDKN2A, and an increase in MKI67 that followed a downward trend with increasing DZNeP concentration. SCC-1 cells also saw a

static decrease in CCND1 following treatment with DZNeP. HPV-negative SCC-9 cells displayed static increases in TP53, MKI67, MET, CCND1, as well as a static decrease in PTEN:PIK3CA following treatment with DZNeP.

EPZ-5687-treated cell lines displayed few expressional changes in both HPV-positive and HPV-negative cell lines. SCC-47 cells showed downward trend of decreased MKI67 expression, and a slight downward trend of decreased CCND1 was seen in SCC-104 cells with increasing EPZ-5687 concentration. A static increase in CDKN2A was seen in HPV-negative SCC-1 cells following treatment with EPZ-5687.

Of note, treatment with DMSO alone altered gene expression of many target genes relative to cells that remained untreated. The most dramatic of these changes were seen in the HPV-positive cell lines (SCC-47 and SCC-104). DMSO-treated SCC-47 cells showed an increased expression in target gene markers EGFR, TP53, MKI67, CDKN2A, CCND1, MET, and EZH2 while PTEN:PIK3CA, CD44, and ALDH1A1 expression remained comparable to untreated cell lines. DMSO-treated SCC-104 cells displayed an increase in target genes EGFR, TP53, MKI67, CDKN2A, MET, PIK3CA, PTEN, EZH2, ALDH1A1, and CD44. CCND1 expression had decreased following treatment with DMSO. HPV-negative SCC-1 cells showed increased expression in TP53, CDKN2A, CCND1, PTEN:PIK3CA, and decreased levels of CD44 following treatment with DMSO alone. SCC-9 cells showed no appreciable changes following treatment with DMSO.

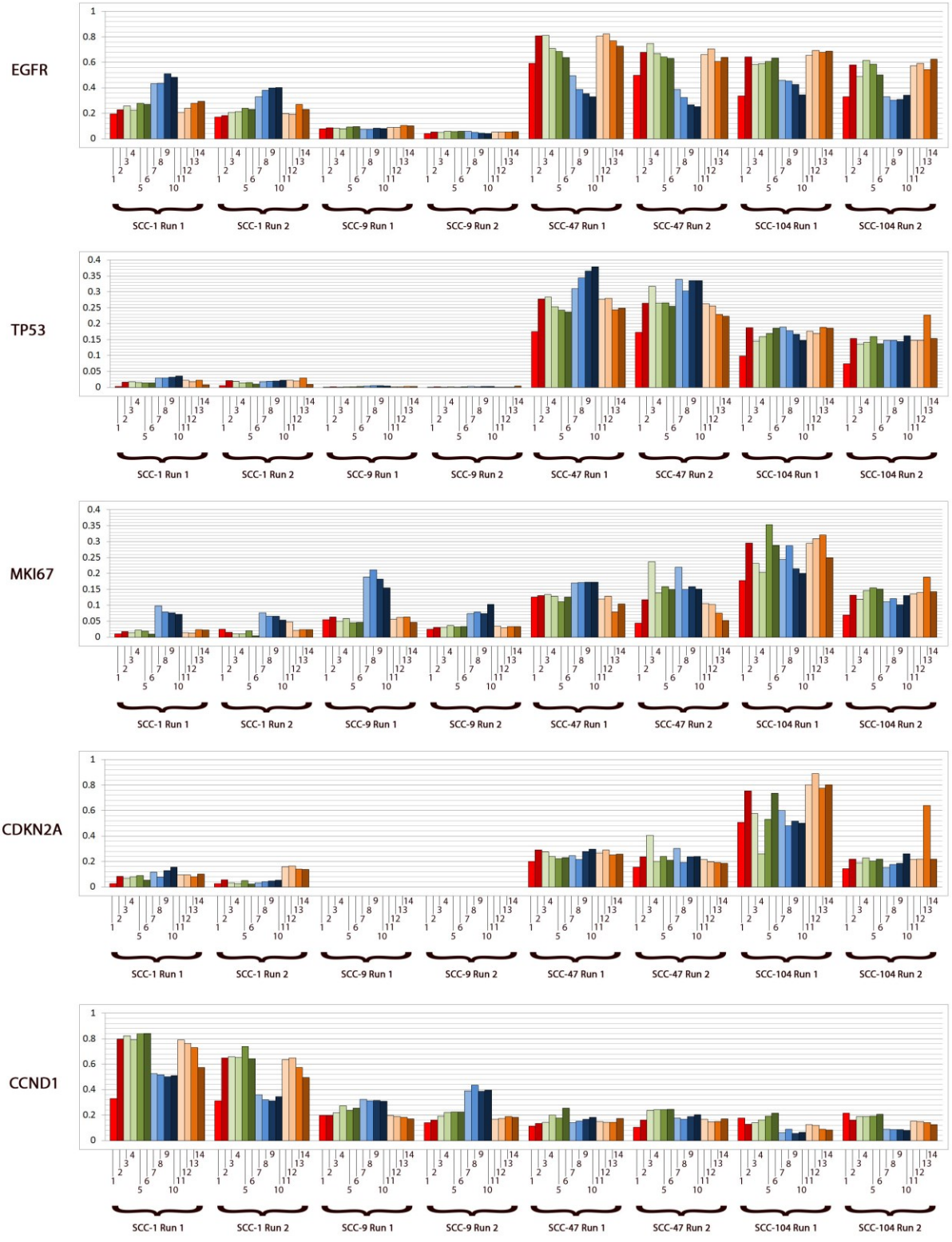
EGFR
TP53
MKI67
CDKN2A
CCND1
SCC-1 Run 1
SCC-1 Run 2
SCC-9 Run 1
SCC-9 Run 2
SCC-47 Run 1
SCC-47 Run 2
SCC-104 Run 1
SCC-104 Run 2


MET
PTEN:
PIK3CA
EZH2
ALDH1A1
CD44
SCC-1 Run 1
SCC-1 Run 2
SCC-9 Run 1
SCC-9 Run 2
SCC-47 Run 1
SCC-47 Run 2
SCC-104 Run 1
SCC-104 Run 2

FIG. 4.4 Treatment with inhibitors variably alters gene expression in all cell lines.

Droplet digital PCR analysis of expressional ratios of 9 target genes (EGFR, TP53, MKI67, CDKN2A, CCND1, MET, PTEN, PIK3CA, EZH2, ALDH1A1, and CD44) following 7-day treatment with GSK-343, DZNeP, or EPZ-5687. EEF2 was utilized as an internal reference, with exception to PTEN:PIK3CA as their gene products are directly antagonistic to one another. Scales vary according to individual expression results. SCC-9 cell line does not express CDKN2A and is therefore not pictured. Lane 1: No treatment, Lane 2: 5.00µM DMSO, 3: 0.10µM GSK-343, Lane 4: 0.25µM GSK-343, Lane 5: 0.50µM GSK-343, Lane 6: 1.00 µM GSK-343, Lane 7: 0.25µM DZNeP, Lane 8: 0.50µM DZNeP, Lane 9: 1.00µM DZNeP, Lane 10: 2.50µM DZNeP, Lane 11: 0.50µM EPZ-5687, Lane 12: 1.0µM EPZ-5687, Lane 13: 5.00µM EPZ-5687, Lane 14: 10.00µM EPZ-5687.

4.4 TREATMENT WITH DZNEP DISPLAYS ANTI-PROLIFERATIVE CHARACTERISTICS

To determine anti-proliferative effects of the inhibitors, as well as establish an approximate timeline of said effects, wound-healing assays were performed with drug application made at two separate time points. The first time point included the addition of the inhibitors on the same day the wound was made (FIG. 4A). The second time point included the addition of inhibitors 5 days prior to the wound being made (FIG. 4B). Of note, SCC-9 cell lines include a transformed fibroblast feeder layer with variably dispersed tumour foci [29]. Due to the nature of the SCC-9 cell line, observed behaviour is likely more representative of this fibroblast layer rather than cancerous cells.

Wounds made on the same day as treatment (FIG. 4A) had closed by 72 hours with no evidence of drug effects on cell proliferation. DZNeP-treated SCC-104 cells initially appear to contradict this statement, as wounds remained open after the 72 hour period. The self-adherent properties of the cell line can be attributed to this result, as the observed rate of cell proliferation in the same day treated cells far exceeded cells pre-treated with DZNeP 5 days prior to wound being made (FIG. 4B). SCC-47 cells with treatment made on the same day as wound had closed by 24 hours. DMSO and EPZ-5687-treated cells wound remained open for a longer duration relative to other

treatments (Not shown; untreated, GSK-343, and DZNeP-treated cell lines had all closed by 12 hours). This difference can most likely be attributed to the slightly larger wound margin, as 5 day DMSO and EPZ-5687 pre-treated cells had closed by a comparable timeline to the untreated cells (FIG. 4.5). These results are comparable to treated SCC-1 cell lines (FIG. 4.5B), with all but the untreated group closing by 36 hours (not shown). The results of untreated SCC-1 cells can also be attributed to a wider wound margin, as their 5 day "pre-treated" counterparts close at an earlier time point of 48 hours (not shown).

All cell lines treated with DZNeP 5 days prior to wound being made (FIG. 4B) displayed clear differences relative to those made on the same day (FIG. 4A), with wounds remaining open after 72 hours in SCC-104, SCC-1, and SCC-9 cells. DZNeP-treated SCC-47 cells had also displayed decreased proliferation; however, wound closure occurred between 24 hours and 36 hours (not shown). GSK-343-treated SCC-1 cells had impartial wound closure after 72 hours, suggesting slight anti-proliferative properties. All other cell lines had complete wound closure by 72 hours. All EPZ-5687-treated cell lines wounds had complete wound closure by 72 hours with timelines comparable to DMSO alone. DMSO appeared to display antiproliferative properties in the SCC-1 cells, with wound closure occurring at a later time point (not shown; between 48 and 60 hours) than the untreated group (between 36 and 48 hours).

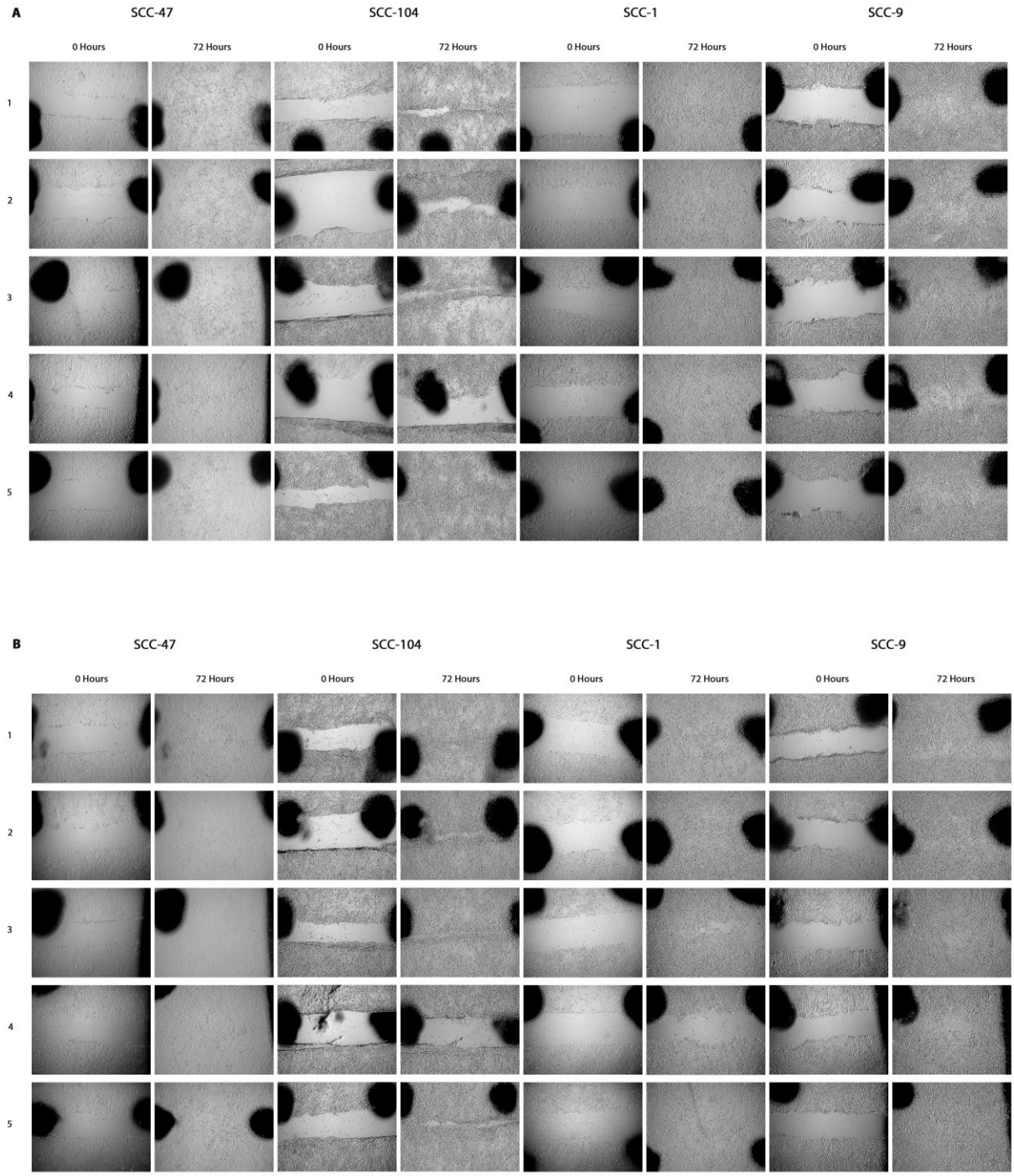

FIG. 4.5 Treatment with DZNeP displays anti-proliferative characteristics.

Wound healing assay 0 hours to 72 hour timeline with Row 1: No treatment, Row 2: 5.00μM DMSO, Row 3: 0.50μM GSK-343, Row 4: 1.00μM DZNeP, or Row 5: 5.00μM EPZ-5687.

Images taken at 0 hours and 72 hours. A. Wound made same time as treatment with inhibitor. B. Wound made 5 days following treatment with inhibitor.

4.5 TREATMENT WITH DZNEP INDUCES APOPTOSIS

To determine if treatment with inhibitors induces apoptosis, activated caspase 3 measurements were taken following 48 hours post-treatment and results were compared against untreated groups or DMSO-treated groups. There was no significant difference between untreated and DMSO-treated groups ($p=0.3515$, 5.000, 1.4455, and 3.633 for SCC-1, SCC-9, SCC-47, and SCC-104, respectively). 1.0 μM staurosporine treated for 4 hours was utilized as a positive control and displayed statistically significant results against both untreated and DMSO-treated groups in all cell lines ($p<0.05$, all cell line p-values versus untreated groups and DMSO-treated groups were $p=0.039$).

GSK-343 treatment induced statistically significant levels of apoptosis in HPV-negative cell lines SCC-1 and SCC-9 when compared to untreated levels ($p<0.05$, $p=0.039$ for both SCC-1 and SCC-9). Statistical significance was not repeated when compared to DMSO-treated cells ($p=3.633$ and 5.0000 for SCC-1 and SCC-9, respectively). No significant changes were observed following treatment with GSK-343 in the HPV-positive cell lines (versus untreated: $p=3.633$ and 1.4455, for SCC-47 and SCC-104, respectively; versus DMSO-treated groups: $p=1.4455$ and 0.3515, for SCC-47 and SCC-104, respectively).

Treatment with DZNeP induced statistically significant levels of apoptosis in both HPV-negative cell lines SCC-1 and SCC-9, as well as HPV-positive SCC-104 when compared to both untreated levels ($p<0.05$, $p=0.039$ for SCC-1, SCC-9, and SCC-104, respectively) as well as DMSO-treated groups ($p<0.05$, $p=0.039$ for SCC-1, SCC-9, and SCC-104, respectively). No statistically significance levels of apoptosis were observed following treatment with DZNeP in HPV-negative SCC-47 cells ($p=1.4455$ and 5.000 versus untreated and versus DMSO-treated groups, respectively).

EPZ-5687 yielded inconsistent levels of apoptosis, inducing apoptosis in HPV-negative SCC-9 when compared to untreated cells ($p<0.05$, $p=0.039$), but not when compared to DMSO-treated

cells (p=1.4455). Interestingly, EPZ-5687 appeared to be rescuing of cells from apoptosis in the HPV-positive SCC-104 cell line when compared to DMSO-treated cells ($p<0.05$, p=0.039), but not when compared to untreated cells (p=0.3515). EPZ-5687 had no apparent effect on apoptosis in HPV-negative SCC-1 (p=1.4455 and 5.000 versus untreated and versus DMSO-treated groups, respectively) and HPV-positive SCC-47 (p=0.3515 versus both untreated and DMSO-treated groups).

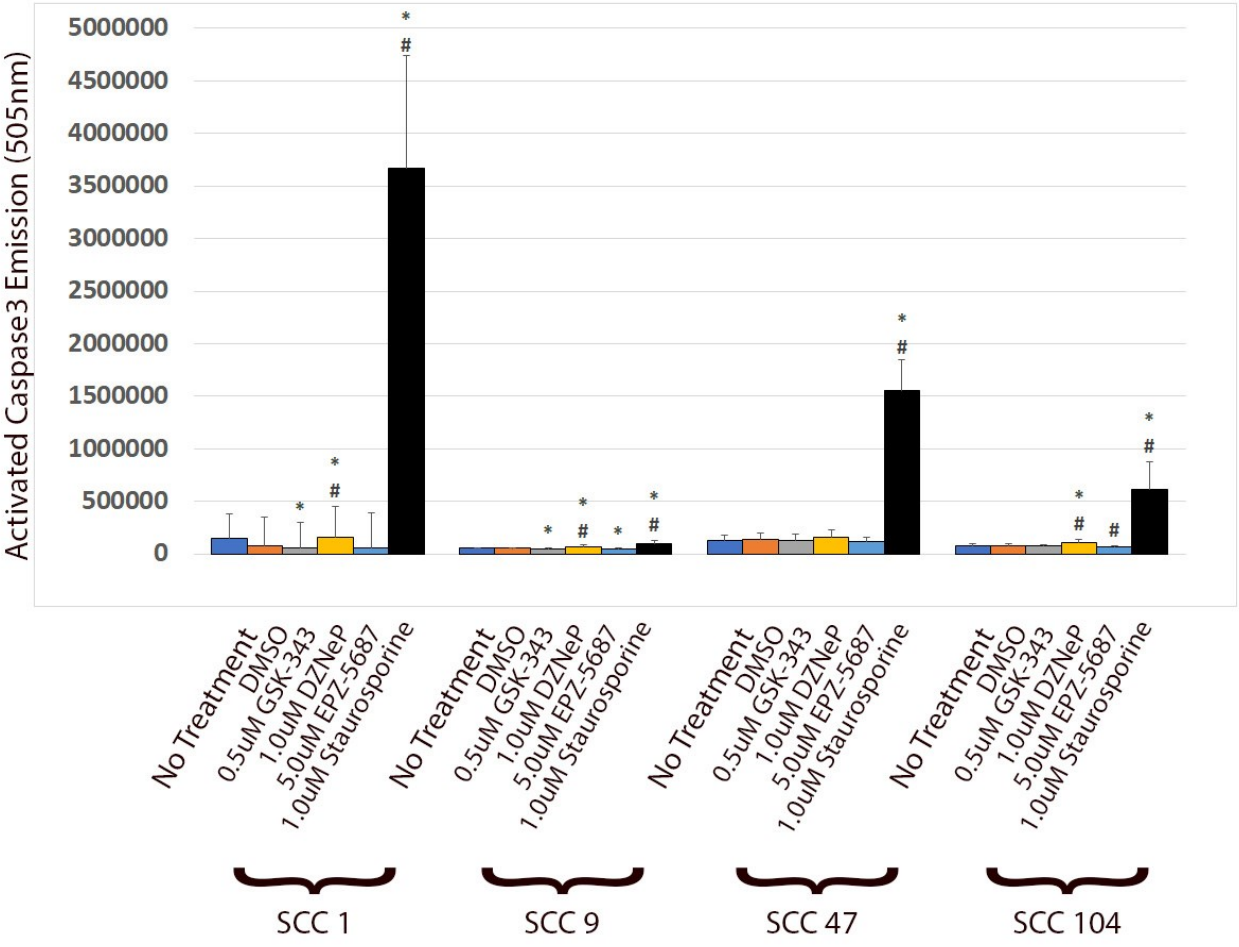

FIG. 4.6 Treatment with DZNeP induced apoptosis.

Caspase 3 assay 48 hours post treatment. 1.0 μM staurosporine (positive control) group treated for 4 hours. *: Statistically significant difference when compared to untreated groups; #: Statistically significant difference when compared to DMSO-treated groups. $p<0.05$. Standard deviation reported as error bars. 1: No treatment, 2: 5.00μM DMSO, 3: 0.50μM GSK-343, 4: 1.00μM DZNeP, 5: 5.00μM EPZ-5687, and 6: 1.0 μM staurosporine.

CHAPTER 5

DISCUSSION

This study aims to investigate the use of EZH2 inhibition as a potential chemotherapeutic target for use in HNSCC. With the incidence of HPV-positive OPSCC rising [423, 424], the need for targeted therapies becomes increasingly more urgent. Given the increased expression of EZH2 in aggressive HPV-positive OPSCC phenotypes as well as other metastatic cancers, EZH2 and its related pathways remain an attractive target for chemotherapeutic agents. Our investigation of three epigenetic inhibitors; GSK-343, DZNeP, and EPZ-5687, suggests targeting of EZH2 pathways may be of therapeutic benefit in HNSCC. EPZ-5687 however, does not appear to be an effective inhibitor of EZH2 in HNSCC.

DZNeP has been shown by others to be effective as an anti-tumoral agent alone or when combined with other agents [387, 395, 425]. DZNeP is one of the first known inhibitors of EZH2 and has well documented epigenetic and anti-proliferative effects [387]. Our findings further support these properties. DZNeP is a small-molecule SAH-hydrolase inhibitor that has been shown to act as a global HMT inhibitor [386]. When used alone as treatment, DZNeP has shown anti-tumor activity in multiple cancer types including breast [386], brain [388], liver [390], lung [391], and prostate [393]. Leukemia and prostate models have demonstrated DZNeP's anti-proliferative [392] and anti-metastatic [393] properties, respectively, and reduced tumor-mitigated angiogenesis in a glioblastoma xenograft model [394]. Our findings suggest its potential to decrease the expression of known HNSCC stem cell marker CD44 [177]. Unfortunately, *in vivo* pharmacological studies have demonstrated DZNeP to have a short half-life [426] and high toxicity in animal models at higher concentrations (DZNeP is generally well tolerated between 1.0 – 5.0μM) [386, 387]. However, gene expression results in our findings display a relatively static trend in all cell lines. This would suggest epigenetic effect to occur in concentrations lower than 0.25μM and potentially lowering cytotoxic properties of the inhibitor. Another interesting result obtained following treatment with DZNeP is the variable H3K27me3 levels with apparent dependence on HPV status. However, expressional data suggests epigenetic effect still remains present in all cell lines. One can speculate that this discrimination may be due potential interactions of HPV viral proteins with DZNeP or its related pathways in combination with DZNePs effects on histone methylation to be global rather than EZH2 specific, leaving the

desired epigenetic effect to carry out via an alternate pathway [386]. DZNeP has shown discriminative properties previously, inducing apoptosis in cancerous cells over normal cells [385, 395]

GSK-343 treated cells displayed H3K27me3 reduction in all cell lines, with no apparent resistance or sensitivity seen with application of DZNeP. The changes in gene expression as a result of GSK-343 were only moderate relative to DZNeP, with evidence of dose-dependence and slight discrimination based on HPV status. These moderate changes could be reflective of the mechanism of action of GSK-343 as a SAM-competitive inhibitor of EZH2, and therefore its increased specificity to EZH2 alone relative to DZNeP. The observed dose-dependent nature of GSK-343 may also play a role the moderate expression results observed. Because our study had utilized low doses of GSK-343 (0.1μM – 1.0μM), future investigations may benefit from increased dosages from those in this investigation. Previous studies have shown GSK-343 treatments have resulted in significant epigenetic effects in breast cancer, colon cancer, and leukemia cell lines [381], as well as inducing autophagy in hepatocellular carcinomas [382]. Additionally, treatment with GSK-343 has shown evidence of phenotypic reprogramming of cervical cancers cell lines from mesenchymal to epithelial both in vitro and in vivo [383]. This reprogramming observed reduced cell proliferation and motility, thereby blocking tumour invasion to nearby tissue. Given the genomic commonalities shared between cervical and HNSCC [427] as well as evidence of epigenetic effect seen in our study, GSK-343 remains a promising agent for combined use with anti-proliferative therapies.

EPZ-5687 showed very little efficacy in both the ability to demethylate H3K27 or lead to desired expressional changes of observed genes within an HNSCC model. These results are curious as EPZ-5687 is also a SAM-competitive inhibitor of EZH2 and has shown >500-fold selectivity to EZH2 over other human protein methylases in lymphoma models [397]. The possibility of this discrimination could be due to EPZ-5687's >5-fold affinity to the A677G mutant over EZH2 wildtype but is unlikely a satisfactory explanation as H3K27me3 inhibition was still present in both variants. However, the Pfeiffer cell line utilized in Knutson and colleagues study showed a much greater sensitivity to EPZ-5687 relative to others they had utilized [397], suggesting the

potential of secondary factors to contribute to EPZ-5687's efficacy of inhibition. Unfortunately, very little published information is available on this inhibitor to identify any consistent trends.

At the transcriptional level, HPV status appeared to play a deterministic role in gene expressional changes as a result of treatment with the EZH2 inhibitors observed. This discrimination in expressed genes may be a result of the differential DNA methylation profiles displayed in HPV-positive carcinomas [126, 194, 195]. Theoretically, varying methylation at promotor regions may limit the epigenetic effects of EZH2 inhibitors, instead only reactivating genes not silenced by DNA methylation. A study performed by Bartke and colleagues provided evidence toward the limitations of HMT and DNMT inhibitors alone by demonstrating reduced regulation of PRC2 following DNA methylation [428]. They observed a far more complex interaction between histone and DNA methylation statuses on transcriptional activity, involving deregulation of one enzyme based on methylation status of DNA or histone. Therefore, desired epigenetic effects of EZH2 inhibitors may be further enhanced by combination with DNMT inhibitors such as 5-azacytidine. Proposed combinations such as this, of course, run the risk of increasing toxic effect. DNA demethylating agents have traditional antiproliferative activity at high doses. 5-azacytidine, for example, has been shown to cause neutropenia [429]. Fortunately, demethylating agents have been shown to be generally mild at lower doses [430] and for the proposed epigenetic action, the use of extremely low doses for both agents (EZH2 inhibitors and DNMT inhibitors) could be utilized to avoid this antiproliferative activity. Our study further supports this notion, as expressional changes occurred in both GSK-343 and DZNeP at low doses. ChIP-sequence analyses performed on colon, breast and leukemia cancer cell lines by Sato and colleagues [381] has already shown evidence for the synergistic effects of DNMT inhibitors with histone methyltransferase inhibitors while maintaining their selectivity towards various oncogenes.

The most prominent limitation of this study is seen in the expression results following treatment with DMSO. The majority of targeted genes in both HPV-negative SCC-1 and HPV-positive SCC-47 and SCC-104 have displayed clear alterations in gene expression following treatment with DMSO as compared to untreated cells. Historically, DMSO has been shown to have multiple effects on cellular functioning [431]. Its most noteworthy trait includes its ability to induce differentiation in malignant tumor cells at low doses, resulting in a loss of tumorigenicity

and altered cell morphology into more mature, differentiated cells in leukemias, colon, prostate, lung, and breast carcinomas [432-434]. The exact mechanism of DMSO's ability to induce differentiation remains relatively unknown; however, a study performed by Iwatani et al suggests DMSO impacting a cells epigenetic profile. Their study had shown the upregulation of DNA methyltransferase Dnmt3a and alteration of genome-wide DNA methylation profiles following the application of DMSO [435]. Contrasting results were seen in a study performed by Kita et al, showing DMSO reducing stemness in association with decreased DNMT3A and DNMT3L expression [436]. Regardless of the contention, genome-wide methylation changes would theoretically be present and it is understandable why our gene target expression levels deviated from untreated baseline levels so dramatically. Given DMSOs already widespread clinical use as a drug vehicle and cryopreservant, as well as the limited amount of solvents available for water-insoluble drug agents, it is an issue that will continue to persist. Additionally, there are inherent limitations of quantifying values from film paper, as overexposure of film runs the potential of film "reverse banding" or "photobleaching", potentially providing lower values in the quantification process than what is representative. The opposite is true as well, with saturated dark values being limited to the darkening capacity of the film following reaction from silver halide molecules [437, 438]. To minimize these issues, lower exposure times were utilized in the quantification process. Other limitations of this study include the use of *in vitro* models on only 4 cell lines.

Both DZNeP and GSK-343 display potential for clinical application as adjunctive therapies in HNSCC, potentially sensitizing tumors to current chemotherapies or limiting cell differentiation. Previous research suggests the use of combination therapies with DNMT inhibitors could have synergistic effects on epigenetic changes within the cell. Future experimentation warrants the use of primary cell cultures as well as tumor xenografts models to further determine clinical efficacy.

5.1 CONCLUSIONS

In HNSCC cell culture models, the targeting of EZH2 and its related pathways appears to have anti-tumorigenic effects which may be dependent on oncogenic HPV status. EPZ-5687 does not

appear to be an effective inhibitor of EZH2 in both HPV positive and negative HNSCC cell lines.

CHAPTER 6

BIBLIOGRAPHY

1. Waddington, C., *Canalization of development and the inheritance of acquired characteristics.* Nature, 1942. **150**(3811): p. 563-565.
2. Wu, C. and J.R. Morris, *Genes, genetics, and epigenetics: a correspondence.* Science, 2001. **293**(5532): p. 1103-5.
3. Feinberg, A.P. and B. Tycko, *The history of cancer epigenetics.* Nat Rev Cancer, 2004. **4**(2): p. 143-53.
4. Kanwal, R., K. Gupta, and S. Gupta, *Cancer epigenetics: an introduction.* Methods Mol Biol, 2015. **1238**: p. 3-25.
5. Lyon, M.F., *Gene action in the X-chromosome of the mouse (Mus musculus L.).* Nature, 1961. **190**: p. 372-3.
6. Kanwal, R. and S. Gupta, *Epigenetic modifications in cancer.* Clin Genet, 2012. **81**(4): p. 303-11.
7. Sharma, S., T.K. Kelly, and P.A. Jones, *Epigenetics in cancer.* Carcinogenesis, 2010. **31**(1): p. 27-36.
8. Gupta, G.P. and J. Massague, *Cancer metastasis: building a framework.* Cell, 2006. **127**(4): p. 679-95.
9. Ducasse, M. and M.A. Brown, *Epigenetic aberrations and cancer.* Mol Cancer, 2006. **5**: p. 60.
10. Perroud, N., et al., *METHYLATION OF SEROTONIN RECEPTOR 3A IN ADHD, BORDERLINE PERSONALITY, AND BIPOLAR DISORDERS: LINK WITH SEVERITY OF THE DISORDERS AND CHILDHOOD MALTREATMENT.* Depress Anxiety, 2015.
11. Jenuwein, T. and C.D. Allis, *Translating the histone code.* Science, 2001. **293**(5532): p. 1074-80.
12. Berger, S.L., *The complex language of chromatin regulation during transcription.* Nature, 2007. **447**(7143): p. 407-12.
13. Kouzarides, T., *Chromatin modifications and their function.* Cell, 2007. **128**(4): p. 693-705.
14. Mattick, J.S. and I.V. Makunin, *Non-coding RNA.* Hum Mol Genet, 2006. **15 Spec No 1**: p. R17-29.
15. Lo, P.K. and S. Sukumar, *Epigenomics and breast cancer.* Pharmacogenomics, 2008. **9**(12): p. 1879-902.
16. Jones, P.A. and S.B. Baylin, *The fundamental role of epigenetic events in cancer.* Nat Rev Genet, 2002. **3**(6): p. 415-28.
17. Feinberg, A.P. and B. Vogelstein, *Hypomethylation distinguishes genes of some human cancers from their normal counterparts.* Nature, 1983. **301**(5895): p. 89-92.
18. Ehrlich, M., *DNA hypomethylation, cancer, the immunodeficiency, centromeric region instability, facial anomalies syndrome and chromosomal rearrangements.* J Nutr, 2002. **132**(8 Suppl): p. 2424S-2429S.
19. Ehrlich, M., *DNA methylation in cancer: too much, but also too little.* Oncogene, 2002. **21**(35): p. 5400-13.
20. Robertson, K.D. and P.A. Jones, *DNA methylation: past, present and future directions.* Carcinogenesis, 2000. **21**(3): p. 461-7.
21. Bestor, T.H., *The DNA methyltransferases of mammals.* Hum Mol Genet, 2000. **9**(16): p. 2395-402.
22. Okano, M., et al., *DNA methyltransferases Dnmt3a and Dnmt3b are essential for de novo methylation and mammalian development.* Cell, 1999. **99**(3): p. 247-57.
23. van Kempen, P.M., et al., *Differences in methylation profiles between HPV-positive and HPV-negative oropharynx squamous cell carcinoma: a systematic review.* Epigenetics, 2014. **9**(2): p. 194-203.
24. Teh, M.T., et al., *FOXM1 induces a global methylation signature that mimics the cancer epigenome in head and neck squamous cell carcinoma.* PLoS One, 2012. **7**(3): p. e34329.

25. Baylin, S.B., *DNA methylation and gene silencing in cancer.* Nat Clin Pract Oncol, 2005. **2 Suppl 1**: p. S4-11.
26. Bakhtiar, S.M., A. Ali, and D. Barh, *Epigenetics in head and neck cancer.* Methods Mol Biol, 2015. **1238**: p. 751-69.
27. Holde, K.E.v., *Chromatin*. 1989, New York: Springer-Verlag.
28. Wolffe, A., *Chromatin: Structure and Function*. 1998: Academic Press.
29. Kornberg, R.D., *Chromatin structure: a repeating unit of histones and DNA.* Science, 1974. **184**(4139): p. 868-71.
30. Felsenfeld, G. and M. Groudine, *Controlling the double helix.* Nature, 2003. **421**(6921): p. 448-53.
31. Shogren-Knaak, M., et al., *Histone H4-K16 acetylation controls chromatin structure and protein interactions.* Science, 2006. **311**(5762): p. 844-7.
32. Martin, C. and Y. Zhang, *The diverse functions of histone lysine methylation.* Nat Rev Mol Cell Biol, 2005. **6**(11): p. 838-49.
33. Wysocka, J., C.D. Allis, and S. Coonrod, *Histone arginine methylation and its dynamic regulation.* Front Biosci, 2006. **11**: p. 344-55.
34. Anayannis, N.V., N.F. Schlecht, and T.J. Belbin, *Epigenetic Mechanisms of Human Papillomavirus-Associated Head and Neck Cancer.* Arch Pathol Lab Med, 2015. **139**(11): p. 1373-8.
35. Gonzalez-Ramirez, I., et al., *Histones and long non-coding RNAs: the new insights of epigenetic deregulation involved in oral cancer.* Oral Oncol, 2014. **50**(8): p. 691-5.
36. Mai, A., et al., *Small-molecule inhibitors of histone acetyltransferase activity: identification and biological properties.* J Med Chem, 2006. **49**(23): p. 6897-907.
37. Choudhuri, S., *From Waddington's epigenetic landscape to small noncoding RNA: some important milestones in the history of epigenetics research.* Toxicol Mech Methods, 2011. **21**(4): p. 252-74.
38. Marmorstein, R. and S.Y. Roth, *Histone acetyltransferases: function, structure, and catalysis.* Curr Opin Genet Dev, 2001. **11**(2): p. 155-61.
39. Sun, X.J., et al., *The Role of Histone Acetyltransferases in Normal and Malignant Hematopoiesis.* Front Oncol, 2015. **5**: p. 108.
40. Holth, L.T., et al., *Chromatin, nuclear matrix and the cytoskeleton: role of cell structure in neoplastic transformation (review).* Int J Oncol, 1998. **13**(4): p. 827-37.
41. Burdelski, C., et al., *HDAC1 overexpression independently predicts biochemical recurrence and is associated with rapid tumor cell proliferation and genomic instability in prostate cancer.* Exp Mol Pathol, 2015. **98**(3): p. 419-26.
42. Fenrick, R. and S.W. Hiebert, *Role of histone deacetylases in acute leukemia.* J Cell Biochem Suppl, 1998. **30-31**: p. 194-202.
43. Strahl, B.D. and C.D. Allis, *The language of covalent histone modifications.* Nature, 2000. **403**(6765): p. 41-5.
44. Chi, P., C.D. Allis, and G.G. Wang, *Covalent histone modifications--miswritten, misinterpreted and mis-erased in human cancers.* Nat Rev Cancer, 2010. **10**(7): p. 457-69.
45. Felsenfeld, G., *A brief history of epigenetics.* Cold Spring Harb Perspect Biol, 2014. **6**(1).
46. Li, C.H. and Y. Chen, *Targeting long non-coding RNAs in cancers: progress and prospects.* Int J Biochem Cell Biol, 2013. **45**(8): p. 1895-910.
47. Esteller, M., *Non-coding RNAs in human disease.* Nat Rev Genet, 2011. **12**(12): p. 861-74.
48. Gasche, J.A. and A. Goel, *Epigenetic mechanisms in oral carcinogenesis.* Future Oncol, 2012. **8**(11): p. 1407-25.
49. Calin, G.A. and C.M. Croce, *MicroRNA signatures in human cancers.* Nat Rev Cancer, 2006. **6**(11): p. 857-66.

50. Ouillette, P., et al., *The prognostic significance of various 13q14 deletions in chronic lymphocytic leukemia.* Clin Cancer Res, 2011. **17**(21): p. 6778-90.
51. Sood, P., et al., *Cell-type-specific signatures of microRNAs on target mRNA expression.* Proc Natl Acad Sci U S A, 2006. **103**(8): p. 2746-51.
52. Lujambio, A., et al., *Genetic unmasking of an epigenetically silenced microRNA in human cancer cells.* Cancer Res, 2007. **67**(4): p. 1424-9.
53. Kugel, J.F. and J.A. Goodrich, *Non-coding RNAs: key regulators of mammalian transcription.* Trends Biochem Sci, 2012. **37**(4): p. 144-51.
54. Waddington, C., *Epigenetics and evolution.* Symp. Soc. Exp. Biol 1953. **7**: p. 186-199.
55. Waddington, C., *The strategy of the genes. A discussion of some aspects of theoretical biology. With an appendix by H. Kacser*, G. Allen, Editor. 1957, Unwin Ltd: London. p. pp. ix +-262 pp.
56. Watson, J.D. and F.H. Crick, *Molecular structure of nucleic acids; a structure for deoxyribose nucleic acid.* Nature, 1953. **171**(4356): p. 737-8.
57. Lewis, E.B., *The theory and application of a new method of detecting chromosomal rearrangements in Drosophila melanogaster.* American Naturalist, 1954: p. 225-239.
58. Brink, R.A., *Paramutation at the R locus in maize.* Cold Spring Harb Symp Quant Biol, 1958. **23**: p. 379-91.
59. Riggs, A.D., *X inactivation, differentiation, and DNA methylation.* Cytogenet Cell Genet, 1975. **14**(1): p. 9-25.
60. Johnson, T.B., & Coghill, R.D., *Researches on pyrimidines. C111. The discovery of 5-methyl-cytosine in tuberculinic acid, the nucleic acid of the tubercle bacillus1.* Journal of the American Chemical Society, 1925. **47**(11): p. 2838-2844.
61. Hotchkiss, R.D., *The quantitative separation of purines, pyrimidines, and nucleosides by paper chromatography.* J Biol Chem, 1948. **175**(1): p. 315-32.
62. Wyatt, G.R., *Occurrence of 5-methyl-cytosine in nucleic acids.* Nature, 1950(166): p. 237-238.
63. Holliday, R. and J.E. Pugh, *DNA modification mechanisms and gene activity during development.* Science, 1975. **187**(4173): p. 226-32.
64. Allfrey, V.G., R. Faulkner, and A.E. Mirsky, *ACETYLATION AND METHYLATION OF HISTONES AND THEIR POSSIBLE ROLE IN THE REGULATION OF RNA SYNTHESIS.* Proc Natl Acad Sci U S A, 1964. **51**: p. 786-94.
65. Riggs, M.G., et al., *n-Butyrate causes histone modification in HeLa and Friend erythroleukaemia cells.* Nature, 1977. **268**(5619): p. 462-4.
66. Chen, D., et al., *Regulation of transcription by a protein methyltransferase.* Science, 1999. **284**(5423): p. 2174-7.
67. Strahl, B.D., et al., *Methylation of histone H3 at lysine 4 is highly conserved and correlates with transcriptionally active nuclei in Tetrahymena.* Proc Natl Acad Sci U S A, 1999. **96**(26): p. 14967-72.
68. Durrin, L.K., et al., *Yeast histone H4 N-terminal sequence is required for promoter activation in vivo.* Cell, 1991. **65**(6): p. 1023-31.
69. Brownell, J.E., et al., *Tetrahymena histone acetyltransferase A: a homolog to yeast Gcn5p linking histone acetylation to gene activation.* Cell, 1996. **84**(6): p. 843-51.
70. Kleff, S., et al., *Identification of a gene encoding a yeast histone H4 acetyltransferase.* J Biol Chem, 1995. **270**(42): p. 24674-7.
71. Brownell, J.E. and C.D. Allis, *An activity gel assay detects a single, catalytically active histone acetyltransferase subunit in Tetrahymena macronuclei.* Proc Natl Acad Sci U S A, 1995. **92**(14): p. 6364-8.

72. Taunton, J., C.A. Hassig, and S.L. Schreiber, *A mammalian histone deacetylase related to the yeast transcriptional regulator Rpd3p.* Science, 1996. **272**(5260): p. 408-11.
73. Shiio, Y. and R.N. Eisenman, *Histone sumoylation is associated with transcriptional repression.* Proc Natl Acad Sci U S A, 2003. **100**(23): p. 13225-30.
74. Lee, R.C., R.L. Feinbaum, and V. Ambros, *The C. elegans heterochronic gene lin-4 encodes small RNAs with antisense complementarity to lin-14.* Cell, 1993. **75**(5): p. 843-54.
75. Fire, A., et al., *Potent and specific genetic interference by double-stranded RNA in Caenorhabditis elegans.* Nature, 1998. **391**(6669): p. 806-11.
76. Brown, C.J., et al., *A gene from the region of the human X inactivation centre is expressed exclusively from the inactive X chromosome.* Nature, 1991. **349**(6304): p. 38-44.
77. Huarte, M. and J.L. Rinn, *Large non-coding RNAs: missing links in cancer?* Hum Mol Genet, 2010. **19**(R2): p. R152-61.
78. Markert, C.L., *Neoplasia: a disease of cell differentiation.* Cancer Res, 1968. **28**(9): p. 1908-14.
79. Holliday, R., *A new theory of carcinogenesis.* Br J Cancer, 1979. **40**(4): p. 513-22.
80. Guo, M. and W. Yan, *Epigenetics of gastric cancer.* Methods Mol Biol, 2015. **1238**: p. 783-99.
81. la Rosa, A.H., et al., *The role of epigenetics in kidney malignancies.* Cent European J Urol, 2015. **68**(2): p. 157-64.
82. Hammoud, S.S., B.R. Cairns, and D.A. Jones, *Epigenetic regulation of colon cancer and intestinal stem cells.* Curr Opin Cell Biol, 2013. **25**(2): p. 177-83.
83. Duenas-Gonzalez, A., et al., *Epigenetics of cervical cancer. An overview and therapeutic perspectives.* Mol Cancer, 2005. **4**: p. 38.
84. Baylin, S.B., et al., *DNA methylation patterns of the calcitonin gene in human lung cancers and lymphomas.* Cancer Res, 1986. **46**(6): p. 2917-22.
85. Greger, V., et al., *Epigenetic changes may contribute to the formation and spontaneous regression of retinoblastoma.* Hum Genet, 1989. **83**(2): p. 155-8.
86. Gonzalez-Zulueta, M., et al., *Methylation of the 5' CpG island of the p16/CDKN2 tumor suppressor gene in normal and transformed human tissues correlates with gene silencing.* Cancer Res, 1995. **55**(20): p. 4531-5.
87. Herman, J.G., et al., *Silencing of the VHL tumor-suppressor gene by DNA methylation in renal carcinoma.* Proc Natl Acad Sci U S A, 1994. **91**(21): p. 9700-4.
88. Lengauer, C., K.W. Kinzler, and B. Vogelstein, *DNA methylation and genetic instability in colorectal cancer cells.* Proc Natl Acad Sci U S A, 1997. **94**(6): p. 2545-50.
89. Bachman, K.E., et al., *Histone modifications and silencing prior to DNA methylation of a tumor suppressor gene.* Cancer Cell, 2003. **3**(1): p. 89-95.
90. Pogo, B.G., V.G. Allfrey, and A.E. Mirsky, *RNA synthesis and histone acetylation during the course of gene activation in lymphocytes.* Proc Natl Acad Sci U S A, 1966. **55**(4): p. 805-12.
91. Struhl, K., *Histone acetylation and transcriptional regulatory mechanisms.* Genes Dev, 1998. **12**(5): p. 599-606.
92. Jones, P.L., et al., *Methylated DNA and MeCP2 recruit histone deacetylase to repress transcription.* Nat Genet, 1998. **19**(2): p. 187-91.
93. Wade, P.A., et al., *Mi-2 complex couples DNA methylation to chromatin remodelling and histone deacetylation.* Nat Genet, 1999. **23**(1): p. 62-6.
94. Nguyen, C.T., et al., *Histone H3-lysine 9 methylation is associated with aberrant gene silencing in cancer cells and is rapidly reversed by 5-aza-2'-deoxycytidine.* Cancer Res, 2002. **62**(22): p. 6456-61.
95. He, L., et al., *A microRNA polycistron as a potential human oncogene.* Nature, 2005. **435**(7043): p. 828-33.

96. O'Donnell, K.A., et al., *c-Myc-regulated microRNAs modulate E2F1 expression.* Nature, 2005. **435**(7043): p. 839-43.
97. Johnson, S.M., et al., *RAS is regulated by the let-7 microRNA family.* Cell, 2005. **120**(5): p. 635-47.
98. Saito, Y., et al., *Specific activation of microRNA-127 with downregulation of the proto-oncogene BCL6 by chromatin-modifying drugs in human cancer cells.* Cancer Cell, 2006. **9**(6): p. 435-43.
99. Ma, L., J. Teruya-Feldstein, and R.A. Weinberg, *Tumour invasion and metastasis initiated by microRNA-10b in breast cancer.* Nature, 2007. **449**(7163): p. 682-8.
100. Tavazoie, S.F., et al., *Endogenous human microRNAs that suppress breast cancer metastasis.* Nature, 2008. **451**(7175): p. 147-52.
101. Medina, P.P., M. Nolde, and F.J. Slack, *OncomiR addiction in an in vivo model of microRNA-21-induced pre-B-cell lymphoma.* Nature, 2010. **467**(7311): p. 86-90.
102. Melo, S.A., et al., *Cancer exosomes perform cell-independent microRNA biogenesis and promote tumorigenesis.* Cancer Cell, 2014. **26**(5): p. 707-21.
103. Chen, J., et al., *A methylenetetrahydrofolate reductase polymorphism and the risk of colorectal cancer.* Cancer Res, 1996. **56**(21): p. 4862-4.
104. Pandey, M., S. Shukla, and S. Gupta, *Promoter demethylation and chromatin remodeling by green tea polyphenols leads to re-expression of GSTP1 in human prostate cancer cells.* Int J Cancer, 2010. **126**(11): p. 2520-33.
105. Siegel, R.L., K.D. Miller, and A. Jemal, *Cancer statistics, 2015.* CA Cancer J Clin, 2015. **65**(1): p. 5-29.
106. Barber, B.R., et al., *Molecular predictors of locoregional and distant metastases in oropharyngeal squamous cell carcinoma.* J Otolaryngol Head Neck Surg, 2013. **42**: p. 53.
107. Stenson KM, B.B., & Ross ME. *Epidemiology and risk factors for head and neck cancer*. UpToDate 2014 2015 [cited 2015 October 16]; Available from: http://www.uptodate.com/contents/epidemiology-and-risk-factors-for-head-and-neck-cancer.
108. Pezzuto, F., et al., *Update on Head and Neck Cancer: Current Knowledge on Epidemiology, Risk Factors, Molecular Features and Novel Therapies.* Oncology, 2015. **89**(3): p. 125-36.
109. Lambert, R., et al., *Epidemiology of cancer from the oral cavity and oropharynx.* Eur J Gastroenterol Hepatol, 2011. **23**(8): p. 633-41.
110. Curado, M.P. and P. Boyle, *Epidemiology of head and neck squamous cell carcinoma not related to tobacco or alcohol.* Curr Opin Oncol, 2013. **25**(3): p. 229-34.
111. Mehanna, H., et al., *Prevalence of human papillomavirus in oropharyngeal and nonoropharyngeal head and neck cancer--systematic review and meta-analysis of trends by time and region.* Head Neck, 2013. **35**(5): p. 747-55.
112. *IARC Monographs on the Evaluation of Carcinogenic Risks to Humans.* 2012. **100B**.
113. zur Hausen, H., *Papillomaviruses and cancer: from basic studies to clinical application.* Nat Rev Cancer, 2002. **2**(5): p. 342-50.
114. de Martel, C., et al., *Worldwide burden of cancer attributable to HPV by site, country and HPV type.* Int J Cancer, 2017. **141**(4): p. 664-670.
115. Yugawa, T. and T. Kiyono, *Molecular mechanisms of cervical carcinogenesis by high-risk human papillomaviruses: novel functions of E6 and E7 oncoproteins.* Rev Med Virol, 2009. **19**(2): p. 97-113.
116. Gillison, M.L. and C. Restighini, *Anticipation of the Impact of Human Papillomavirus on Clinical Decision Making for the Head and Neck Cancer Patient.* Hematol Oncol Clin North Am, 2015. **29**(6): p. 1045-60.
117. Doorbar, J., et al., *Human papillomavirus molecular biology and disease association.* Rev Med Virol, 2015. **25 Suppl 1**: p. 2-23.

118. Sapp, M. and M. Bienkowska-Haba, *Viral entry mechanisms: human papillomavirus and a long journey from extracellular matrix to the nucleus.* FEBS J, 2009. **276**(24): p. 7206-16.
119. Selinka, H.C., et al., *Inhibition of transfer to secondary receptors by heparan sulfate-binding drug or antibody induces noninfectious uptake of human papillomavirus.* J Virol, 2007. **81**(20): p. 10970-80.
120. Surviladze, Z., A. Dziduszko, and M.A. Ozbun, *Essential roles for soluble virion-associated heparan sulfonated proteoglycans and growth factors in human papillomavirus infections.* PLoS Pathog, 2012. **8**(2): p. e1002519.
121. Surviladze, Z., et al., *Cellular entry of human papillomavirus type 16 involves activation of the phosphatidylinositol 3-kinase/Akt/mTOR pathway and inhibition of autophagy.* J Virol, 2013. **87**(5): p. 2508-17.
122. Bergant Marusic, M., et al., *Human papillomavirus L2 facilitates viral escape from late endosomes via sorting nexin 17.* Traffic, 2012. **13**(3): p. 455-67.
123. Jeon, S. and P.F. Lambert, *Integration of human papillomavirus type 16 DNA into the human genome leads to increased stability of E6 and E7 mRNAs: implications for cervical carcinogenesis.* Proc Natl Acad Sci U S A, 1995. **92**(5): p. 1654-8.
124. Kumar Gupta, A. and M. Kumar, *HPVbase--a knowledgebase of viral integrations, methylation patterns and microRNAs aberrant expression: As potential biomarkers for Human papillomaviruses mediated carcinomas.* Sci Rep, 2015. **5**: p. 12522.
125. Akagi, K., et al., *Genome-wide analysis of HPV integration in human cancers reveals recurrent, focal genomic instability.* Genome Res, 2014. **24**(2): p. 185-99.
126. Sartor, M.A., et al., *Genome-wide methylation and expression differences in HPV(+) and HPV(-) squamous cell carcinoma cell lines are consistent with divergent mechanisms of carcinogenesis.* Epigenetics, 2011. **6**(6): p. 777-87.
127. Maruya, S., et al., *Differential methylation status of tumor-associated genes in head and neck squamous carcinoma: incidence and potential implications.* Clin Cancer Res, 2004. **10**(11): p. 3825-30.
128. Scholzen, T. and J. Gerdes, *The Ki-67 protein: from the known and the unknown.* J Cell Physiol, 2000. **182**(3): p. 311-22.
129. Gerdes, J., et al., *Cell cycle analysis of a cell proliferation-associated human nuclear antigen defined by the monoclonal antibody Ki-67.* J Immunol, 1984. **133**(4): p. 1710-5.
130. Wei, S.H., et al., *Prognostic DNA methylation biomarkers in ovarian cancer.* Clin Cancer Res, 2006. **12**(9): p. 2788-94.
131. Koturbash, I., F.A. Beland, and I.P. Pogribny, *Role of epigenetic events in chemical carcinogenesis--a justification for incorporating epigenetic evaluations in cancer risk assessment.* Toxicol Mech Methods, 2011. **21**(4): p. 289-97.
132. Kidani, K., et al., *High expression of EZH2 is associated with tumor proliferation and prognosis in human oral squamous cell carcinomas.* Oral Oncol, 2009. **45**(1): p. 39-46.
133. Zhao, L., et al., *Role of EZH2 in oral squamous cell carcinoma carcinogenesis.* Gene, 2014. **537**(2): p. 197-202.
134. Orellana, E.A. and A.L. Kasinski, *MicroRNAs in Cancer: A Historical Perspective on the Path from Discovery to Therapy.* Cancers (Basel), 2015. **7**(3): p. 1388-405.
135. Sherr, C.J. and F. McCormick, *The RB and p53 pathways in cancer.* Cancer Cell, 2002. **2**(2): p. 103-12.
136. Suh, Y., et al., *Clinical update on cancer: molecular oncology of head and neck cancer.* Cell Death Dis, 2014. **5**: p. e1018.

137. Vogelstein, B., D. Lane, and A.J. Levine, *Surfing the p53 network.* Nature, 2000. **408**(6810): p. 307-10.
138. Polager, S. and D. Ginsberg, *p53 and E2f: partners in life and death.* Nat Rev Cancer, 2009. **9**(10): p. 738-48.
139. Giacinti, C. and A. Giordano, *RB and cell cycle progression.* Oncogene, 2006. **25**(38): p. 5220-7.
140. Agrawal, N., et al., *Exome sequencing of head and neck squamous cell carcinoma reveals inactivating mutations in NOTCH1.* Science, 2011. **333**(6046): p. 1154-7.
141. Poeta, M.L., et al., *TP53 mutations and survival in squamous-cell carcinoma of the head and neck.* N Engl J Med, 2007. **357**(25): p. 2552-61.
142. Stransky, N., et al., *The mutational landscape of head and neck squamous cell carcinoma.* Science, 2011. **333**(6046): p. 1157-60.
143. Smeets, S.J., et al., *Genome-wide DNA copy number alterations in head and neck squamous cell carcinomas with or without oncogene-expressing human papillomavirus.* Oncogene, 2006. **25**(17): p. 2558-64.
144. Scheffner, M., et al., *The E6 oncoprotein encoded by human papillomavirus types 16 and 18 promotes the degradation of p53.* Cell, 1990. **63**(6): p. 1129-36.
145. Huibregtse, J.M., M. Scheffner, and P.M. Howley, *A cellular protein mediates association of p53 with the E6 oncoprotein of human papillomavirus types 16 or 18.* EMBO J, 1991. **10**(13): p. 4129-35.
146. Dyson, N., et al., *The human papilloma virus-16 E7 oncoprotein is able to bind to the retinoblastoma gene product.* Science, 1989. **243**(4893): p. 934-7.
147. Huh, K., et al., *Human papillomavirus type 16 E7 oncoprotein associates with the cullin 2 ubiquitin ligase complex, which contributes to degradation of the retinoblastoma tumor suppressor.* J Virol, 2007. **81**(18): p. 9737-47.
148. Wang, H., et al., *P16INK4A as a surrogate biomarker for human papillomavirus-associated oropharyngeal carcinoma: consideration of some aspects.* Cancer Sci, 2013. **104**(12): p. 1553-9.
149. Leevers, S.J., B. Vanhaesebroeck, and M.D. Waterfield, *Signalling through phosphoinositide 3-kinases: the lipids take centre stage.* Curr Opin Cell Biol, 1999. **11**(2): p. 219-25.
150. Lamorte, L. and M. Park, *The receptor tyrosine kinases: role in cancer progression.* Surg Oncol Clin N Am, 2001. **10**(2): p. 271-88, viii.
151. Engelman, J.A., *Targeting PI3K signalling in cancer: opportunities, challenges and limitations.* Nat Rev Cancer, 2009. **9**(8): p. 550-62.
152. Martelli, A.M., et al., *Targeting the translational apparatus to improve leukemia therapy: roles of the PI3K/PTEN/Akt/mTOR pathway.* Leukemia, 2011. **25**(7): p. 1064-79.
153. Sparks, C.A. and D.A. Guertin, *Targeting mTOR: prospects for mTOR complex 2 inhibitors in cancer therapy.* Oncogene, 2010. **29**(26): p. 3733-44.
154. Betz, C., et al., *Feature Article: mTOR complex 2-Akt signaling at mitochondria-associated endoplasmic reticulum membranes (MAM) regulates mitochondrial physiology.* Proc Natl Acad Sci U S A, 2013. **110**(31): p. 12526-34.
155. Abraham, R.T., *mTOR as a positive regulator of tumor cell responses to hypoxia.* Curr Top Microbiol Immunol, 2004. **279**: p. 299-319.
156. Molinolo, A.A., et al., *mTOR as a molecular target in HPV-associated oral and cervical squamous carcinomas.* Clin Cancer Res, 2012. **18**(9): p. 2558-68.
157. Qiu, W., et al., *PIK3CA mutations in head and neck squamous cell carcinoma.* Clin Cancer Res, 2006. **12**(5): p. 1441-6.
158. Cancer Genome Atlas, N., *Comprehensive genomic characterization of head and neck squamous cell carcinomas.* Nature, 2015. **517**(7536): p. 576-82.

159. Yarden, Y. and M.X. Sliwkowski, *Untangling the ErbB signalling network.* Nat Rev Mol Cell Biol, 2001. **2**(2): p. 127-37.
160. De Luca, A., et al., *The role of the EGFR signaling in tumor microenvironment.* J Cell Physiol, 2008. **214**(3): p. 559-67.
161. Roskoski, R., Jr., *ErbB/HER protein-tyrosine kinases: Structures and small molecule inhibitors.* Pharmacol Res, 2014. **87**: p. 42-59.
162. Lin, S.Y., et al., *Nuclear localization of EGF receptor and its potential new role as a transcription factor.* Nat Cell Biol, 2001. **3**(9): p. 802-8.
163. Sok, J.C., et al., *Mutant epidermal growth factor receptor (EGFRvIII) contributes to head and neck cancer growth and resistance to EGFR targeting.* Clin Cancer Res, 2006. **12**(17): p. 5064-73.
164. Temam, S., et al., *Epidermal growth factor receptor copy number alterations correlate with poor clinical outcome in patients with head and neck squamous cancer.* J Clin Oncol, 2007. **25**(16): p. 2164-70.
165. Reya, T., et al., *Stem cells, cancer, and cancer stem cells.* Nature, 2001. **414**(6859): p. 105-11.
166. Brunner, T.B., et al., *Cancer stem cells as a predictive factor in radiotherapy.* Semin Radiat Oncol, 2012. **22**(2): p. 151-74.
167. Wang, S.J. and L.Y. Bourguignon, *Role of hyaluronan-mediated CD44 signaling in head and neck squamous cell carcinoma progression and chemoresistance.* Am J Pathol, 2011. **178**(3): p. 956-63.
168. Naor, D., et al., *Involvement of CD44, a molecule with a thousand faces, in cancer dissemination.* Semin Cancer Biol, 2008. **18**(4): p. 260-7.
169. Joshua, B., et al., *Frequency of cells expressing CD44, a head and neck cancer stem cell marker: correlation with tumor aggressiveness.* Head Neck, 2012. **34**(1): p. 42-9.
170. Prince, M.E., et al., *Identification of a subpopulation of cells with cancer stem cell properties in head and neck squamous cell carcinoma.* Proc Natl Acad Sci U S A, 2007. **104**(3): p. 973-8.
171. Yoshihara, S., et al., *A hyaluronan synthase suppressor, 4-methylumbelliferone, inhibits liver metastasis of melanoma cells.* FEBS Lett, 2005. **579**(12): p. 2722-6.
172. Wobus, M., et al., *CD44 mediates constitutive type I receptor signaling in cervical carcinoma cells.* Gynecol Oncol, 2001. **83**(2): p. 227-34.
173. Bourguignon, L.Y., et al., *Hyaluronan-CD44 interaction with leukemia-associated RhoGEF and epidermal growth factor receptor promotes Rho/Ras co-activation, phospholipase C epsilon-Ca2+ signaling, and cytoskeleton modification in head and neck squamous cell carcinoma cells.* J Biol Chem, 2006. **281**(20): p. 14026-40.
174. Mack, B. and O. Gires, *CD44s and CD44v6 expression in head and neck epithelia.* PLoS One, 2008. **3**(10): p. e3360.
175. Ma, I. and A.L. Allan, *The role of human aldehyde dehydrogenase in normal and cancer stem cells.* Stem Cell Rev, 2011. **7**(2): p. 292-306.
176. Chen, Y.C., et al., *Aldehyde dehydrogenase 1 is a putative marker for cancer stem cells in head and neck squamous cancer.* Biochem Biophys Res Commun, 2009. **385**(3): p. 307-13.
177. Krishnamurthy, S., et al., *Endothelial cell-initiated signaling promotes the survival and self-renewal of cancer stem cells.* Cancer Res, 2010. **70**(23): p. 9969-78.
178. Tomita, H., et al., *Aldehyde dehydrogenase 1A1 in stem cells and cancer.* Oncotarget, 2016. **7**(10): p. 11018-32.
179. Duester, G., F.A. Mic, and A. Molotkov, *Cytosolic retinoid dehydrogenases govern ubiquitous metabolism of retinol to retinaldehyde followed by tissue-specific metabolism to retinoic acid.* Chem Biol Interact, 2003. **143-144**: p. 201-10.

180. Appel, B. and J.S. Eisen, *Retinoids run rampant: multiple roles during spinal cord and motor neuron development.* Neuron, 2003. **40**(3): p. 461-4.
181. Zhao, D., et al., *Molecular identification of a major retinoic-acid-synthesizing enzyme, a retinaldehyde-specific dehydrogenase.* Eur J Biochem, 1996. **240**(1): p. 15-22.
182. Kastan, M.B., et al., *Direct demonstration of elevated aldehyde dehydrogenase in human hematopoietic progenitor cells.* Blood, 1990. **75**(10): p. 1947-50.
183. Moreb, J., et al., *Role of aldehyde dehydrogenase in the protection of hematopoietic progenitor cells from 4-hydroperoxycyclophosphamide by interleukin 1 beta and tumor necrosis factor.* Cancer Res, 1992. **52**(7): p. 1770-4.
184. Yu, C.C., et al., *Targeting CD133 in the enhancement of chemosensitivity in oral squamous cell carcinoma-derived side population cancer stem cells.* Head Neck, 2016. **38 Suppl 1**: p. E231-8.
185. Fukusumi, T., et al., *CD10 as a novel marker of therapeutic resistance and cancer stem cells in head and neck squamous cell carcinoma.* Br J Cancer, 2014. **111**(3): p. 506-14.
186. Swanson, M.S., N. Kokot, and U.K. Sinha, *The Role of HPV in Head and Neck Cancer Stem Cell Formation and Tumorigenesis.* Cancers (Basel), 2016. **8**(2).
187. La Rocca, G., et al., *Isolation and characterization of Oct-4+/HLA-G+ mesenchymal stem cells from human umbilical cord matrix: differentiation potential and detection of new markers.* Histochem Cell Biol, 2009. **131**(2): p. 267-82.
188. Marcus, A.J. and D. Woodbury, *Fetal stem cells from extra-embryonic tissues: do not discard.* J Cell Mol Med, 2008. **12**(3): p. 730-42.
189. Martens-de Kemp, S.R., et al., *CD98 marks a subpopulation of head and neck squamous cell carcinoma cells with stem cell properties.* Stem Cell Res, 2013. **10**(3): p. 477-88.
190. Tsai, L.L., et al., *Markedly increased Oct4 and Nanog expression correlates with cisplatin resistance in oral squamous cell carcinoma.* J Oral Pathol Med, 2011. **40**(8): p. 621-8.
191. Yin, X., et al., *Coexpression of gene Oct4 and Nanog initiates stem cell characteristics in hepatocellular carcinoma and promotes epithelial-mesenchymal transition through activation of Stat3/Snail signaling.* J Hematol Oncol, 2015. **8**: p. 23.
192. Talora, C., et al., *Specific down-modulation of Notch1 signaling in cervical cancer cells is required for sustained HPV-E6/E7 expression and late steps of malignant transformation.* Genes Dev, 2002. **16**(17): p. 2252-63.
193. Lin, T., et al., *p53 induces differentiation of mouse embryonic stem cells by suppressing Nanog expression.* Nat Cell Biol, 2005. **7**(2): p. 165-71.
194. Parfenov, M., et al., *Characterization of HPV and host genome interactions in primary head and neck cancers.* Proc Natl Acad Sci U S A, 2014. **111**(43): p. 15544-9.
195. Lleras, R.A., et al., *Unique DNA methylation loci distinguish anatomic site and HPV status in head and neck squamous cell carcinoma.* Clin Cancer Res, 2013. **19**(19): p. 5444-55.
196. Richards, K.L., et al., *Genome-wide hypomethylation in head and neck cancer is more pronounced in HPV-negative tumors and is associated with genomic instability.* PLoS One, 2009. **4**(3): p. e4941.
197. Schlecht, N.F., et al., *Epigenetic changes in the CDKN2A locus are associated with differential expression of P16INK4A and P14ARF in HPV-positive oropharyngeal squamous cell carcinoma.* Cancer Med, 2015. **4**(3): p. 342-53.
198. Sawada, M., et al., *Increased expression of DNA methyltransferase 1 (DNMT1) protein in uterine cervix squamous cell carcinoma and its precursor lesion.* Cancer Lett, 2007. **251**(2): p. 211-9.
199. van Kempen, P.M., et al., *HPV-positive oropharyngeal squamous cell carcinoma is associated with TIMP3 and CADM1 promoter hypermethylation.* Cancer Med, 2014. **3**(5): p. 1185-96.

200. Werness, B.A., A.J. Levine, and P.M. Howley, *Association of human papillomavirus types 16 and 18 E6 proteins with p53.* Science, 1990. **248**(4951): p. 76-9.
201. Mantovani, F. and L. Banks, *The human papillomavirus E6 protein and its contribution to malignant progression.* Oncogene, 2001. **20**(54): p. 7874-87.
202. McCance, D.J., *Transcriptional regulation by human papillomaviruses.* Curr Opin Genet Dev, 2005. **15**(5): p. 515-9.
203. Burgers, W.A., et al., *Viral oncoproteins target the DNA methyltransferases.* Oncogene, 2007. **26**(11): p. 1650-5.
204. Hafkamp, H.C., et al., *A subset of head and neck squamous cell carcinomas exhibits integration of HPV 16/18 DNA and overexpression of p16INK4A and p53 in the absence of mutations in p53 exons 5-8.* Int J Cancer, 2003. **107**(3): p. 394-400.
205. Gemenetzidis, E., et al., *FOXM1 upregulation is an early event in human squamous cell carcinoma and it is enhanced by nicotine during malignant transformation.* PLoS One, 2009. **4**(3): p. e4849.
206. Schuettengruber, B., et al., *Genome regulation by polycomb and trithorax proteins.* Cell, 2007. **128**(4): p. 735-45.
207. Akasaka, T., et al., *A role for mel-18, a Polycomb group-related vertebrate gene, during theanteroposterior specification of the axial skeleton.* Development, 1996. **122**(5): p. 1513-22.
208. van der Lugt, N.M., et al., *The Polycomb-group homolog Bmi-1 is a regulator of murine Hox gene expression.* Mech Dev, 1996. **58**(1-2): p. 153-64.
209. Boyer, L.A., et al., *Polycomb complexes repress developmental regulators in murine embryonic stem cells.* Nature, 2006. **441**(7091): p. 349-53.
210. Heard, E., *Delving into the diversity of facultative heterochromatin: the epigenetics of the inactive X chromosome.* Curr Opin Genet Dev, 2005. **15**(5): p. 482-9.
211. Ringrose, L. and R. Paro, *Epigenetic regulation of cellular memory by the Polycomb and Trithorax group proteins.* Annu Rev Genet, 2004. **38**: p. 413-43.
212. Huber, G.F., et al., *Expression patterns of Bmi-1 and p16 significantly correlate with overall, disease-specific, and recurrence-free survival in oropharyngeal squamous cell carcinoma.* Cancer, 2011. **117**(20): p. 4659-70.
213. Hyland, P.L., et al., *Evidence for alteration of EZH2, BMI1, and KDM6A and epigenetic reprogramming in human papillomavirus type 16 E6/E7-expressing keratinocytes.* J Virol, 2011. **85**(21): p. 10999-1006.
214. Shao, Z., et al., *Stabilization of chromatin structure by PRC1, a Polycomb complex.* Cell, 1999. **98**(1): p. 37-46.
215. Biron, V.L., et al., *Epigenetic differences between human papillomavirus-positive and -negative oropharyngeal squamous cell carcinomas.* J Otolaryngol Head Neck Surg, 2012. **41 Suppl 1**: p. S65-70.
216. Nishioka, K., et al., *PR-Set7 is a nucleosome-specific methyltransferase that modifies lysine 20 of histone H4 and is associated with silent chromatin.* Mol Cell, 2002. **9**(6): p. 1201-13.
217. Fang, J., et al., *Purification and functional characterization of SET8, a nucleosomal histone H4-lysine 20-specific methyltransferase.* Curr Biol, 2002. **12**(13): p. 1086-99.
218. Pannetier, M., et al., *PR-SET7 and SUV4-20H regulate H4 lysine-20 methylation at imprinting control regions in the mouse.* EMBO Rep, 2008. **9**(10): p. 998-1005.
219. Schotta, G., et al., *A silencing pathway to induce H3-K9 and H4-K20 trimethylation at constitutive heterochromatin.* Genes Dev, 2004. **18**(11): p. 1251-62.
220. Oda, H., et al., *Monomethylation of histone H4-lysine 20 is involved in chromosome structure and stability and is essential for mouse development.* Mol Cell Biol, 2009. **29**(8): p. 2278-95.

221. Di Croce, L. and K. Helin, *Transcriptional regulation by Polycomb group proteins.* Nat Struct Mol Biol, 2013. **20**(10): p. 1147-55.
222. Pasini, D., et al., *Suz12 is essential for mouse development and for EZH2 histone methyltransferase activity.* EMBO J, 2004. **23**(20): p. 4061-71.
223. Cao, R. and Y. Zhang, *SUZ12 is required for both the histone methyltransferase activity and the silencing function of the EED-EZH2 complex.* Mol Cell, 2004. **15**(1): p. 57-67.
224. Yamamoto, K., et al., *Polycomb group suppressor of zeste 12 links heterochromatin protein 1alpha and enhancer of zeste 2.* J Biol Chem, 2004. **279**(1): p. 401-6.
225. Margueron, R. and D. Reinberg, *The Polycomb complex PRC2 and its mark in life.* Nature, 2011. **469**(7330): p. 343-9.
226. Margueron, R., et al., *Ezh1 and Ezh2 maintain repressive chromatin through different mechanisms.* Mol Cell, 2008. **32**(4): p. 503-18.
227. Bracken, A.P., et al., *EZH2 is downstream of the pRB-E2F pathway, essential for proliferation and amplified in cancer.* EMBO J, 2003. **22**(20): p. 5323-35.
228. Volkel, P., et al., *Diverse involvement of EZH2 in cancer epigenetics.* Am J Transl Res, 2015. **7**(2): p. 175-93.
229. Morin, R.D., et al., *Somatic mutations altering EZH2 (Tyr641) in follicular and diffuse large B-cell lymphomas of germinal-center origin.* Nat Genet, 2010. **42**(2): p. 181-5.
230. Ernst, T., et al., *Inactivating mutations of the histone methyltransferase gene EZH2 in myeloid disorders.* Nat Genet, 2010. **42**(8): p. 722-6.
231. Schwartzentruber, J., et al., *Driver mutations in histone H3.3 and chromatin remodelling genes in paediatric glioblastoma.* Nature, 2012. **482**(7384): p. 226-31.
232. Holland, D., et al., *Activation of the enhancer of zeste homologue 2 gene by the human papillomavirus E7 oncoprotein.* Cancer Res, 2008. **68**(23): p. 9964-72.
233. Tang, X., et al., *Activated p53 suppresses the histone methyltransferase EZH2 gene.* Oncogene, 2004. **23**(34): p. 5759-69.
234. Oeggerli, M., et al., *E2F3 amplification and overexpression is associated with invasive tumor growth and rapid tumor cell proliferation in urinary bladder cancer.* Oncogene, 2004. **23**(33): p. 5616-23.
235. Coe, B.P., et al., *Genomic deregulation of the E2F/Rb pathway leads to activation of the oncogene EZH2 in small cell lung cancer.* PLoS One, 2013. **8**(8): p. e71670.
236. Fujii, S., et al., *MEK-ERK pathway regulates EZH2 overexpression in association with aggressive breast cancer subtypes.* Oncogene, 2011. **30**(39): p. 4118-28.
237. Koh, C.M., et al., *Myc enforces overexpression of EZH2 in early prostatic neoplasia via transcriptional and post-transcriptional mechanisms.* Oncotarget, 2011. **2**(9): p. 669-83.
238. Kunderfranco, P., et al., *ETS transcription factors control transcription of EZH2 and epigenetic silencing of the tumor suppressor gene Nkx3.1 in prostate cancer.* PLoS One, 2010. **5**(5): p. e10547.
239. Garipov, A., et al., *NF-YA underlies EZH2 upregulation and is essential for proliferation of human epithelial ovarian cancer cells.* Mol Cancer Res, 2013. **11**(4): p. 360-9.
240. Lin, Y.W., et al., *Role of STAT3 and vitamin D receptor in EZH2-mediated invasion of human colorectal cancer.* J Pathol, 2013. **230**(3): p. 277-90.
241. Kalashnikova, E.V., et al., *ANCCA/ATAD2 overexpression identifies breast cancer patients with poor prognosis, acting to drive proliferation and survival of triple-negative cells through control of B-Myb and EZH2.* Cancer Res, 2010. **70**(22): p. 9402-12.

242. Richter, G.H., et al., *EZH2 is a mediator of EWS/FLI1 driven tumor growth and metastasis blocking endothelial and neuro-ectodermal differentiation.* Proc Natl Acad Sci U S A, 2009. **106**(13): p. 5324-9.
243. Chang, C.J., et al., *EZH2 promotes expansion of breast tumor initiating cells through activation of RAF1-beta-catenin signaling.* Cancer Cell, 2011. **19**(1): p. 86-100.
244. Wu, H., et al., *Structure of the catalytic domain of EZH2 reveals conformational plasticity in cofactor and substrate binding sites and explains oncogenic mutations.* PLoS One, 2013. **8**(12): p. e83737.
245. Berg, T., et al., *A transgenic mouse model demonstrating the oncogenic role of mutations in the polycomb-group gene EZH2 in lymphomagenesis.* Blood, 2014. **123**(25): p. 3914-24.
246. McCabe, M.T., et al., *Mutation of A677 in histone methyltransferase EZH2 in human B-cell lymphoma promotes hypertrimethylation of histone H3 on lysine 27 (H3K27).* Proc Natl Acad Sci U S A, 2012. **109**(8): p. 2989-94.
247. Majer, C.R., et al., *A687V EZH2 is a gain-of-function mutation found in lymphoma patients.* FEBS Lett, 2012. **586**(19): p. 3448-51.
248. Ott, H.M., et al., *A687V EZH2 is a driver of histone H3 lysine 27 (H3K27) hypertrimethylation.* Mol Cancer Ther, 2014. **13**(12): p. 3062-73.
249. Huether, R., et al., *The landscape of somatic mutations in epigenetic regulators across 1,000 paediatric cancer genomes.* Nat Commun, 2014. **5**: p. 3630.
250. Muto, T., et al., *Concurrent loss of Ezh2 and Tet2 cooperates in the pathogenesis of myelodysplastic disorders.* J Exp Med, 2013. **210**(12): p. 2627-39.
251. Makishima, H., et al., *Novel homo- and hemizygous mutations in EZH2 in myeloid malignancies.* Leukemia, 2010. **24**(10): p. 1799-804.
252. He, A., et al., *PRC2 directly methylates GATA4 and represses its transcriptional activity.* Genes Dev, 2012. **26**(1): p. 37-42.
253. Wu, Z., et al., *Polycomb protein EZH2 regulates cancer cell fate decision in response to DNA damage.* Cell Death Differ, 2011. **18**(11): p. 1771-9.
254. Gao, F., et al., *Direct ChIP-bisulfite sequencing reveals a role of H3K27me3 mediating aberrant hypermethylation of promoter CpG islands in cancer cells.* Genomics, 2014. **103**(2-3): p. 204-10.
255. Schlesinger, Y., et al., *Polycomb-mediated methylation on Lys27 of histone H3 pre-marks genes for de novo methylation in cancer.* Nat Genet, 2007. **39**(2): p. 232-6.
256. Velichutina, I., et al., *EZH2-mediated epigenetic silencing in germinal center B cells contributes to proliferation and lymphomagenesis.* Blood, 2010. **116**(24): p. 5247-55.
257. Qi, W., et al., *Selective inhibition of Ezh2 by a small molecule inhibitor blocks tumor cells proliferation.* Proc Natl Acad Sci U S A, 2012. **109**(52): p. 21360-5.
258. Kazanets, A., et al., *Epigenetic silencing of tumor suppressor genes: Paradigms, puzzles, and potential.* Biochim Biophys Acta, 2016. **1865**(2): p. 275-88.
259. Moison, C., et al., *Synergistic chromatin repression of the tumor suppressor gene RARB in human prostate cancers.* Epigenetics, 2014. **9**(4): p. 477-82.
260. Beckedorff, F.C., et al., *The intronic long noncoding RNA ANRASSF1 recruits PRC2 to the RASSF1A promoter, reducing the expression of RASSF1A and increasing cell proliferation.* PLoS Genet, 2013. **9**(8): p. e1003705.
261. Paul, T.A., et al., *Signatures of polycomb repression and reduced H3K4 trimethylation are associated with p15INK4b DNA methylation in AML.* Blood, 2010. **115**(15): p. 3098-108.
262. Riising, E.M., et al., *Gene silencing triggers polycomb repressive complex 2 recruitment to CpG islands genome wide.* Mol Cell, 2014. **55**(3): p. 347-60.

263. De Raedt, T., et al., *PRC2 loss amplifies Ras-driven transcription and confers sensitivity to BRD4-based therapies.* Nature, 2014. **514**(7521): p. 247-51.
264. Wassef, M., et al., *Impaired PRC2 activity promotes transcriptional instability and favors breast tumorigenesis.* Genes Dev, 2015. **29**(24): p. 2547-62.
265. Martin, C., R. Cao, and Y. Zhang, *Substrate preferences of the EZH2 histone methyltransferase complex.* J Biol Chem, 2006. **281**(13): p. 8365-70.
266. Vire, E., et al., *The Polycomb group protein EZH2 directly controls DNA methylation.* Nature, 2006. **439**(7078): p. 871-4.
267. Mohammad, H.P., et al., *Polycomb CBX7 promotes initiation of heritable repression of genes frequently silenced with cancer-specific DNA hypermethylation.* Cancer Res, 2009. **69**(15): p. 6322-30.
268. Rush, M., et al., *Targeting of EZH2 to a defined genomic site is sufficient for recruitment of Dnmt3a but not de novo DNA methylation.* Epigenetics, 2009. **4**(6): p. 404-14.
269. Xu, K., et al., *EZH2 oncogenic activity in castration-resistant prostate cancer cells is Polycomb-independent.* Science, 2012. **338**(6113): p. 1465-9.
270. Kim, E., et al., *Phosphorylation of EZH2 activates STAT3 signaling via STAT3 methylation and promotes tumorigenicity of glioblastoma stem-like cells.* Cancer Cell, 2013. **23**(6): p. 839-52.
271. Cha, T.L., et al., *Akt-mediated phosphorylation of EZH2 suppresses methylation of lysine 27 in histone H3.* Science, 2005. **310**(5746): p. 306-10.
272. Chen, S., et al., *Cyclin-dependent kinases regulate epigenetic gene silencing through phosphorylation of EZH2.* Nat Cell Biol, 2010. **12**(11): p. 1108-14.
273. Kaneko, S., et al., *Phosphorylation of the PRC2 component Ezh2 is cell cycle-regulated and up-regulates its binding to ncRNA.* Genes Dev, 2010. **24**(23): p. 2615-20.
274. Wei, Y., et al., *CDK1-dependent phosphorylation of EZH2 suppresses methylation of H3K27 and promotes osteogenic differentiation of human mesenchymal stem cells.* Nat Cell Biol, 2011. **13**(1): p. 87-94.
275. Khalil, A.M., et al., *Many human large intergenic noncoding RNAs associate with chromatin-modifying complexes and affect gene expression.* Proc Natl Acad Sci U S A, 2009. **106**(28): p. 11667-72.
276. Davidovich, C. and T.R. Cech, *The recruitment of chromatin modifiers by long noncoding RNAs: lessons from PRC2.* RNA, 2015. **21**(12): p. 2007-22.
277. Wu, S.C. and Y. Zhang, *Cyclin-dependent kinase 1 (CDK1)-mediated phosphorylation of enhancer of zeste 2 (Ezh2) regulates its stability.* J Biol Chem, 2011. **286**(32): p. 28511-9.
278. Shi, B., et al., *Integration of estrogen and Wnt signaling circuits by the polycomb group protein EZH2 in breast cancer cells.* Mol Cell Biol, 2007. **27**(14): p. 5105-19.
279. Jung, H.Y., et al., *PAF and EZH2 induce Wnt/beta-catenin signaling hyperactivation.* Mol Cell, 2013. **52**(2): p. 193-205.
280. Lee, S.T., et al., *Context-specific regulation of NF-kappaB target gene expression by EZH2 in breast cancers.* Mol Cell, 2011. **43**(5): p. 798-810.
281. Lajer, C.B., et al., *The role of miRNAs in human papilloma virus (HPV)-associated cancers: bridging between HPV-related head and neck cancer and cervical cancer.* Br J Cancer, 2012. **106**(9): p. 1526-34.
282. Sethi, N., et al., *MicroRNAs and head and neck cancer: reviewing the first decade of research.* Eur J Cancer, 2014. **50**(15): p. 2619-35.
283. Zheng, Z.M. and X. Wang, *Regulation of cellular miRNA expression by human papillomaviruses.* Biochim Biophys Acta, 2011. **1809**(11-12): p. 668-77.

284. Jamali, Z., et al., *MicroRNAs as prognostic molecular signatures in human head and neck squamous cell carcinoma: a systematic review and meta-analysis.* Oral Oncol, 2015. **51**(4): p. 321-31.
285. Zhao, Y., et al., *Helicobacter pylori enhances CIP2A expression and cell proliferation via JNK2/ATF2 signaling in human gastric cancer cells.* Int J Mol Med, 2014. **33**(3): p. 703-10.
286. Hudson, R.S., et al., *MicroRNA-106b-25 cluster expression is associated with early disease recurrence and targets caspase-7 and focal adhesion in human prostate cancer.* Oncogene, 2013. **32**(35): p. 4139-47.
287. Lu, Z., et al., *MicroRNA-21 promotes cell transformation by targeting the programmed cell death 4 gene.* Oncogene, 2008. **27**(31): p. 4373-9.
288. Childs, G., et al., *Low-level expression of microRNAs let-7d and miR-205 are prognostic markers of head and neck squamous cell carcinoma.* Am J Pathol, 2009. **174**(3): p. 736-45.
289. Pekarsky, Y., et al., *Tcl1 expression in chronic lymphocytic leukemia is regulated by miR-29 and miR-181.* Cancer Res, 2006. **66**(24): p. 11590-3.
290. Friedman, J.M., et al., *The putative tumor suppressor microRNA-101 modulates the cancer epigenome by repressing the polycomb group protein EZH2.* Cancer Res, 2009. **69**(6): p. 2623-9.
291. Yan, F., et al., *Restoration of miR-101 suppresses lung tumorigenesis through inhibition of DNMT3a-dependent DNA methylation.* Cell Death Dis, 2014. **5**: p. e1413.
292. Ge, X.S., et al., *HOTAIR, a prognostic factor in esophageal squamous cell carcinoma, inhibits WIF-1 expression and activates Wnt pathway.* Cancer Sci, 2013. **104**(12): p. 1675-82.
293. Maass, P.G., F.C. Luft, and S. Bahring, *Long non-coding RNA in health and disease.* J Mol Med (Berl), 2014. **92**(4): p. 337-46.
294. Gibb, E.A., C.J. Brown, and W.L. Lam, *The functional role of long non-coding RNA in human carcinomas.* Mol Cancer, 2011. **10**: p. 38.
295. Li, D., et al., *Long intergenic noncoding RNA HOTAIR is overexpressed and regulates PTEN methylation in laryngeal squamous cell carcinoma.* Am J Pathol, 2013. **182**(1): p. 64-70.
296. Nie, Y., et al., *Long non-coding RNA HOTAIR is an independent prognostic marker for nasopharyngeal carcinoma progression and survival.* Cancer Sci, 2013. **104**(4): p. 458-64.
297. Kogo, R., et al., *Long noncoding RNA HOTAIR regulates polycomb-dependent chromatin modification and is associated with poor prognosis in colorectal cancers.* Cancer Res, 2011. **71**(20): p. 6320-6.
298. Kim, K., et al., *HOTAIR is a negative prognostic factor and exhibits pro-oncogenic activity in pancreatic cancer.* Oncogene, 2013. **32**(13): p. 1616-25.
299. Gupta, R.A., et al., *Long non-coding RNA HOTAIR reprograms chromatin state to promote cancer metastasis.* Nature, 2010. **464**(7291): p. 1071-6.
300. Yang, Z., et al., *Overexpression of long non-coding RNA HOTAIR predicts tumor recurrence in hepatocellular carcinoma patients following liver transplantation.* Ann Surg Oncol, 2011. **18**(5): p. 1243-50.
301. Zhang, S., et al., *Potential role of differentially expressed lncRNAs in the pathogenesis of oral squamous cell carcinoma.* Arch Oral Biol, 2015. **60**(10): p. 1581-7.
302. Shahryari, A., et al., *Long non-coding RNA SOX2OT: expression signature, splicing patterns, and emerging roles in pluripotency and tumorigenesis.* Front Genet, 2015. **6**: p. 196.
303. Lee, H.S., et al., *Epigenetic silencing of the non-coding RNA nc886 provokes oncogenes during human esophageal tumorigenesis.* Oncotarget, 2014. **5**(11): p. 3472-81.
304. Lindsay, C., H. Seikaly, and V.L. Biron, *Epigenetics of oropharyngeal squamous cell carcinoma: opportunities for novel chemotherapeutic targets.* J Otolaryngol Head Neck Surg, 2017. **46**(1): p. 9.

305. Pickering, C.R., et al., *Integrative genomic characterization of oral squamous cell carcinoma identifies frequent somatic drivers.* Cancer Discov, 2013. **3**(7): p. 770-81.
306. Leemans, C.R., B.J. Braakhuis, and R.H. Brakenhoff, *The molecular biology of head and neck cancer.* Nat Rev Cancer, 2011. **11**(1): p. 9-22.
307. Masterson, L., et al., *De-escalation treatment protocols for human papillomavirus-associated oropharyngeal squamous cell carcinoma: a systematic review and meta-analysis of current clinical trials.* Eur J Cancer, 2014. **50**(15): p. 2636-48.
308. Iyer, N.G., et al., *Detailed Analysis of Clinicopathologic Factors Demonstrate Distinct Difference in Outcome and Prognostic Factors Between Surgically Treated HPV-Positive and Negative Oropharyngeal Cancer.* Ann Surg Oncol, 2015. **22**(13): p. 4411-21.
309. Biron, V.L., et al., *Detection of human papillomavirus type 16 in oropharyngeal squamous cell carcinoma using droplet digital polymerase chain reaction.* Cancer, 2016. **122**(10): p. 1544-51.
310. Mallick, I. and J.N. Waldron, *Radiation therapy for head and neck cancers.* Semin Oncol Nurs, 2009. **25**(3): p. 193-202.
311. Dische, S., et al., *A randomised multicentre trial of CHART versus conventional radiotherapy in head and neck cancer.* Radiother Oncol, 1997. **44**(2): p. 123-36.
312. Waldron, J., et al., *A dose escalation study of hyperfractionated accelerated radiation delivered with integrated neck surgery (HARDWINS) for the management of advanced head and neck cancer.* Radiother Oncol, 2008. **87**(2): p. 173-80.
313. Horiot, J.C., et al., *Hyperfractionation versus conventional fractionation in oropharyngeal carcinoma: final analysis of a randomized trial of the EORTC cooperative group of radiotherapy.* Radiother Oncol, 1992. **25**(4): p. 231-41.
314. Fu, K.K., et al., *A Radiation Therapy Oncology Group (RTOG) phase III randomized study to compare hyperfractionation and two variants of accelerated fractionation to standard fractionation radiotherapy for head and neck squamous cell carcinomas: first report of RTOG 9003.* Int J Radiat Oncol Biol Phys, 2000. **48**(1): p. 7-16.
315. Bourhis, J., et al., *Hyperfractionated or accelerated radiotherapy in head and neck cancer: a meta-analysis.* Lancet, 2006. **368**(9538): p. 843-54.
316. Pedruzzi, P.A., et al., *Analysis of prognostic factors in patients with oropharyngeal squamous cell carcinoma treated with radiotherapy alone or in combination with systemic chemotherapy.* Arch Otolaryngol Head Neck Surg, 2008. **134**(11): p. 1196-204.
317. Jabbari, S., et al., *Matched case-control study of quality of life and xerostomia after intensity-modulated radiotherapy or standard radiotherapy for head-and-neck cancer: initial report.* Int J Radiat Oncol Biol Phys, 2005. **63**(3): p. 725-31.
318. Jha, N., et al., *Submandibular salivary gland transfer prevents radiation-induced xerostomia.* Int J Radiat Oncol Biol Phys, 2000. **46**(1): p. 7-11.
319. Jha, N., et al., *Phase III randomized study: oral pilocarpine versus submandibular salivary gland transfer protocol for the management of radiation-induced xerostomia.* Head Neck, 2009. **31**(2): p. 234-43.
320. Edward C. Halperin, C.A.P., Luther W. Brady, *Head and Neck Tumors*, in *Perez and Brady's Principles and Practice of Radiation Oncology*, J.W. Pine, Editor. 2008, Lippincott Williams & Wilkins, a Wolters Kluwer business: Philadelphia, PA, USA. p. 915-957.
321. Higgins, G.S., et al., *Drug radiotherapy combinations: review of previous failures and reasons for future optimism.* Cancer Treat Rev, 2015. **41**(2): p. 105-13.
322. Lo, T.C., et al., *Combined radiation therapy and 5-fluorouracil for advanced squamous cell carcinoma of the oral cavity and oropharynx: a randomized study.* AJR Am J Roentgenol, 1976. **126**(2): p. 229-35.

323. Lawrence, T.S., A.W. Blackstock, and C. McGinn, *The mechanism of action of radiosensitization of conventional chemotherapeutic agents.* Semin Radiat Oncol, 2003. **13**(1): p. 13-21.
324. Mauro, D.J., et al., *Mechanisms of excision of 5-fluorouracil by uracil DNA glycosylase in normal human cells.* Mol Pharmacol, 1993. **43**(6): p. 854-7.
325. Noordhuis, P., et al., *5-Fluorouracil incorporation into RNA and DNA in relation to thymidylate synthase inhibition of human colorectal cancers.* Ann Oncol, 2004. **15**(7): p. 1025-32.
326. Bartelink, H., et al., *Therapeutic enhancement in mice by clinically relevant dose and fractionation schedules of cis-diamminedichloroplatinum (II) and irradiation.* Radiother Oncol, 1986. **6**(1): p. 61-74.
327. Richmond, R.C., *Toxic variability and radiation sensitization by dichlorodiammineplatinum(II) complexes in Salmonella typhimurium cells.* Radiat Res, 1984. **99**(3): p. 596-608.
328. Yang, L.X., E.B. Douple, and H.J. Wang, *Irradiation enhances cellular uptake of carboplatin.* Int J Radiat Oncol Biol Phys, 1995. **33**(3): p. 641-6.
329. Amorino, G.P., et al., *Radiopotentiation by the oral platinum agent, JM216: role of repair inhibition.* Int J Radiat Oncol Biol Phys, 1999. **44**(2): p. 399-405.
330. Servidei, T., et al., *The novel trinuclear platinum complex BBR3464 induces a cellular response different from cisplatin.* Eur J Cancer, 2001. **37**(7): p. 930-8.
331. Moreland, N.J., et al., *Modulation of drug resistance mediated by loss of mismatch repair by the DNA polymerase inhibitor aphidicolin.* Cancer Res, 1999. **59**(9): p. 2102-6.
332. Yousef, M.I., A.A. Saad, and L.K. El-Shennawy, *Protective effect of grape seed proanthocyanidin extract against oxidative stress induced by cisplatin in rats.* Food Chem Toxicol, 2009. **47**(6): p. 1176-1183.
333. Arany, I. and R.L. Safirstein, *Cisplatin nephrotoxicity.* Semin Nephrol, 2003. **23**(5): p. 460-4.
334. dos Santos, N.A., et al., *Dimethylthiourea protects against mitochondrial oxidative damage induced by cisplatin in liver of rats.* Chem Biol Interact, 2007. **170**(3): p. 177-86.
335. Al-Majed, A.A., *Carnitine deficiency provokes cisplatin-induced hepatotoxicity in rats.* Basic Clin Pharmacol Toxicol, 2007. **100**(3): p. 145-50.
336. Al-Majed, A.A., et al., *Propionyl-L-carnitine prevents the progression of cisplatin-induced cardiomyopathy in a carnitine-depleted rat model.* Pharmacol Res, 2006. **53**(3): p. 278-86.
337. Dasari, S. and P.B. Tchounwou, *Cisplatin in cancer therapy: molecular mechanisms of action.* Eur J Pharmacol, 2014. **740**: p. 364-78.
338. Go, R.S. and A.A. Adjei, *Review of the comparative pharmacology and clinical activity of cisplatin and carboplatin.* J Clin Oncol, 1999. **17**(1): p. 409-22.
339. Dean, M., T. Fojo, and S. Bates, *Tumour stem cells and drug resistance.* Nat Rev Cancer, 2005. **5**(4): p. 275-84.
340. Jain, R.K., *Barriers to drug delivery in solid tumors.* Sci Am, 1994. **271**(1): p. 58-65.
341. Raghunand, N., R.A. Gatenby, and R.J. Gillies, *Microenvironmental and cellular consequences of altered blood flow in tumours.* Br J Radiol, 2003. **76 Spec No 1**: p. S11-22.
342. Tannock, I.F. and D. Rotin, *Acid pH in tumors and its potential for therapeutic exploitation.* Cancer Res, 1989. **49**(16): p. 4373-84.
343. Tannock, I., *Cell kinetics and chemotherapy: a critical review.* Cancer Treat Rep, 1978. **62**(8): p. 1117-33.
344. Hirst, D.G. and J. Denekamp, *Tumour cell proliferation in relation to the vasculature.* Cell Tissue Kinet, 1979. **12**(1): p. 31-42.
345. Bonner, J.A., et al., *Radiotherapy plus cetuximab for locoregionally advanced head and neck cancer: 5-year survival data from a phase 3 randomised trial, and relation between cetuximab-induced rash and survival.* Lancet Oncol, 2010. **11**(1): p. 21-8.

346. Lewis, C.M., et al., *A phase II study of gefitinib for aggressive cutaneous squamous cell carcinoma of the head and neck.* Clin Cancer Res, 2012. **18**(5): p. 1435-46.
347. Magrini, S.M., et al., *Cetuximab and Radiotherapy Versus Cisplatin and Radiotherapy for Locally Advanced Head and Neck Cancer: A Randomized Phase II Trial.* J Clin Oncol, 2016. **34**(5): p. 427-35.
348. Greene, F.L. and L.H. Sobin, *A worldwide approach to the TNM staging system: collaborative efforts of the AJCC and UICC.* J Surg Oncol, 2009. **99**(5): p. 269-72.
349. Ang, K.K., et al., *Human papillomavirus and survival of patients with oropharyngeal cancer.* N Engl J Med, 2010. **363**(1): p. 24-35.
350. Dahlstrom, K.R., et al., *An evolution in demographics, treatment, and outcomes of oropharyngeal cancer at a major cancer center: a staging system in need of repair.* Cancer, 2013. **119**(1): p. 81-9.
351. Huang, S.H., et al., *Refining American Joint Committee on Cancer/Union for International Cancer Control TNM stage and prognostic groups for human papillomavirus-related oropharyngeal carcinomas.* J Clin Oncol, 2015. **33**(8): p. 836-45.
352. Bernier, J., et al., *Postoperative irradiation with or without concomitant chemotherapy for locally advanced head and neck cancer.* N Engl J Med, 2004. **350**(19): p. 1945-52.
353. Lewis, J.S., Jr., et al., *Extracapsular extension is a poor predictor of disease recurrence in surgically treated oropharyngeal squamous cell carcinoma.* Mod Pathol, 2011. **24**(11): p. 1413-20.
354. (UICC), U.f.I.C.C., *TNM Classification of Malignant Tumours - 8th edition*. 8 ed, ed. M.K.G. James D. Brierley, Christian Wittekind. 2016, Hoboken, New Jersey, USA: Wiley Blackwell.
355. Pan, L.N., J. Lu, and B. Huang, *HDAC inhibitors: a potential new category of anti-tumor agents.* Cell Mol Immunol, 2007. **4**(5): p. 337-43.
356. USFDA. *FDA approves Farydak for treatment of multiple myeloma*. US Food and Drug Administration Releases 2015 [cited 2015 22 October 2015]; Available from: http://www.fda.gov/NewsEvents/Newsroom/PressAnnouncements/ucm435296.htm.
357. Duvic, M., *Histone Deacetylase Inhibitors for Cutaneous T-Cell Lymphoma.* Dermatol Clin, 2015. **33**(4): p. 757-64.
358. Venugopal, B., et al., *A phase I study of quisinostat (JNJ-26481585), an oral hydroxamate histone deacetylase inhibitor with evidence of target modulation and antitumor activity, in patients with advanced solid tumors.* Clin Cancer Res, 2013. **19**(15): p. 4262-72.
359. Gros, C., et al., *DNA methylation inhibitors in cancer: recent and future approaches.* Biochimie, 2012. **94**(11): p. 2280-96.
360. Leone, G., et al., *Inhibitors of DNA methylation in the treatment of hematological malignancies and MDS.* Clin Immunol, 2003. **109**(1): p. 89-102.
361. Santi, D.V., A. Norment, and C.E. Garrett, *Covalent bond formation between a DNA-cytosine methyltransferase and DNA containing 5-azacytosine.* Proc Natl Acad Sci U S A, 1984. **81**(22): p. 6993-7.
362. Stresemann, C. and F. Lyko, *Modes of action of the DNA methyltransferase inhibitors azacytidine and decitabine.* Int J Cancer, 2008. **123**(1): p. 8-13.
363. Amatori, S., et al., *DNA demethylating antineoplastic strategies: a comparative point of view.* Genes Cancer, 2010. **1**(3): p. 197-209.
364. Gnyszka, A., Z. Jastrzebski, and S. Flis, *DNA methyltransferase inhibitors and their emerging role in epigenetic therapy of cancer.* Anticancer Res, 2013. **33**(8): p. 2989-96.
365. Huilgol, N.G., *A phase I study to study arsenic trioxide with radiation and hyperthermia in advanced head and neck cancer.* Int J Hyperthermia, 2006. **22**(5): p. 391-7.

366. Fu, H.Y., et al., *Arsenic trioxide inhibits DNA methyltransferase and restores expression of methylation-silenced CDKN2B/CDKN2A genes in human hematologic malignant cells.* Oncol Rep, 2010. **24**(2): p. 335-43.
367. Winquist, E., et al., *Phase II trial of DNA methyltransferase 1 inhibition with the antisense oligonucleotide MG98 in patients with metastatic renal carcinoma: a National Cancer Institute of Canada Clinical Trials Group investigational new drug study.* Invest New Drugs, 2006. **24**(2): p. 159-67.
368. Davis, A.J., et al., *Phase I and pharmacologic study of the human DNA methyltransferase antisense oligodeoxynucleotide MG98 given as a 21-day continuous infusion every 4 weeks.* Invest New Drugs, 2003. **21**(1): p. 85-97.
369. Ben-Kasus, T., et al., *Metabolic activation of zebularine, a novel DNA methylation inhibitor, in human bladder carcinoma cells.* Biochem Pharmacol, 2005. **70**(1): p. 121-33.
370. Richon, V.M., et al., *Histone deacetylase inhibitor selectively induces p21WAF1 expression and gene-associated histone acetylation.* Proc Natl Acad Sci U S A, 2000. **97**(18): p. 10014-9.
371. Sandor, V., et al., *P21-dependent g(1)arrest with downregulation of cyclin D1 and upregulation of cyclin E by the histone deacetylase inhibitor FR901228.* Br J Cancer, 2000. **83**(6): p. 817-25.
372. Mascolo, M., et al., *Epigenetic disregulation in oral cancer.* Int J Mol Sci, 2012. **13**(2): p. 2331-53.
373. Duvic, M., et al., *Phase 2 trial of oral vorinostat (suberoylanilide hydroxamic acid, SAHA) for refractory cutaneous T-cell lymphoma (CTCL).* Blood, 2007. **109**(1): p. 31-9.
374. Modesitt, S.C., et al., *A phase II study of vorinostat in the treatment of persistent or recurrent epithelial ovarian or primary peritoneal carcinoma: a Gynecologic Oncology Group study.* Gynecol Oncol, 2008. **109**(2): p. 182-6.
375. Stein, E.M., Garcia-Manero, G., Rizzieri, D. A., Savona, M., Tibes, R., Altman, J. K., ... & Tallman, M. S, *The DOT1L inhibitor EPZ-5676: safety and activity in relapsed/refractory patients with MLL-rearranged leukemia.* Blood, 2014. **124**(21): p. 387-387.
376. Xu, B., et al., *Selective inhibition of EZH2 and EZH1 enzymatic activity by a small molecule suppresses MLL-rearranged leukemia.* Blood, 2015. **125**(2): p. 346-57.
377. Song, X., et al., *Selective inhibition of EZH2 by ZLD1039 blocks H3K27 methylation and leads to potent anti-tumor activity in breast cancer.* Sci Rep, 2016. **6**: p. 20864.
378. Kung, P.P., et al., *Design and Synthesis of Pyridone-Containing 3,4-Dihydroisoquinoline-1(2H)-ones as a Novel Class of Enhancer of Zeste Homolog 2 (EZH2) Inhibitors.* J Med Chem, 2016. **59**(18): p. 8306-25.
379. Kung, P.P., et al., *Correction to Design and Synthesis of Pyridone-Containing 3,4-Dihydroisoquinoline-1(2H)-ones as a Novel Class of Enhancer of Zeste Homolog 2 (EZH2) Inhibitors.* J Med Chem, 2016. **59**(24): p. 11196.
380. Verma, S.K., et al., *Identification of Potent, Selective, Cell-Active Inhibitors of the Histone Lysine Methyltransferase EZH2.* ACS Med Chem Lett, 2012. **3**(12): p. 1091-6.
381. Sato, T., et al., *Transcriptional Selectivity of Epigenetic Therapy in Cancer.* Cancer Res, 2016.
382. Liu, T.P., et al., *In silico and experimental analyses predict the therapeutic value of an EZH2 inhibitor GSK343 against hepatocellular carcinoma through the induction of metallothionein genes.* Oncoscience, 2016. **3**(1): p. 9-20.
383. Ding, M., et al., *The polycomb group protein enhancer of zeste 2 is a novel therapeutic target for cervical cancer.* Clin Exp Pharmacol Physiol, 2015. **42**(5): p. 458-64.
384. Tsai, J.H. and J. Yang, *Epithelial-mesenchymal plasticity in carcinoma metastasis.* Genes Dev, 2013. **27**(20): p. 2192-206.

385. Glazer, R.I., et al., *3-Deazaneplanocin: a new and potent inhibitor of S-adenosylhomocysteine hydrolase and its effects on human promyelocytic leukemia cell line HL-60.* Biochem Biophys Res Commun, 1986. **135**(2): p. 688-94.
386. Miranda, T.B., et al., *DZNep is a global histone methylation inhibitor that reactivates developmental genes not silenced by DNA methylation.* Mol Cancer Ther, 2009. **8**(6): p. 1579-88.
387. Tan, J., et al., *Pharmacologic disruption of Polycomb-repressive complex 2-mediated gene repression selectively induces apoptosis in cancer cells.* Genes Dev, 2007. **21**(9): p. 1050-63.
388. Suva, M.L., et al., *EZH2 is essential for glioblastoma cancer stem cell maintenance.* Cancer Res, 2009. **69**(24): p. 9211-8.
389. Hayden, A., et al., *S-adenosylhomocysteine hydrolase inhibition by 3-deazaneplanocin A analogues induces anti-cancer effects in breast cancer cell lines and synergy with both histone deacetylase and HER2 inhibition.* Breast Cancer Res Treat, 2011. **127**(1): p. 109-19.
390. Chiba, T., et al., *3-Deazaneplanocin A is a promising therapeutic agent for the eradication of tumor-initiating hepatocellular carcinoma cells.* Int J Cancer, 2012. **130**(11): p. 2557-67.
391. Kemp, C.D., et al., *Polycomb repressor complex-2 is a novel target for mesothelioma therapy.* Clin Cancer Res, 2012. **18**(1): p. 77-90.
392. Fiskus, W., et al., *Combined epigenetic therapy with the histone methyltransferase EZH2 inhibitor 3-deazaneplanocin A and the histone deacetylase inhibitor panobinostat against human AML cells.* Blood, 2009. **114**(13): p. 2733-43.
393. Crea, F., et al., *Pharmacologic disruption of Polycomb Repressive Complex 2 inhibits tumorigenicity and tumor progression in prostate cancer.* Mol Cancer, 2011. **10**: p. 40.
394. Smits, M., et al., *Down-regulation of miR-101 in endothelial cells promotes blood vessel formation through reduced repression of EZH2.* PLoS One, 2011. **6**(1): p. e16282.
395. Fiskus, W., et al., *Superior efficacy of a combined epigenetic therapy against human mantle cell lymphoma cells.* Clin Cancer Res, 2012. **18**(22): p. 6227-38.
396. Sun, F., et al., *Loading 3-deazaneplanocin A into pegylated unilamellar liposomes by forming transient phenylboronic acid-drug complex and its pharmacokinetic features in Sprague-Dawley rats.* Eur J Pharm Biopharm, 2012. **80**(2): p. 323-31.
397. Knutson, S.K., et al., *A selective inhibitor of EZH2 blocks H3K27 methylation and kills mutant lymphoma cells.* Nat Chem Biol, 2012. **8**(11): p. 890-6.
398. Shen, J.K., et al., *Targeting EZH2-mediated methylation of H3K27 inhibits proliferation and migration of Synovial Sarcoma in vitro.* Sci Rep, 2016. **6**: p. 25239.
399. Khaleghian, A., et al., *Metabolism of arsenic trioxide in acute promyelocytic leukemia cells.* J Cell Biochem, 2014. **115**(10): p. 1729-39.
400. Kramer, O.H., et al., *The histone deacetylase inhibitor valproic acid selectively induces proteasomal degradation of HDAC2.* EMBO J, 2003. **22**(13): p. 3411-20.
401. Ma, J., et al., *Histone Deacetylase Inhibitor Phenylbutyrate Exaggerates Heart Failure in Pressure Overloaded Mice independently of HDAC inhibition.* Sci Rep, 2016. **6**: p. 34036.
402. Epizyme, I. *An Open-Label, Multicenter, Phase 1/2 Study of E7438 (EZH2 Histone Methyl Transferase [HMT] Inhibitor) as a Single Agent in Subjects With Advanced Solid Tumors or With B-cell Lymphomas*. 2015 [cited 2015 November 16]; Available from: https://clinicaltrials.gov/ct2/show/NCT01897571.
403. Poirier, J.T., et al., *DNA methylation in small cell lung cancer defines distinct disease subtypes and correlates with high expression of EZH2.* Oncogene, 2015. **34**(48): p. 5869-78.
404. Medicine, U.N.L.o. *A Study to Investigate the Safety, Pharmacokinetics, Pharmacodynamics and Clinical Activity of GSK2816126 in Subjects With Relapsed/Refractory Diffuse Large B Cell Lymphoma, Transformed Follicular Lymphoma, Other Non-Hodgkin's Lymphomas, Solid Tumors*

and Multiple Myeloma. 2014 [cited 2017 June 8, 2017]; Available from: https://clinicaltrials.gov/ct2/show/NCT02082977.
405. Medicine, U.N.L.o. *A Study Evaluating CPI-1205 in Patients With B-Cell Lymphomas*. 2015 [cited 2017 June 8, 2017]; Available from: https://clinicaltrials.gov/ct2/show/NCT02395601.
406. Valentino, K. and C.B. Poronsky, *Human Papillomavirus Infection and Vaccination.* J Pediatr Nurs, 2015.
407. Merck & Co, I. *Gardasil: Human Papillomavirus Quadrivalent (Types 6, 11, 16, 18) Vaccine, Recombinant*. 2015 [cited 2015 December 4]; Available from: http://www.fda.gov/BiologicsBloodVaccines/Vaccines/ApprovedProducts/UCM094042.
408. Lee, J., V. Taneja, and R. Vassallo, *Cigarette smoking and inflammation: cellular and molecular mechanisms.* J Dent Res, 2012. **91**(2): p. 142-9.
409. Merck & Co, I. *Package Insert – GARDASIL 9*. 2015 [cited 2015 December 4]; Available from: http://www.fda.gov/downloads/BiologicsBloodVaccines/Vaccines/ApprovedProducts/UCM426457.pdf.
410. US Department of Health and Human Services. *Immunization and Infections Diseases*. 2015 [cited 2015 December 4]; Available from: http://www.healthypeople.gov/2020/topics-objectives/topic/immunization-and-infectious-diseases.
411. Stokley, S., et al., *Human papillomavirus vaccination coverage among adolescents, 2007-2013, and postlicensure vaccine safety monitoring, 2006-2014--United States.* MMWR Morb Mortal Wkly Rep, 2014. **63**(29): p. 620-4.
412. Williams, W.W., et al., *Noninfluenza vaccination coverage among adults - United States, 2012.* MMWR Morb Mortal Wkly Rep, 2014. **63**(5): p. 95-102.
413. Tonini, G., et al., *New molecular insights in tobacco-induced lung cancer.* Future Oncol, 2013. **9**(5): p. 649-55.
414. Spira, A., et al., *Effects of cigarette smoke on the human airway epithelial cell transcriptome.* Proc Natl Acad Sci U S A, 2004. **101**(27): p. 10143-8.
415. Yu, H.S., et al., *Formation of acetaldehyde-derived DNA adducts due to alcohol exposure.* Chem Biol Interact, 2010. **188**(3): p. 367-75.
416. Brown, J.M. and A.J. Giaccia, *The unique physiology of solid tumors: opportunities (and problems) for cancer therapy.* Cancer Res, 1998. **58**(7): p. 1408-16.
417. Guimaraes, E.P., et al., *Cyclin D1 and Ki-67 expression correlates to tumor staging in tongue squamous cell carcinoma.* Med Oral Patol Oral Cir Bucal, 2015. **20**(6): p. e657-63.
418. Rheinwald, J.G. and M.A. Beckett, *Tumorigenic keratinocyte lines requiring anchorage and fibroblast support cultured from human squamous cell carcinomas.* Cancer Res, 1981. **41**(5): p. 1657-63.
419. Brenner, J.C., et al., *Genotyping of 73 UM-SCC head and neck squamous cell carcinoma cell lines.* Head Neck, 2010. **32**(4): p. 417-26.
420. Inc., T.F.S. *Useful information for various sizes of cell culture dishes and flasks*. Useful Numbers for Cell Culture 2017 [cited 2017 February 2]; Available from: https://www.thermofisher.com/ca/en/home/references/gibco-cell-culture-basics/cell-culture-protocols/cell-culture-useful-numbers.html.
421. Inc., T.F.S. *Histone extraction protocol for western blot*. Western Blot 2017 [cited 2017 February 2].
422. Varambally, S., et al., *The polycomb group protein EZH2 is involved in progression of prostate cancer.* Nature, 2002. **419**(6907): p. 624-9.
423. Chaturvedi, A.K., et al., *Incidence trends for human papillomavirus-related and -unrelated oral squamous cell carcinomas in the United States.* J Clin Oncol, 2008. **26**(4): p. 612-9.

424. Chaturvedi, A.K., et al., *Worldwide trends in incidence rates for oral cavity and oropharyngeal cancers.* J Clin Oncol, 2013. **31**(36): p. 4550-9.
425. Crea, F., et al., *EZH2 inhibition: targeting the crossroad of tumor invasion and angiogenesis.* Cancer Metastasis Rev, 2012. **31**(3-4): p. 753-61.
426. Coulombe, R.A., Jr., R.P. Sharma, and J.W. Huggins, *Pharmacokinetics of the antiviral agent 3-deazaneplanocin A.* Eur J Drug Metab Pharmacokinet, 1995. **20**(3): p. 197-202.
427. Adams, A.K., T.M. Wise-Draper, and S.I. Wells, *Human papillomavirus induced transformation in cervical and head and neck cancers.* Cancers (Basel), 2014. **6**(3): p. 1793-820.
428. Bartke, T., et al., *Nucleosome-interacting proteins regulated by DNA and histone methylation.* Cell, 2010. **143**(3): p. 470-84.
429. Braiteh, F., et al., *Phase I study of epigenetic modulation with 5-azacytidine and valproic acid in patients with advanced cancers.* Clin Cancer Res, 2008. **14**(19): p. 6296-301.
430. Nervi, C., E. De Marinis, and G. Codacci-Pisanelli, *Epigenetic treatment of solid tumours: a review of clinical trials.* Clin Epigenetics, 2015. **7**: p. 127.
431. Santos, N.C., et al., *Multidisciplinary utilization of dimethyl sulfoxide: pharmacological, cellular, and molecular aspects.* Biochem Pharmacol, 2003. **65**(7): p. 1035-41.
432. Collins, S.J., et al., *Terminal differentiation of human promyelocytic leukemia cells induced by dimethyl sulfoxide and other polar compounds.* Proc Natl Acad Sci U S A, 1978. **75**(5): p. 2458-62.
433. Seidenfeld, J., *Effects of difluoromethylornithine on proliferation, polyamine content and plating efficiency of cultured human carcinoma cells.* Cancer Chemother Pharmacol, 1985. **15**(3): p. 196-202.
434. Carvalho, L., K. Foulkes, and D.D. Mickey, *Effect of DMSO and DFMO on rat prostate tumor growth.* Prostate, 1989. **15**(2): p. 123-33.
435. Iwatani, M., et al., *Dimethyl sulfoxide has an impact on epigenetic profile in mouse embryoid body.* Stem Cells, 2006. **24**(11): p. 2549-56.
436. Kita, H., et al., *Dimethyl sulfoxide induces chemotherapeutic resistance in the treatment of testicular embryonal carcinomas.* Oncol Lett, 2015. **10**(2): p. 661-666.
437. Gassmann, M., et al., *Quantifying Western blots: pitfalls of densitometry.* Electrophoresis, 2009. **30**(11): p. 1845-55.
438. Alegria-Schaffer, A., A. Lodge, and K. Vattem, *Performing and optimizing Western blots with an emphasis on chemiluminescent detection.* Methods Enzymol, 2009. **463**: p. 573-99.